OPEN ACCESS

African Journal of Environmental Science and Technology

December 2019
ISSN 1996-0786
DOI: 10.5897/AJEST
www.academicjournals.org

ACADEMIC JOURNALS
expand your knowledge

About AJEST

African Journal of Environmental Science and Technology (AJEST) provides rapid publication (monthly) of articles in all areas of the subject such as Biocidal activity of selected plant powders, evaluation of biomass gasifier, green energy, Food technology etc. The Journal welcomes the submission of manuscripts that meet the general criteria of significance and scientific excellence. Papers will be published shortly after acceptance. All articles are peer-reviewed

Indexing

The African Journal of Environmental Science and Technology is indexed in:
CAB Abstracts, CABI's Global Health Database, Chemical Abstracts (CAS Source Index), China National Knowledge Infrastructure (CNKI), Dimensions Database, Google Scholar, Matrix of Information for The Analysis of Journals (MIAR), Microsoft Academic

AJEST has an h5-index of 14 on Google Scholar Metrics

Open Access Policy

Open Access is a publication model that enables the dissemination of research articles to the global community without restriction through the internet. All articles published under open access can be accessed by anyone with internet connection.

The African Journal of Environmental Science and Technology is an Open Access journal. Abstracts and full texts of all articles published in this journal are freely accessible to everyone immediately after publication without any form of restriction.

Article License

Memberships and Standards

Academic Journals strongly supports the Open Access initiative. Abstracts and full texts of all articles published by Academic Journals are freely accessible to everyone immediately after publication.

All articles published by Academic Journals are licensed under the Creative Commons Attribution 4.0 International License (CC BY 4.0). This permits anyone to copy, redistribute, remix, transmit and adapt the work provided the original work and source is appropriately cited.

Crossref is an association of scholarly publishers that developed Digital Object Identification (DOI) system for the unique identification published materials. Academic Journals is a member of Crossref and uses the DOI system. All articles published by Academic Journals are issued DOI.

Similarity Check powered by iThenticate is an initiative started by CrossRef to help its members actively engage in efforts to prevent scholarly and professional plagiarism. Academic Journals is a member of Similarity Check.

CrossRef Cited-by Linking (formerly Forward Linking) is a service that allows you to discover how your publications are being cited and to incorporate that information into your online publication platform. Academic Journals is a member of CrossRef Cited-by.

Academic Journals is a member of the International Digital Publishing Forum (IDPF). The IDPF is the global trade and standards organization dedicated to the development and promotion of electronic publishing and content consumption.

Contact

Editorial Office: ajest@academicjournals.org

Help Desk: helpdesk@academicjournals.org

Website: http://www.academicjournals.org/journal/AJEST

Submit manuscript online http://ms.academicjournals.org

Academic Journals
73023 Victoria Island, Lagos, Nigeria
ICEA Building, 17th Floor,
Kenyatta Avenue, Nairobi, Kenya.

Table of Content

Vol. 13(12), pp. 456-463, December 2019
DOI: 10.5897/AJEST2018.2570
Article Number: 80902C262328
ISSN: 1996-0786

http://www.academicjournals.org/AJEST

African Journal of Environmental Science and Technology

Full Length Research Paper

Characterization of the development and productivity of *Jatropha curcas* L. plants according to provenance and tillage in Bargny, Senegal

Barro Lamine[1*], Samba Ndiaye Arona Samba[2], Diatta Malaïny[3], Diop Babacar[1] and Akpo Elie Leonard[1]

[1]Department of Plant Biology, Sciences and Technologies Faculty, University of Cheikh Anta Diop of Dakar, Senegal.
[2]Department of Plant Production, National Higher School of Agriculture, University of Thiès, Senegal.
[3]National Forest Research Center, ISRA, Senegal.

Receive 3 September, 2018; Accepted 10 December, 2018

Among the crops that can potentially be used to provide the raw material needed for liquid biofuel production *Jatropha curcas* L. is the one that generates most interest in many development projects. The aim of this study is to evaluate the production and development of 3-year-old *J. curcas* L. seedlings in 2012. The results showed that after three years of planting, subsoiling and provenance have no effect on growth variables and on the major part of foliar functional traits. However, the number of branches in bloom (p = 0.0041) and in fruiting (p = 0.0091) varied significantly under the effect of subsoiling. Branching is significantly higher in the prepared plot than in the control. As a conclusion, tillage has increased branching, while provenance has improved growth in height of *J. curcas* L. plants.

Key words: Tillage, provenance, branching, growth.

INTRODUCTION

Among the crops that can potentially be used to provide the raw material needed for liquid biofuel production, *Jatropha curcas* L. is the one that is of most interest to various development organizations in the tropical and subtropical areas. These biofuels are extracts of renewable sources that bring about environmental benefits, and make it possible to create jobs, both in the collection phase and in the treatment.

J. curcas is a shrub, of the Euphorbiaceae family, originating from Central America (Nicolas, 2010). It exists in all the arid and semi-arid tropical regions of the world (Henning, 2002). In Africa, it can be found in the Sudanese and Guinean savannas and extends from Senegal to Cameroon (Assogbadjo et al., 2010).

According to its most convinced promoters, *J. curcas* can produce large quantities of high quality inedible fuel

*Corresponding author. E-mail: lbarro2@gmail.com. Tel: (221) 774596626.

oil, restore marginal soils, improve the fertility of all types of soil, reforest degraded lands, promote land safety, limit cattle damages on crops, diversify farmers' income and obtain by-products with phytosanitary and therapeutic uses (Mergeai, 2011).

The exploitation of *Jatropha* is recent and needs to be established over the long term. Therefore, our current knowledge and studies must be deepened. *Jatropha* and its by-products are promising, yet technical and agronomic knowledge must be strengthened.

A study carried out two years after having planted in Bargny (Senegal) showed that: subsoiling seems to improve the growth of the upright part (neck, crown) of *Jatropha* (Barro, 2010). Similarly, growth variables, tree architecture, and fruit numbers also vary significantly between *Jatropha* provenances (Barro, 2010).

This present study is based on studies (Barro, 2010) in order to further them. It aims at evaluating the production (fruit and leaves) and development (growth variables and architecture of air ports) of *J. curcas* (JCL) plants aged 4 years in 2012. Two hypotheses were tested: (i) provenance and tillage have affected the growth and productivity of *J. curcas* plants; (ii) some functional features (leaf thickness, leaf stretch, leaf area, specific leaf area (SLA) and leaf dry matter content (LDMC)) of *J. curcas* vary according to provenance and soil work.

MATERIALS AND METHODS

The plant material of *J. curcas* comes from the industrial plantation of SOCOCIM located in Bargny. The plants are located next to the limestone quarries and consist of two provenances: "Diobass" and "Casamance". The studied plants were 4 years old. They were first studied for the first time 2 years after being planted by Barro (2010) in the same site.

The small tools used to carry out this study consisted of an electronic vernier caliper to determine the thickness of the leaves, a nesting perch measuring the height of the JCL plants, plastic bags for the conservation of samples taken, a pruning shears pruner and a tape measure for measuring lengths (branches), circumferences (collar) and diameters (crowns).

Experimental plan

The planting was carried out in 2008 at the SOCOCIM site located in Bargny, with the provenances of JCL "Diobass" and "Casamance". It was fulfilled in rows at a density of 625 plants/ha (4 m × 4 m). A crossed subsoiling of 1 tooth (dent semat) was made to a depth of 40 cm on a part of the plot before planting while the rest of the plot was not subject to any land preparation.

The plants of *J. curcas* were irrigated for 12 months after being planted, at the rate of two waterings of 16 L/plant/week. The main plot provenance factor and the soil tillage factor in secondary plots are the only factors studied in this experiment, the experimental device of which was a split-block with three repetitions, the second factor (tillage) being randomized at the block scale and not within each main plot.

The factors studied had each two levels: "provenances" (Diobass and Casamance) and "tillage" (subsoil and control). Three gross plots of 36 m, that is, 1,296 m^2, containing 100 *J. curcas*, were demarcated. Within each of these plots, a batch of 10 randomly selected and labeled plants constituted the experimental unit. The combination of the different levels of the factors studied gave a total of 4 treatments. Each treatment was repeated 3 times, that means 12 experimental units each one containing 10 JCL plants.

Measured traits

At the scale of the experimental unit (lot of 10 plants), the following variables were determined: the number of low primary branches (0 - 15 cm of the soil), the number of high primary branches (height greater than 15 cm), the number of secondary branches, the number of flowering branches, the number of fruiting branches, the total height (length of the longest strand), the diameter at the neck of the main stem, the diameter of the crown in the direction parallel to the planting line and following the direction perpendicular to the planting line, the state of maturity of the fruit (number of green fruits, number of yellow fruit, number of black fruits or chestnuts, number of total fruits) taking into account the order of branches. At the gross plot scale, survival rates were evaluated.

Measurements also focused on the following functional features: i) leaf thickness, ii) leaf surface, iii) leaf surface area (SLA), iiii) leaf stretching.

According to Violle et al. (2007), a "functional trait" is defined as any morphological, physiological or phenological characteristic, measurable at the individual level without reference to the environment and intervening in the adaptive or fitness value of the species.

To achieve this, three plants from each source were randomly selected, in a well-lit environment, in the prepared plot and in the control. A well-lit branch with a diameter of about 1 cm and at least 1 m long per plant was selected. Six intact fresh leaves of the branch were chosen for the measurements. The selected leaves were kept cool in aluminium foil, placed in a box in the dark, and used throughout the next 24 h.

At first, the leaves were tagged and weighed with a scale to determine their fresh weight (g). Subsequent to these measurements, they were then placed in small aluminium foil bags and dried for at least 48 h at 72°C (up to constant weight) in order to obtain the dry mass of the leaf. It consists of an approximation of the leaf tissue density (when the leaf is not spongy), and is positively correlated with the retention of nutrients in the leaf. By this definition, the leaf dry-matter content (LDMC) was determined by the ratio between the mass of a dry leaf and its weight in the fresh state (g g^{-1}):

$$\text{LDMC (Leaf dry-matter content)} = (\text{Dry mass}) / (\text{Fresh mass}) \quad (1)$$

Then for the thickness of the leaf (mm), the measurements were made at 6 points for each leaf in its fresh state, using a digital caliper. The main veins and the midrib have been avoided. Then, each leaf was scanned to obtain a digital image. The leaves have been flattened as much as possible so that the leaf covers the largest possible area, but not crushed to avoid tissue damage.

The cross section of the leaves was supposed to be circular, and an adjustment was made accordingly to calculate the average thickness (Em) by multiplying the diameter by π / 4.

$$Em = (\Sigma Ei) / 6 \times \pi / 4 \quad (2)$$

where E represents the thickness of the leaf; i ranging from 1 to 6 leaves.

In the same process, the area of each projected leaf was determined using the Midbmp software. The Foliar Specific Surface (SLA) was obtained by the relation between the surface of a leaf in m^2 and its mass in kg.

SLA (Specific leaf area) = (Specific surface area of the leaf) / (Mass of leaf) (3)

Each scanned image (the entire leaf) had a corresponding weight allowing us to calculate the Specific leaf area (SLA). SLA of the branch leaves (expressed in $m^2.kg^{-1}$) was calculated by averaging the specific areas of the six leaves taken from that branch.

(SLA) mean = (ΣSLA) / 6 (4)

For the stretching of the leaves, three plants in each treatment were targeted. Six leaf buds from one branch per plant were selected and labeled and followed until one month of age. The stretching of one-month-old leaves was determined, followed by that of the two-month-old leaves.

The measurements of lengths were carried out with a tape measure in meters except for the height which was measured using a nesting perch of measurement (8 m). Mass measurements were obtained with a precision balance (1/10 000).

Statistical analysis

All the collected data were entered into ExcelTM and analyzed for variance (ANOVA) followed by a mean comparison test (Tukey test) to identify significantly different treatments. The analysis was performed with Statistix 10 software.

RESULTS

Effect of tillage and provenance on growth and survival of *J. curcas* L.

The analysis of the results showed considerable differences (Table 1) in the total height ($p = 0.0202$) and in the survival rate ($p = 0.0095$) of JCL plants under the effect of the interaction between the factors "provenance" and "subsoiling" (Interaction Prov α SS).

The Tukey test enabled us to identify two homogeneous groups: group A composed of Casamance with an average of 1.90 ± 0.01 m and group B composed of Diobass provenance with an average of 2.10 ± 0.01 m (Figure 1). The Tukey test (Table 1) revealed two significantly different groups: group A composed of Casamance provenance with subsoiling (Casa SS) treatment with an average height of 2.07 ± 0.07 m and the group B composed of the treatment "Casamance without subsoiling (control)", noted CasaTem with 1.91 ± 0.07 m. In the "source of cultivation and subsoiling" interaction, the "source Casamance × subsoiling" treatment recorded, on the total height, significantly higher values compared to the "source Casamance × control without subsoiling" treatment.

The same observation was made on the Diobass provenance with two distinct groups revealed by the Tukey test: group A composed of the plot (Diob SS) worked (subsoiling) with an average height of 2.02 ± 0.03 m and group B composed of the unworked plot (DiobTem) (control) with 2.23 ± 0.04 m. The same trend was noted for the survival rate of 98 and 87%, respectively, in the plots worked from Casamance (Casa SS) and Diobass (Diob SS) provenances. The survival rate in the control (non-tillage) plots of Casamance and Diobass provenances was 74.3 and 94%, respectively.

In the "provenance and tillage" interaction, the treatment "Provenance Casamance × subsoiling" recorded, on the survival rate, significantly higher values compared to the treatment "source Casamance × control without subsoiling". The reverse has been registered with the Diobass provenance. Subsoiling was only favorable for the Casamance provenance.

The main factors “provenance and tillage” and their interactions did not affect the crown diameter of the main stem of JCL plants, crown diameter, and survival rate. These variables did not vary significantly under their influence (Table 1).

Due to provenance, Diobass recorded a diameter at the neck of the main stem (11.5 ± 6.2 cm) slightly greater than that of Casamance (11.2 ± 6.2 cm). The same trend is observed for the height, the crown diameter and the survival rate. Similarly, the interaction of factors provenance and subsoiling (Table 1) showed that plots with a diameter at the neck of the stem of the higher JCL plants had higher survival rates, crown diameters and heights. However the plots with small neck diameters of JCL plants have recorded low survival rates, crown height and crown diameter. These results show that the larger the neck diameter of the main stem, the more the plants have better growth and survival rate.

Effect of tillage and provenance on the branching of *J. curcas* L.

The results showed that the number of high primary branches (NR1h>15 cm from soil) with $p = 0.0408$, the total number of primary branches (NR1) with $p = 0.0381$ and the number of primary branches in leaf (NF1) with $p = 0.0381$ significantly varied under the effect of subsoiling (Table 2). The Tukey test revealed two distinct homogeneous groups: the group A composed of the worked plot (subsoiling) and the group B composed of the control (not worked) respectively produced 8.63 ± 1 and 9.98 ± 1, 0 for NR1h; 11.28 ± 0.60 and 12.47 ± 0.60 for NR1 and 11.28 ± 0.60 and 12.47 ± 0.60 for NF1 (Figure 2).

The source and the interaction between the two factors (source and subsoil) did not have a significant effect on the number of low primary branches (NR1b <15 cm of the soil), the number of high primary branches (>15

Table 1. Effect of tillage (subsoiling) and provenance on growth (Main stem crown diameter (DCTP), crown diameter (DH), total height (H) and survival rate (Tx) *Jatropha curcas* plants, three years after planting.

Variable	Provenances		P>F	Subsoiling (SS)		P>F	Interaction ProvαSS				P>F
	Casa	Diobas		SS	Tem		Casa SS	Diob SS	CasaTem	DiobTem	
H (m)	1.90±0.01	2.10±0.01	0.0602	2.04±0.01	2.07±0.01	0.6655	2.07±0.071	2.02±0.03	1.91±0.07	2.23±0.04	0.0202*
DCTP (cm)	11.2±6.2	11.5±6.2	0.5611	11.3±6.2	11.3±6.2	0.9911	11.5±0.47	11.1 ±1.6	10.8±1.35	11.8±1.7	0.1850
DH (m)	2.0±0.1	2.2±0.1	0.1835	2.16±0.1	2.05±0.1	0.5511	2.28±0.11	2.05±0.05	1.66±0.3	2.44±0.13	0.325
Tx (%)	86.2±50	90.5±50	0.3297	92.5±50	84.17±50	0.0875	98.0±1.52	87.0±5	74.3±3.84	94.0±3.51	0.0095*

Casamance = Casa; Diobass = Diob; Under soling = SS; Witness = Tem. *Significant at the 0.05 level. Analysis software: Statistix 10.

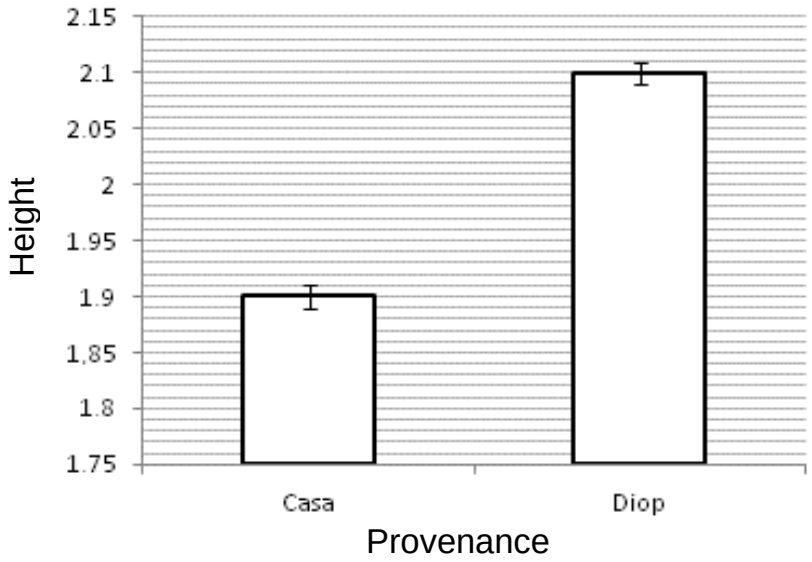

Figure 1. Effect of provenance on the total height of *Jatropha curcas* L. plants.

cm soil = NR1h), the total number of primary branches (NR1), the number of secondary branches (NR2), the number of primary branches in leaf (NF1) and the number of secondary branches (NF2) in leafing (Table 2).

Branching was significantly better for Diobass than for Casamance (Table 2). The total number of primary branches (NR1) and the number of secondary branches (NR2) were 12.1 ± 0.6 and 92.3, respectively on Diobass whereas

Casamance provenance had 11.7 ± 0.6 and 77.8, respectively in the same order. Subsoiling had a depressive effect on primary branching (Table 2), the control of which recorded the highest number (12.47 ± 0.6) compared to the worked plot (11.28

Table 2. Effect of subsoiling and provenance on number of low primary branches (<15 cm of soil = NR1b), number of high primary branches (> 15 cm of soil = NR1h), total number of primary branches (NR1), the number of secondary branches (NR2), the number of primary branches in leaf (NF1) and the number of secondary branches in leafing (NF2).

Variable	Provenances		P>F	Subsoiling		P>F	Interaction prov α SS				P>F
	Casa	Diob		SS	Tem		Casa SS	Diob SS	CasaTem	DiobTem	
NR1b	2.6±0.1	2.5±0.1	0.3668	2.65±0.10	2.48±0.10	0.3668	2.57±0.40	2.73±0.2	2.73±0.2	2.23±0.3	0.098
NR1h	9.03±1	9.6±1	0.3307	8.63±1.0[a]	9.98±1.0[b]	0.0408*	8.50±0.50	8.77±1.0	9.57±0.3	10.4±0.5	0.605
NR1	11.7±0.6	12.1±0.6	0.4239	11.28±0.60[a]	12.47±0.60[b]	0.0381*	11.07±0.14	11.5±1.0	12.30±0.5	12.6±0.5	0.9145
NR2	77.8	92.3	0.1733	87.90	82.18	0.5652	85.80±6.0	90±5.0	69.80±11	94.6±12	0.3142
NF1	11.7±0.6	12.07±0.6	0.4239	11.28±0.60[a]	12.47±0.60[b]	0.0381*	11.07±0.14	11.5±1.0	12.30±0.5	11.5±0.5	0.9145
NF2	77.15	90.6	0.2495	87.90	79.82	0.4715	85.80±6.0	90±5.0	68.50±12	91.1±14	0.4148

Casamance = Casa; Diobass = Diob; Under soling = SS; Witness = Tem. *Significant at the 0.05 level. Analysis software: Statistix 10.

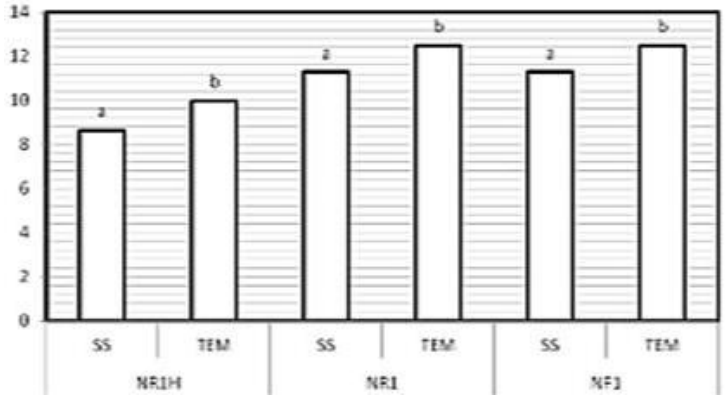

Figure 2. Effect of tillage on branching.

± 0.60). Although subsoiling did not affect the number of secondary branches (NR2), the prepared plot had the highest number.

The interaction of source and subsoiling factors has shown that tillage has a depressive effect on primary and secondary branching for the Diobass. While for the Casamance provenance, soil preparation improved the number of primary branches and was negative for the number of secondary branches. We have the same trend for the number of branches in leaf from each source.

Productivity of *J. curcas* L. plants as a result of soil preparation and provenance

The number of secondary branches in flowering (NR2FL, p = 0.0041), the number of green fruit (NV, p = 0.0225), the number of primary fruiting branches (NB1fr, p = 0.0011), the number of secondary fruiting branches (NB2fr, p = 0.0205), and the total number of fruiting branches (NBfrt, p = 0.0091) significantly varied under the effect of subsoil (Table 3). The Tukey test enabled us to identify two distinct groups under the effect of subsoiling: group A composed of the worked plot and group B represented by the control recorded as 69.38 and 43.17, respectively for NR2FL"; 0.233 and 11.73 for "NV"; 0.1 and 1.8 ± 0.3 for "NB1FR"; 0.1 and 3.4 for "NB2FR"; 0.1 and 5.2 for

Table 3. Estimated flowering by branch order and fruiting (number of fruits and fruiting branches) due to subsoiling and provenance.

Variable	Provenances		P>F	Subsoiling		P>F	Interaction prov α ss				P>+F
	Casa	Diob		SS	Tem		Casa SS	Diob SS	CasaTem	DiobTem	
NR1FL	11.48±0.6	12.07±0.6	0.2509	11.30±0.6	12.20±0.6	0.1027	11.20±0.1	11.50±1	11.80±1	12.60±0.5	0.6057
NR2FL	57.3	55.23	0.7332	69.38[a]	43.17[b]	0.0041*	72.2±4.2	66.60±7	42.40±6.3	43.90±8.3	0.5651
NV	2.85	9.12	0.1476	0.23[a]	11.73[b]	0.0225*	0.13±0.1	0.70±0.2	5.60±2.2	17.90±7.4	0.1588
NB1FR	0.6±0.3	1.233±0.3	0.0894	0.10±0.3[a]	1.80±0.3[b]	0.0011*	0.07±0.03	0.70±0.03	1.20±0.4	2.40±0.5	0.0894
NB2FR	0.8±3.5	2.7±3.5	0.1447	0.10±3.5[a]	3.40±3.5[b]	0.0205*	0.07±0.03	0.70±0.03	1.60±0.7	5.30±2.1	0.1447
NBFRT	1.4±5.6	3.8±5.6	0.1293	0.10±5.6[a]	5.20±5.6[b]	0.0091*	0.07±0.03	0.70±0.03	2.80±1.2	7.60±2.5	0.1293
NFT	132.5	132.7	0.9949	148.93	116.26	0.3497	143.6±35	154±54	121.40±10	111.10±21	0.7550

Analysis software: Statistix 10. *Significant at the threshold of 0.05. Casa = Casamance; Diob = Diobass; SS = under solage; Casa SS = plot worked from Casamance; Diob SS = control plot from Casamance; CasaTem = plot worked from Diobass; DiobTem = control plot from Diobass; NR1FL = Number of primary branches in flowering; NR2FL = number of secondary branches in flowering; NV = number of green fruits; NB1FR = number of primary branches in fruiting; NB2FR = number of secondary branches in fruiting; NBFRT = total number of branches in fruiting; NFT = total number of fruits.

"NBfrt" (Table 3).

However, in addition to the variables mentioned earlier (Table 3), the source and the interaction of the two factors (source and subsoil) did not have a significant effect on all the supervised variables. The number of secondary productive branches (number of secondary branches in flowering and fruiting) was much higher than the number of primary productive branches (number of primary branches in fruiting and flowering) for the Casamance provenance (respectively 58.1 and 18, 08) as for Diobass (respectively 57.93 and 13.3). During the period of data collecting, the fruits were all green; that is why there are no results on the number of yellow and black fruits.

Effect of tillage and provenance on some functional traits of *J. curcas* L.

After planting, the measures taken on the average leaf thickness (Epmf) taken from the 4-year-old *J. curcas* varied significantly (Casamance: 0.334 mm, Diobass: 0.371 mm) depending on the source (p = 0.05) (Table 4). On the contrary, subsoiling and factors interaction did not have a significant effect on this variable (Epmf).

However, leaf fresh weight (p = 0.009) (Table 4) and two-month-old leaf stretch (p = 0.014) (Table 4) significantly varied due to the interaction between the two factors (source and subsoiling).

DISCUSSION

The diameter at the neck of the main stem and the diameter of the crown did not significantly vary under the effect of tillage and provenance factors after 3 years of planting. On the other hand, the height significantly varied under the effect of the interaction of the two factors; although Casa Tem plots gave the lowest heights. The total height of 3-year-old *J. curcas* was 1.90 ± 0.01 m for the Casamance provenance and 2.12 ± 0.01 for Diobass. It reached 2.04 m in the worked plot and 2.07 m in the control plot. These results are substantially similar to other studies (Chehaibi et al., 2008), where evidence is presented that tillage has a favorable effect on the plants' development. It improves in particular the speed of growth.

This same plantation was studied by Barro (2010) with a total height of 1.8 ± 0.004 m for the provenance Casamance, 1.5 ± 0.004 m for Diobass, 1.7 m in the worked plot and in the control. The new results show a clear increase in height growth of *J. curcas* plants. Huwe (2003) noted that tillage influences the biotic and abiotic processes, including the modification of soil structural properties such as cracks, aggregates and pore continuity, as well as soil aeration, temperature levels and humidity, what should promote the growth of plants. In this study, tillage has improved height growth for the Casamance provenance and was depressive for Diobass. Similarly, the preparation of the soil has positively influenced the survival rate for the Casamance provenance and has negatively impacted on the Diobass provenance. Overall, the worked plot had the highest survival rate. The present results are

Table 4. Effect of tillage and provenance on some functional traits: leaf thickness (Epmf), fresh (Pff) and dry (Psf) weights of leaves, dry matter content of leaf (LDMC)), leaf stretching by one month (Etir 1) and two months (Etir 2), leaf surface (Surf F) and leaf surface area (SLA)) of *Jatropha curcas* years, planted under irrigated conditions on the site of SOCOCIM (Bargny, Senegal).

Variable	Provenances		P>F	Subsoiling		P>F	Interaction prov α ss				P>F
	Casa	Diob		SS	Tem		Casa SS	Diob SS	Casa Tem	Diob Tem	
Epmf	0.3±0.001	0.4±0.001	0.05	0.34±0.001	0.36±0.001	0.153	0.316±0.02	0.364±0.02	0.35±0.01	0.4±0.15	0.47
Pff (en g)	2.9±0.045	2.9±0.045	0.74	3.08±0.045[a]	2.7±0.045[b]	0.018	0.3±0.2	2.8±0.2	2.5±0.03	2.9±0.15	0.009
Psf (en g)	0.6±0.01	0.5±0.01	0.72	0.60±0.01	0.50±0.01	0.063	0.6±0.05	0.5±0.06	0.5±0.02	0.5±0.02	0.106
LDMC (mg g^{-1})	0.2±0.001	0.2±0.001	0.78	0.2±0.001	0.2±0.001	0.57	0.2±0.03	0.19±0.01	0.2±0.01	0.2±0.004	0.983
Etir 1	508.3	458.3	0.34	483.3	483.3	1.000	533.3±25	433.3±60	483.3±58	483.3±10	0.342
Etir 2	547.2	552.8	0.83	522.2	577.8	0.064	477.8±40.1	566.7±78	616.7±73	538.9±45	0.014
Surf F(en cm^2)	4986	980	0.37	459	5507	0.273	230.1	688.5	9742.2	1271.5	0.33
SLA (en $cm^2.g^{-1}$)	0.011±0.0003	0.002±0.0003	0.36	0.012±0.0003	0.001±0.0003	0.276	0.0006±0.05	0.001±0.001	0.02±0.02	0.002±0.001	0.33

Analysis software: Statistix 10. *Significant at the threshold of 0.05. Casa = Casamance; Diob = Diobass; SS = under solage; Casa SS = worked plot from Casamance; Casa Tem = sample plot from Casamance; Diob SS = worked plot from Diobass; Diob Tem = sample plot from Diobass.

better than those of Kobilke (1989) in Cape Verde and Heller (1992) in Senegal who reported 5 to 50% survival rates with direct seeding.

Tillage (subsoiling) has an important outcome on the number of primary branches, the number of high primary branches, the number of primary branches in leafing, the number of secondary branches in bloom and the number of branches in fruiting. These results corroborate with the observations of Domergue and Pirot (2008) who noted that the preparation of the soil leads to a faster tree development of the plant, with a broad crown. Similarly, Kouyaté et al. (2008) reported that tillage directly influences crop development. In the same vein, Eléonore et al. (2012) report that the more soil is worked in depth with a high frequency, the greater the amount of mineralized organic matter that can lead to a good development of *Jatropha* plants.

However, tillage does not have a significant effect on the low primary branching and secondary branching. Nevertheless, the prepared plots had the highest number of branches. The results have shown an increase in the growth and branching of *J. curcas* under the effect of provenance and tillage between 2 (Barro, 2010) and 3 years (Barro, 2013) at the SOCOCIM site. The number of branches correlates well with production, indicating that an early branching of JCL would have a decisive effect on the yield because the inflorescences only develop at the end of branches (Domergue and Pirot, 2008; Legendre, 2008). So the more branches the tree has, the more fruit it produces, thus increasing the yield in this SOCOCIM plantation.

The choice of more productive provenance is a very delicate parameter, since production can vary from one year to the next and is even dependent on several factors. Comparative tests of 13 varieties made in Keur Samba Gueye and Toubacouta (Heller, 1992) have shown that the best results were obtained with the local variety (collected at Santhie Ram).

Legendre (2008) reveals that the results obtained at Beude Dieng by the Italian-Senegalese SBE Senegal project tend to indicate that, out of a dozen origins from all the continents, the plants coming from the Sokone zone are the most homogeneous and present the best vegetative development. Similarly, seed size (length, width and thickness), weight (100 seeds, hull and kernel), and germination rate of two provenances (Kaffrine and Nioro) were followed by Ly et al. (2015).

Growth in height, neck diameter, and number of leaves were measured after 60 days. The results obtained showed that the Kaffrine origin had significantly heavier seeds (weight 100 seeds = 71.50 ± 1.22 g, weight = 14.50 ± 0.41 g and weight almond = 22.75 ± 0, 50 g), longer (18.82 ± 0.78 mm) and wider (11.41 ± 0.42 mm) with germination rates (90%) higher than those of Nioro (Ly et al., 2015).

Most of the functional traits (Epmf, Psf, LDMC, Etir1, Etir2, Surf f, SLA) did not vary between provenances or even under the effect of

subsoiling. A dense, thick-leafed leaf has a strong LDMC, which is not the case for a leaf rich in photosynthetic tissues. A high LDMC is often associated with a long leaf life because it gives better mechanical resistance to damage caused by drought and friction (wind) (Bumb, 2012).

However, the dry substance content (LDMC) and specific leaf area values obtained in this study are very low and the JCL plants showed more or less slow growth. These results confirm the previous studies (Westoby, 1998) showing that high SLA values characterize fast-growing plants with large leaves but low longevity; whereas high LDMC values characterize plants leaf organs of which accumulate nutrients and constitute important storage pools with low tissue turnover.

According to Westoby et al. (2002), high ALS species have strategies for rapid leaf material production and frequent leaf turnover. They are efficient in acquiring resources, but poor in the conservation of nutrients in their tissues. These assertions show that *J. curcas* plants do not grow rapidly and have a low frequency for leaf renewal at the Bargny site.

Conclusion

The purpose of this study was to evaluate the effect of tillage and provenance on the growth and the productivity of *J. curcas* plants. The study has revealed that subsoiling and provenance did not affect growth variables and most foliar traits. However, the number of blooming and fruiting branches varied significantly under the effect of subsoiling. Branching is significantly higher in the prepared plot than in the control plot. Likewise, the survival rate is better in the worked field compared to the control.

The interaction of provenance and subsoiling factors had an effect on height growth and survival rate of JCL plants. On the other hand, it has no effect on the branching of JCL plants.

The production of a plant of *J. curcas* L. would, therefore, depend on the branching. Based on these current findings, additional questions arise: which method to apply to *Jatropha* plants to increase the number of branches? Is the size of the branches a good strategy to stimulate branching? These questions have justified the next studies to be pursued in our research.

CONFLICT OF INTERESTS

The authors have not declared any conflict of interests.

REFERENCES

Assogbadjo AE, Sinsin B (2010). Current state of plant diversity in Benin. In Atlas of the Biodiversity of West Africa (Volume 1), Sinsin B, Kanpman D (eds). pp. 222-227.

Barro L (2010). Effect of tillage on the agronomic performance of *Jatropha curcas* in Bargny. Master's thesis, Agroforestry, Ecology, Adaptation. University Cheikh Anta Diop of Dakar; Department of Plant Biology.

Barro L, Samba NAS, Diatta M, Akpo EL (2013). Effect of tillage on the productivity of different provenances of *Jatropha curcas*. OCL 20(3):165-170.

Bumb I (2012). Effects of the functional composition of subalpine grassland communities on primary production and forage quality. Montpellier II University, Place Eugene Battalion, CC 065, 34095 MONTPELLIER Cedex 05.

Chehaibi S, Hannachi C, Pieters JG, Verschoore RA (2008). Keywords, Effects of plowing tools on soil structural condition and yield of a potato crop Re-plowing- Resistance penetration- Voluminous mass-Plant biomass- Tubers yield-Tunisia.

Domergue M, Pirot R (2008). *Jatropha curcas* L, bibliographic synthesis report. CIRAD, Agropolis Avenue 34398 Montpellier Cedex 5 AGROgeneration, 45-47 rue de Monceau 75008 Paris.

Eléonore B, Gérard G, Didier J, Blaise L, Yves N (2012). Adapting Organic Inputs on the Ground "http://www.casasso.com/uploads/rte/File/ Press files /% 20sols% 20vivants% 20Bio / 3_ Adapt_the_apports.pdf ». Accessed at 12hours 15mn on 27/09/2015.

Heller J (1992). Untersuchugen über Gentopische Eigenschaften und Vermehrungsung und An-bauVerfähren bei des Pürgiernuss (*Jatropha curcas* L.). 1992: Hamburg.

Henning RK (2002). Jatropha curcas in Africa, The Global Facilitation Unit for Underutilized Species (GFUUS), Weissensberg, Germany, P 49.

Huwe B (2003). The role of soil for soil structure. In: El Titi A (ed) Soil tillage in agroecosys-tems. CRC, Boca Raton, Florida pp. 27-49.

Kobilke H (1989). Untersuchungen zur Bestandesbegrundung von Purgiernuß (*Jatropha curcas* L.). in University. 1989, Hohenheim: Stuttgart.

Kouyaté AM, Van Damme P, Goyens S, De Neve S, Hofman G (2008). Evaluation of soil fertility at Detarium microcarpum Guill. & Perr. Detarium microcarpum- Soil fertility- Physicochem-ical properties- C / N- Mali.

Legendre B (2008). *Jatropha curcas* (Tabanani), Agronomic Note. Performance Company RC 96B1982 - Dakar Ninea 190263 2B2.

Ly MO, Kumar D, Diouf M, Nautiyal S, Diop T (2015). Morphological traits of seed and vigor of seedlings of two provenances of *Jatropha curcas* L. in Senegal. Journal of Applied Biosciences 88:8249-8255. ISSN 1997-5902.

Mergeai Guy (2011). *Jatropha curcas* L: miraculous plant or devil tree? Tropicultura 29:1-2.

Nicolas C (2010). Jatropha curcas L: a review. Progress of Botanical Research 2(50): 39-86. DOI: 10./016/s0065-2296, 2010.

Violle C, Navas ML, Vile D, Kazakou E, Fortunel C, Hummel I & Garnier E (2007). Let the concept of be functional, Oikos 116(5):882-892.

Westoby M (1998). A leaf height seed (LHS), Plant ecology strategy scheme. Plant Soil 199:213-227.

Westoby M, Falster DS, Moles AT, Vesk PA & Wright IJ (2002). Plant ecological strategies: Some leading dimensions of variation between species. Annual Review of Ecology, Evolution, and Systematics 33:125-159.

Vol. 13(12), pp. 464-480, December 2019
DOI: 10.5897/AJEST2019.2726
Article Number: 3815D8062330
ISSN: 1996-0786

http://www.academicjournals.org/AJEST

African Journal of Environmental Science and Technology

Full Length Research Paper

Spatial patterns of climatic variability and water budget over Sudan Savannah Region of Nigeria

Butu A. W.[1] and Emeribe C. N.[2*]

[1]Department of Geography, Faculty of Arts and Social Sciences, Nigerian Defense Academy, Kaduna, Nigeria.
[2]National Centre for Energy and Environment, Energy Commission of Nigeria, University of Benin, Benin City, Edo State, Nigeria.

Received 29 June, 2019; Accepted 4 November, 2019

The study examined the effect of climatic variability on climatic water balance over Sudan Savannah, Nigeria. Temperature and Rainfall data were collected for the period 1943-2012 from the Nigerian Meteorological Agency. The data were divided into two climatic years 1943-1977 and 1978-2012. On the whole, rainfall amount decreased from a very high mean value of 981.5 mm in Yelwa (Lat. 10.88 N; Long. 4.75 E) to a very low value of 656.1mm in Katsina (Lat. 13.02 N; Long.7.68 E). This pattern reveals gradual/potential extension of dryness from the Lake Chad area in Nigeria in northeast, towards the Sudan savannah, northwest of Nigeria. Annual temperature, PET, moisture deficit distributions revealed very strong evidence of upward trend at α<0.01 with corresponding decrease in rainfall in the second climatic period, an indication of changing climate. However, in Yelwa, Sokoto and Gusau, there was little evidences of significant downward trend in annual rainfall distribution at α =0.10, but rather a quasi–periodic pattern, even though there were signs of statistical rise in temperature. The general pattern of deviation in PET from the first climate period were 1.4, 3.7, 2.7, 1.9% for Yelwa, Sokoto, Gusau and Katsina respectively, while moisture deficits were 5.0, 4.2, 4.0 and 7.9% for Yelwa, Sokoto, Gusau and Katsina respectively. This general observation may suggest that water balance parameters during the second climatic period deviated from patterns Observed in the first climatic period (1943-1977). Repetition of drought within the present climate regime could be expected and should be planned for. For temperature, there is strong evidence of increasing trends for all the stations in the region which agrees with global trend. This has implications for socio-economic development of the study area especially coupled with the attendant consequences of increasing population and economic activities in the region. There is thus need to plan for and design sustainable water resources management techniques in different sectors-agriculture, irrigation and dams, water supply to adapt to the quasi-periodic patterns of rainfall fluctuation.

Key words: Thornthwaite, Sudan Savannah, water balance, climate change, rainfall and temperature.

INTRODUCTION

The hydrological cycle is one of the main components of the earth's system, regulating life in the ecosystem. As a

*Corresponding author. E-mail: emeribe.c@ncee.org.ng. Tel: 08063581430.

result, the sustainability of the hydrological cycle is key toward the continued existence of man, animals and plants. Regrettably, over the past decades beginning from the 18th century, the stability of the hydrological cycle has come under threat essentially due to global warming. The Intergovernmental Panel on Climate Change (IPCC) reported in 2001 that the global climate is changing, largely because of human activities (IPCC, 2007). Exponential increase in demography now puts pressure on land use/ water resources, fossil fuels utilization and natural resources (Van Asselen et al., 2013; Avis et al., 2011; Romero et al., 2014).

The resultant effects of these actions have been drastic changes in the natural environment, including climate change with noticeable implications on the climatic water distribution. These changes can be seen from the frequency of water crises (UNGC, 2009, IPCC, 2017), repeated drought (Vicente-Serrano et al*.,* 2010; Koutroulis et al., 2011; Kwak et al., 2013), water pollution (Jutla et al., 2011; Reyburn et al., 2011) and other hydrological extremes with far reaching effects on the economy, social, political and cultural wellbeing of mankind. Studies have shown that while one consequence of global warming is an increase in temperature, and thus the water holding capacity of the atmosphere, other consequence is an increase in evaporation over the ocean or evapotranspiration on land. This will speed up the hydrological cycle. Finding from all climatic models as they relate to climate change predict an increased evapotranspiration in the presence of water. However, in the absence of precipitation, this will results in increased risk of drought due to enhanced surface dryness (Westerling and Swetnam, 2003), heat wave (Lyon, 2009; Lau and Nath, 2012) and wild fires (Whitman, et al., 2015).

This is true of the Sudan the Savannah Region of Nigeria, which is characterized by acute rainfall variability and in the last 40 years has witnessed dramatic reductions in mean annual rainfall throughout the region (Dai et al., 2004; Ekpoh and Nsa, 2011). Note that this is not new in this region as the region is a significant portion of the Sudan-Sahel ecological zone of West Africa. However, since the early 1970s, climatic anomalies in the form of recurrent droughts, frightening dust storms and rampaging floods have overprinted their rhythms, creating short-duration climatic oscillations as against the normal cycles of larger amplitudes (Camberlin and Diop, 2003; Ekpoh and Nsa, 2011). The persistence of drought in parts in the Sudano-Sahel Nigeria has been attributed to the prevalence of a stagnated anti-cyclonic circulation of the tropical atmosphere over areas that normally should be exposed to the rising arm of the tropical Hadley Cell circulation by mid-summer (Kalu, 1987; Kamara, 1986). These conditions are themselves related to the tropical component of the global general circulation system. Tropical circulation patterns are particularly influenced by heat inputs from such sources as warm ocean surfaces acting through latent heat released in deep cumulus convection (Lockwood, 1979). Related heat sources which also have an important bearing on tropical circulations are high plateaus and equatorial rainforests (Nicholson and Tucker, 1998). These heat sources display visible latitudinal and longitudinal variations, and also a marked tendency to vary on both annual and, in the case of oceans, non-annual scales. One of the consequences of these circulation patterns is that rainfall patterns in West Africa, including northern Nigeria, show both annual and greater than annual variations and also marked tele-connections with distant locations (Nicholson, 1993). Ikhatua (2010) shows that in Nigeria and by extension globally, climate change will affect all four dimensions of food security, namely food availability (production and trade), access to food, stability of food supplies, and food utilization.

The Sudan Savanah region of Nigeria is considered most suitable for the cultivation of grain crops such as millet, sorghum, *acha* and rice, and grain legumes such as beans, cowpea etc. It is also important to mention that the main concentration of cattle production in the country occurs in the zone primarily because it is relatively free from tsetse fly infestation (Oguntoyinbo et al., 1983). Consequently, agricultural production in this region will be affected by moisture deficiency as water is required for photosynthesis and transpiration. In an attempt to attain sustainable food production, there is need to develop adaptation measures. One step towards achieving this however is to gain an understanding of the changes in water balance indices and effects on climatological drought over the region. This is the main focus of this study.

MATERIALS AND METHODS

The study area is Sudan Savannah region of Nigeria. Five synoptic stations in the region were selected for the study; Kano (12.05 N; 8.20 E; 472.5 m), Katsina (13.02 N; 7.68 E; 517.6 m), Yelwa (10.88 N; 4.75 E; 244.0 m), Gusau (12.17 N; 6.70 E; 463.9 m) and Sokoto (13.02 N; 5.25 E; 350.8 m). The region runs east to west of the North occupying an over 250 km band width. Mean annual rainfall is between 510 - 1,140 mm and the dry season lasts between 5 - 7 months (Figure 1). The vegetation is made up of tall grasses and trees which vary in density from place to place. Most of these have umbrella-shaped canopies which become smaller as one move northwards. Cultivation is intense in this region, coupled with heavy grazing, bush burning and cutting trees for fuel and building has promoted desertification in this zone (Agabi, 1995).

Data collection

Monthly temperature and rainfall data were collected for the period 1943-2012 from the Nigerian Meteorological Agency (NIMET), Lagos State. Climatic data were divided into two climatic periods 1943-1977 and 1978-2012 for ease of discussion. The Thornthwaite water balance computer software version 1.10, developed by the United States Geological Survey Department was used to estimate potential evapotranspiration based on Hamon equation (Hamon,

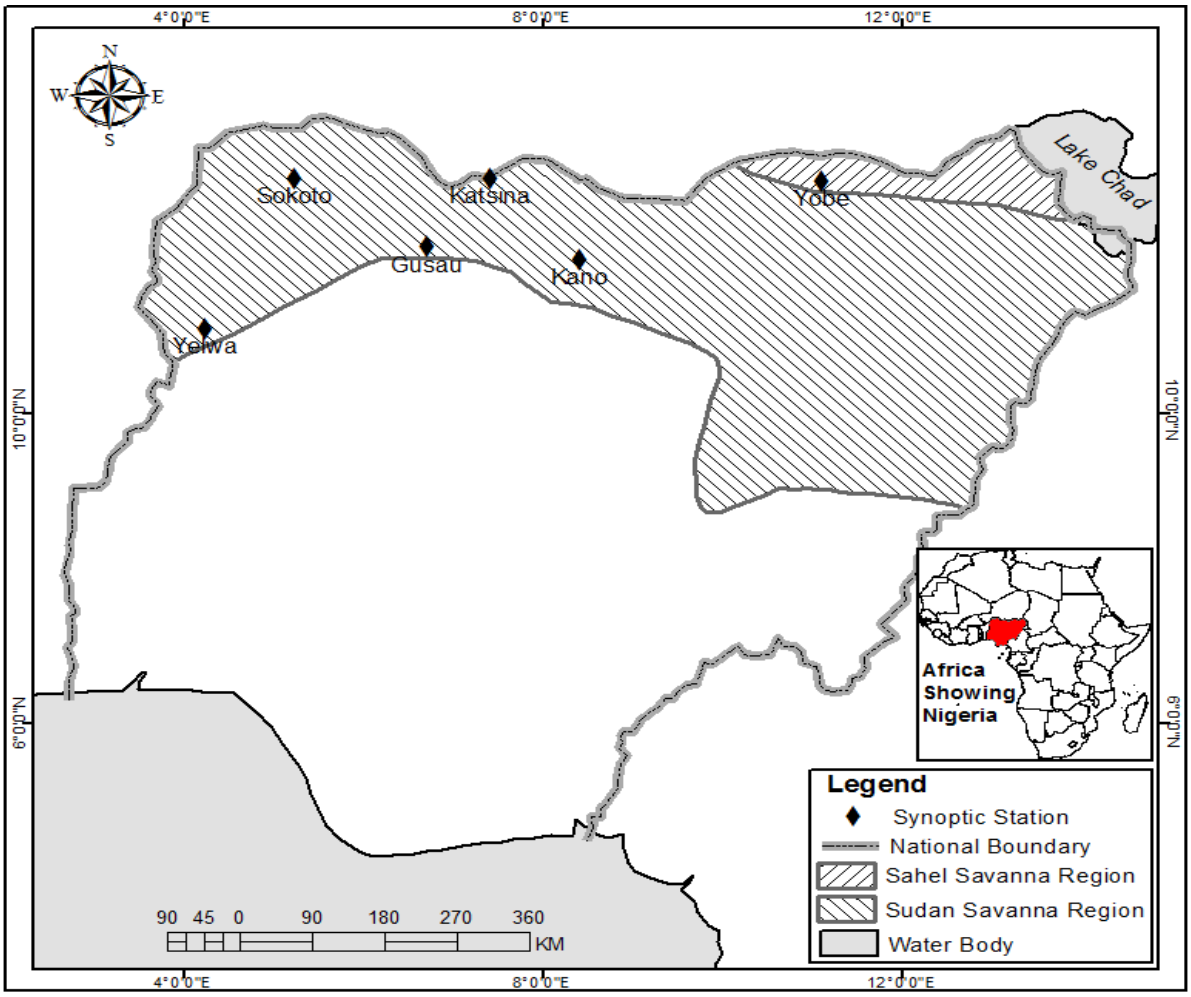

Figure 1. Sudan-Sahelian Region of Nigeria.

1961). The equation estimates monthly *PET* from mean monthly temperature (*T*).

The choice of this model is based on the nature of physical processes that interact to produce the phenomena under investigation (that is, temperature rainfall relationship), availability of the required model components/data and wide applicability of the model for hydrological impact of climate change assessment. Although studies have shown the Penman (1948) equation is considered to be the most accurate and has widespread application (Ayoade, 1983; Anyadike, 1987), unfortunately, the model demands a great deal of data which may not be readily available particularly in most developing countries for example where net radiation data and soil heat flux are important. Like the FAO Penman model, the Thornthwaite software version 1.10 also takes into account the geographical location of the area of concern, assumed soil moisture capacity. But more importantly, the authors preferred the Thornthwaite software version 1.10 mainly due to availability of input data such as temperature, rainfall, longitude and latitudes, available moisture capacity, unlike Penman model most of whose inputs data are not available for the country.

The Hamon equation is given as:

$$PET_{Hamon} = 13.97 \times d \times D_2 \times W_t \quad (1)$$

where PET_{Hamon} is *PET* in millimeters per month, *d* is the number of days in a month, *D* is the mean monthly hours of daylight in units of 12 h, and W_t is the saturated water vapor density term, in grams per cubic meter, calculated using Equation 2:

$$W_t = \frac{4.95 \times e^{0.062 \times T}}{100} \quad (2)$$

Where *T* is the mean monthly temperature in degrees Celsius (Hamon, 1961).

With the knowledge of the monthly precipitation, potential evapotranspiration values and soil moisture holding capacity of the study area, other water budget elements such as actual evapotranspiration, change in storage, soil moisture deficit and surplus were calcula

ted as arithmetical differences, either positive or negative, between precipitation and potential evapotranspiration values.

Analysis for trend

Mann-Kendall, Spearman's Rho and Linear Regression were carried out using TREND software and were determined using a

Trend/change detection software (TREND) version 1.0.2 developed by the Cooperative Research Centre for Catchment Hydrology's (CRCCH) Climate Variability Program, in Australia.

Mann-Kendall test

This tool is used test whether there is a significant trend in the time series data. The n time series values (X1, X2, X3, ….., Xn) were first replaced by their relative ranks (R1, R2, R3,….., Rn) (starting at 1 for the lowest up to n). The test statistic S is:

$$s = \sum_{i=1}^{n-1} [\sum_{j=i+1}^{n} \mathrm{sgn}(R_i - R_i)]. \quad (3)$$

Where Sgn(x) = 1 for x > 0
Sgn(x) =0 for x = 0
Sgn(x) = -1 for x <0
If the null hypothesis Ho is true, then S is approximately normally distributed with:μ = 0

$$\sigma = n(n-1)(2n+5)/18 \quad (4)$$

The z-statistic is therefore (critical test statistic values for various significance levels may be obtained from normal probability tables):

$$Z = | s | / \sigma^{0.5} \quad (5)$$

A positive value of S indicates that there is an increasing trend and vice versa.

Spearman's Rho test

This was used to determine whether the correlation between two variables is significant. One variable was taken as the time itself (years) and the other as the corresponding time series data. Like the Mann-Kendall Test, the n time series values were replaced by their ranks. The test statistic *ρs* is the correlation coefficient, which is obtained in the same way as the usual sample correlation coefficient, but using ranks. The equation is expressed as-:

$$\rho_S \; S_{xy} / (S_x S_y)^{0.5} \quad (6)$$

$$where \quad S_x = \sum_{i=1}^{n} \left(x_i - \overline{X} \right)^2 \quad (7)$$

$$S_y = \sum_{i=1}^{n} \left(y_i - \overline{Y} \right)^2 \quad (8)$$

$$S_{xy} = \sum_{i=1}^{n} \left(x_i - \overline{X} \right)^2 \left(y_i - \overline{Y} \right). \quad (9)$$

and x_i (time), y_i (variable of interest), $\bar{x}$ and $\bar{y}$ refer to the ranks ($\bar{x}$, $\bar{y}$, S_x and S_y have the same value in a trend analysis).

Linear regression test

It tests whether there is a linear trend by examining the relationship between time (x) and the variable of interest (y). The regression gradient is estimated by:

$$b = \frac{\sum_{i=1}^{n} (x_i - \bar{x})(y_i - \bar{y})}{\sum_{i=1}^{n} (x_i - \bar{x})^2}. \quad (10)$$

and the intercept is estimated as:

$$a = y - bx \quad (11)$$

The test statistic S is:

$$where \quad \sigma = \sqrt{\frac{12 \sum_{i=1}^{n} (y_i - a - bx_i)}{n(n-2)(n^2-1)}}. \quad (12)$$

The test statistic S follows a Student-t distribution with n-2 degrees of freedom under the null hypothesis (critical test statistic values for various significance levels was obtained from Student's t statistic tables).

Analysis of moisture index

Moisture index was determined using the Thornthwaite (1953) method as follows:

$$\mathrm{Im} = \frac{100S - 100D}{PET}$$

Where, Im is the moisture index, S is the sum of monthly surpluses, D is the sum of monthly moisture deficit and PET is evapotranspiration.

$$\mathrm{Ia} = \frac{100D}{PET}$$

Where Ia is the Index of aridity, D is the sum of monthly moisture deficit and PET is evapotranspiration.

$$\mathrm{Ih} = \frac{100S}{PET}$$

Where Ih is the index of humidity, S is the sum of monthly surpluses and PET is evapotranspiration.

RESULTS AND DISCUSSION

In Figures 2 to 10, the long-term annual rainfall and temperature patterns are presented. Annual rainfall was generally random. However, for locations such as Yelwa and Sokoto there was evidence of a gentle decrease in rainfall amount first between 1940s and 1950 and between 1970 and 1990 (Figures 2 and 4). For Gusau, annual rainfall was generally low with a sign of a sharp increase towards the end of the 1990s. In Katsina and Kano annual rainfall revealed decreasing trend from 1980

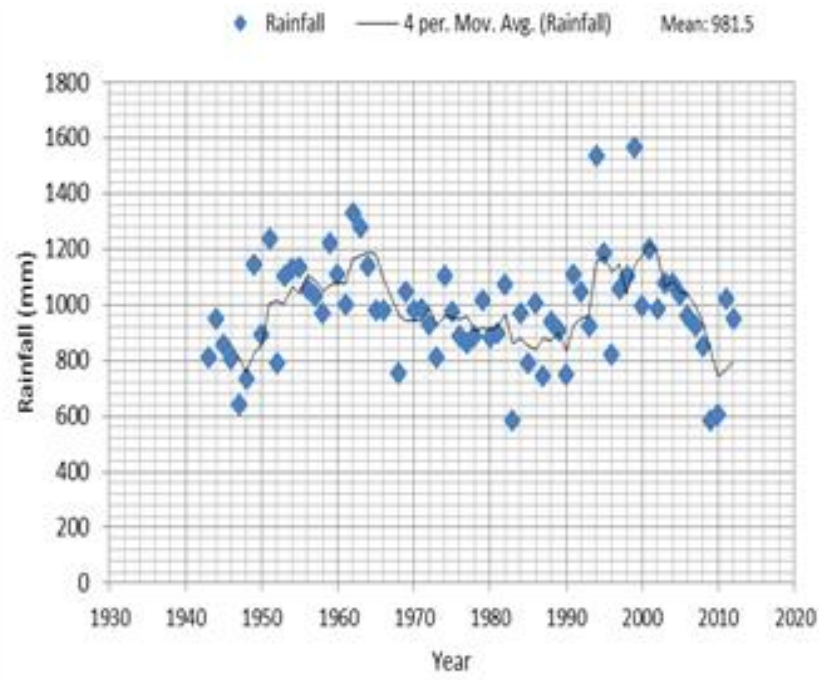

Figure 2. Annual rainfall distribution over Yelwa.

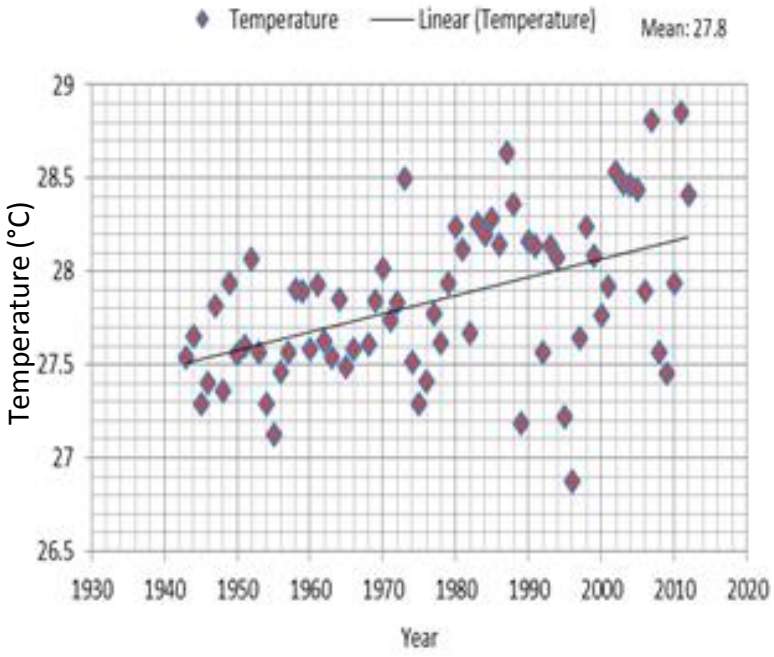

Figure 3. Annual temperature distribution over Yelwa.

for Katsina and 1990 for Kano station. Annual temperature distribution on the other hand revealed very strong evidence of an upward trend at $\alpha<0.01$ for all the synoptic stations (Figures, 3, 4, 6, 8, 10 and Table 1). The observed decreasing trends in the 1940s and 1950 and between 1970 and 1990 coincides with the Sahel droughts of the 1940s, 1960-1973 and 1980-1987 (Amissah-Arthur, 1999); it is attributed to the prevalence of a stagnated anti-cyclonic circulation of the tropical atmosphere over areas that normally should be exposed

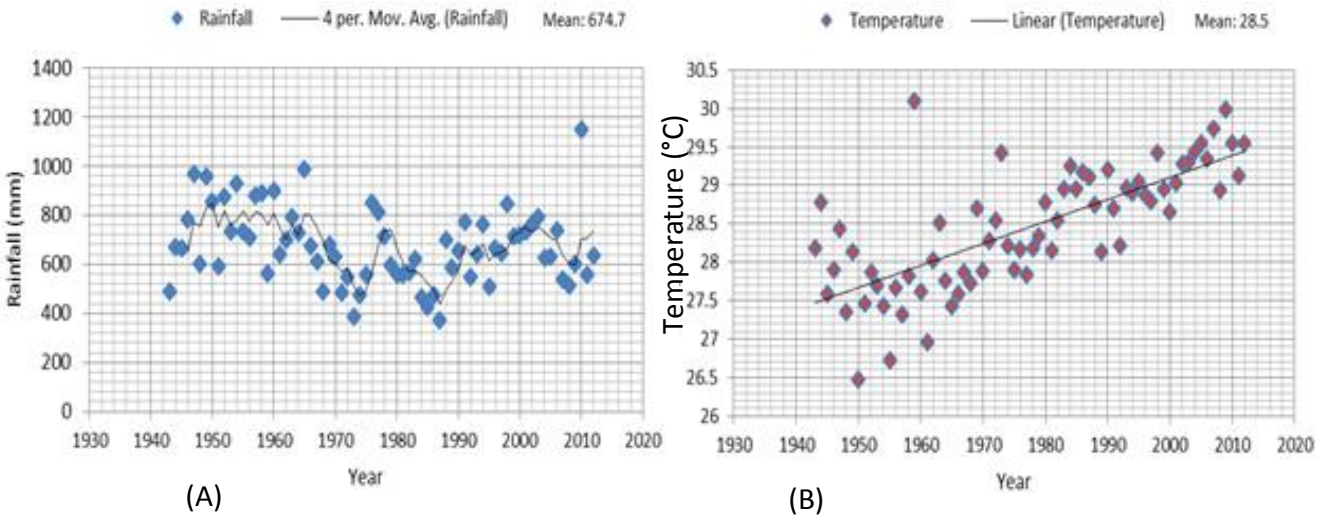

Figure 4. (a) Annual rainfall distribution over Sokoto, (b) Annual temperature distribution over Sokoto.

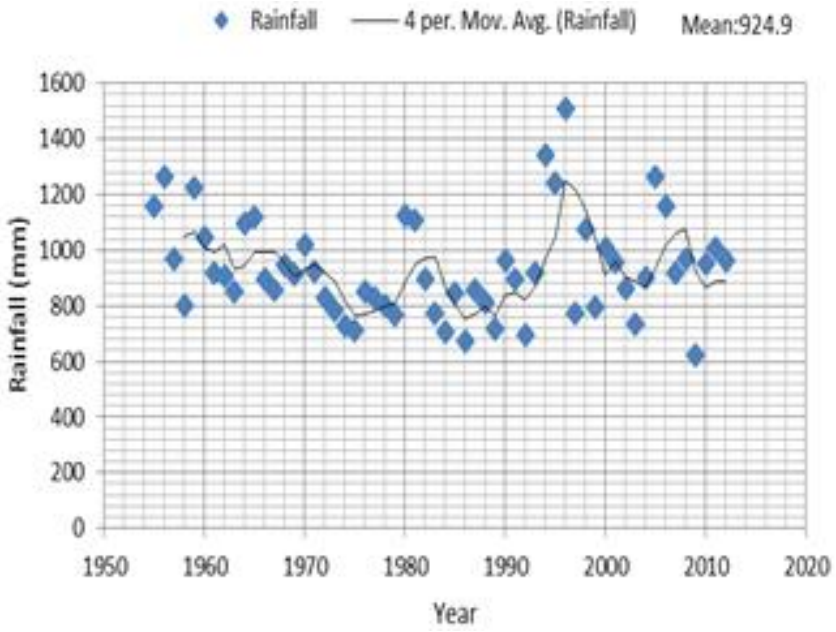

Figure 5. Annual rainfall distribution over Gusau.

to the rising arm of the tropical Hadley Cell circulation by mid-summer (Kamara, 1986). More so the abnormally high rainfall at the end of 80s, and within the decade 90s attest to the study area is characterized by unstable annual rainfall character. In Table 1, results of long-term trend patterns of rainfall and temperature over Sudan savannah (1943-2012) are presented. In locations such as Yelwa, Sokoto and Gusau, there is little or no evidence of statistical downward trends in annual rainfall distribution at $\alpha = 0.10$, but rather quasi –periodic patterns in nature. However for Katsina and Kano there is strong evidence of statistical downward trends in annual rainfall patterns at $\alpha < 0.05$.

In Table 2, descriptive statistics of long-term annual rainfall and temperature are presented. Rainfall amount decreased from a very high value of 981.5 mm in Yelwa (Lat. 10.88 N; Long. 4.75 E) to a very low value of 656.1 mm in Katsina (Lat. 13.02 N; Long.7.68 E), followed by Sokoto (Lat. 13.02 N; Long. 5.25 E). Kano also recorded a low annual value of 841.9 mm compared to stations in the extreme northwest. This pattern also reveals gradual outward spread of dryness from the Lake Chad basin in

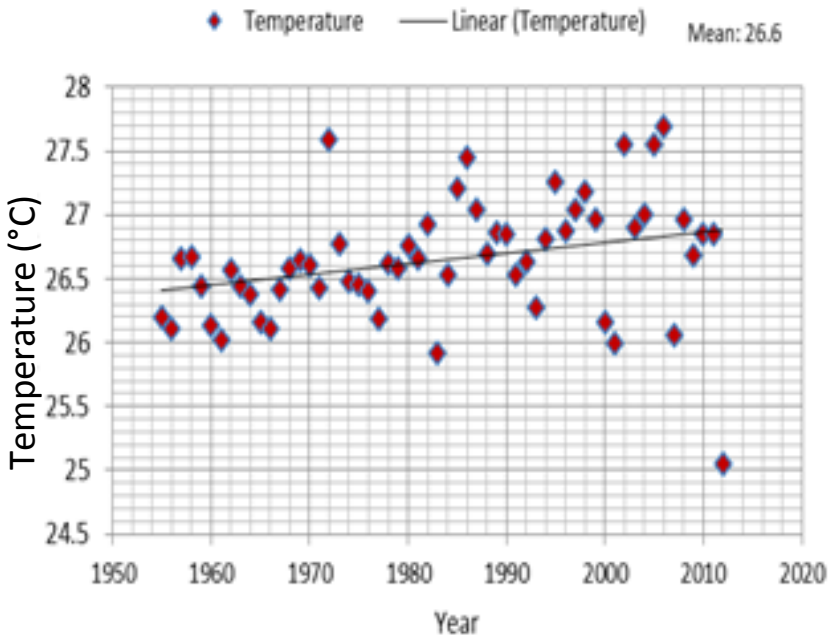

Figure 6. Annual temperature distribution over Gusau.

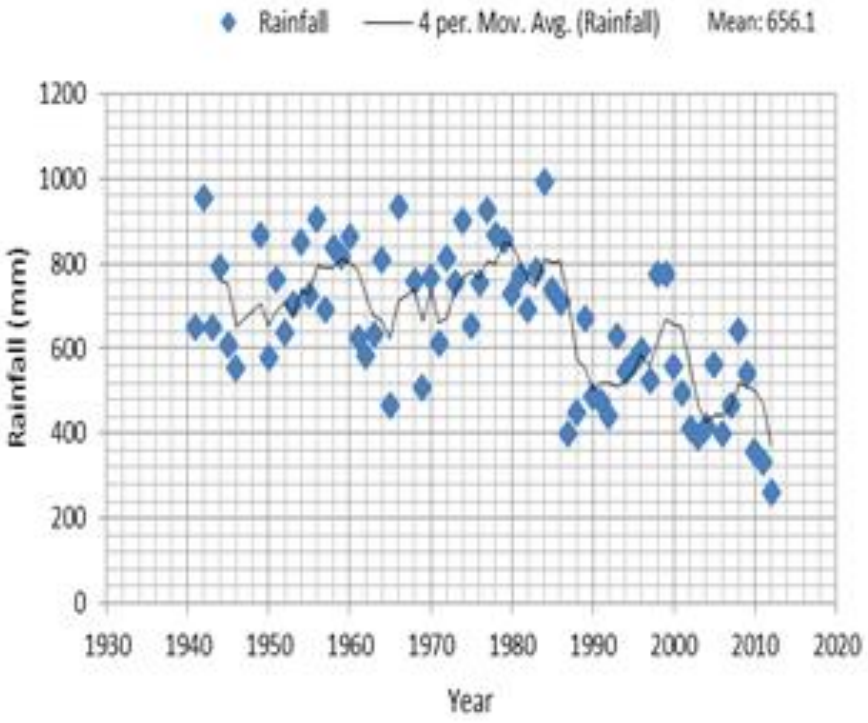

Figure 7. Annual rainfall distribution over Katsina.

the northeast part of the region towards the Sudan savannah, northwest of Nigeria. Mean annual temperature also followed a pattern similar to rainfall. Sokoto recorded the highest temperature in the region in the period under consideration. Coefficient of variation values for Katsina, Sokoto and Kano also confirm that rainfall amounts and temperatures were very erratic in these stations. This observations confirm the report of USAID (2012), that the

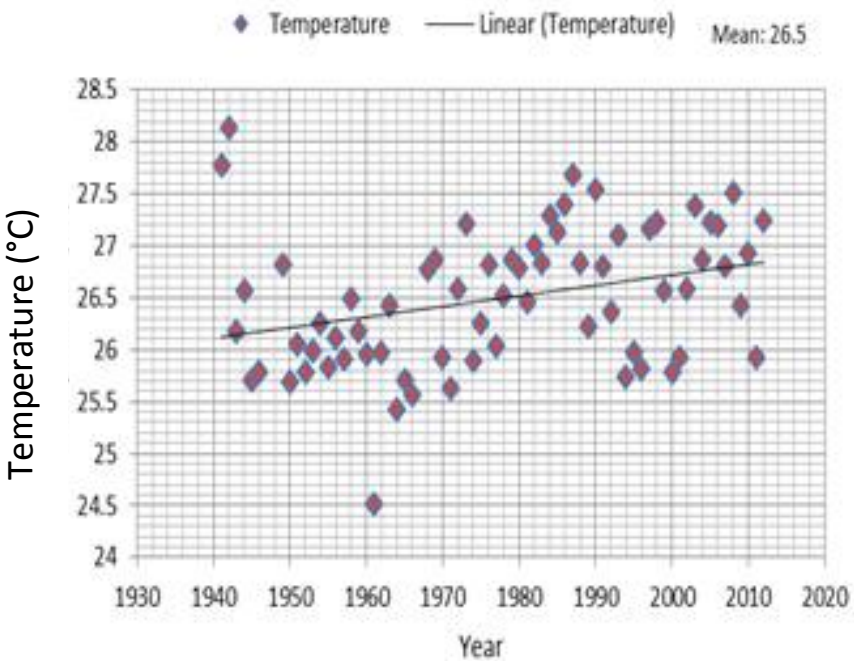

Figure 8. Annual temperature distribution over Gusau.

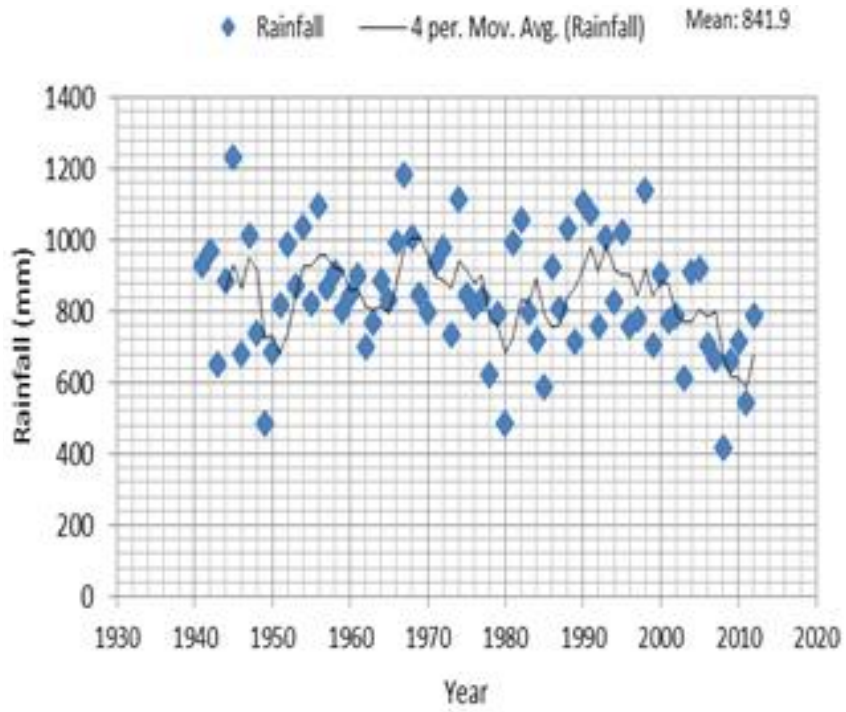

Figure 9. Annual rainfall distribution over Kano.

greatest food insecurity concerns in Nigeria remains in the extreme north, particularly in the northern most parts of Borno, Yobe and Jigawa states in the northeast, and the northern most parts of Kano, Katsina and Sokoto in the northwest. Similarly the National Action Programme to Combat Desertification in Nigeria estimates, about 50

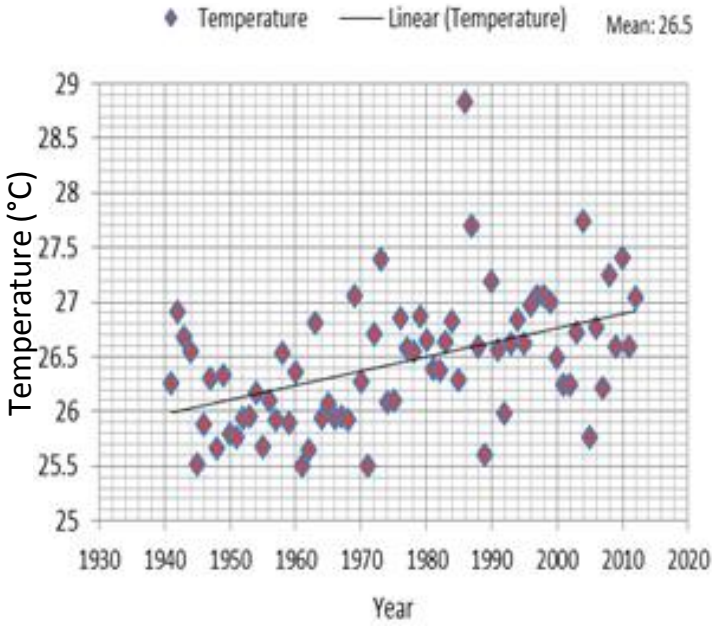

Figure 10. Annual temperature distribution over Kano.

Table 1. Long-term trend patterns of rainfall and temperature over Sudan Savannah (1943-2012).

Climatic station	Time series	Mann-Kendal	Significance level	Spearman's Rho	Significance level	Linear regression	Significance level
	Annual	z-test		z-test		t-test	
Yelwa	Rainfall (mm)	-0.269	α =0.10	-0.085	α =0.10	0.046	α =0.10
	Temp (°C)	4.113	α <0.01	3.95	α <0.01	4.422	α <0.01
Sokoto	Rainfall (mm)	-1.774	α =0.10	-1.787	α =0.10	-1.631	α =0.10
	Temp (°C)	7.148	α <0.01	6.36	α <0.01	8.982	α <0.01
Gusau	Rainfall (mm)	-0.51	α =0.10	-0.226	α =0.10	-0.256	α =0.10
	Temp (°C)	3.481	α <0.01	3.242	α <0.01	2.34	α <0.05
Katsina	Rainfall (mm)	-4.563	α <0.01	-4.463	α <0.01	-5.461	α <0.01
	Temp (°C)	3..279	α <0.01	α <0.01	3.029	2.782	α <0.01
Kano	Rainfall (mm)	-2.047	α <0.05	-1.977	α <0.05	-1.95	α =0.10
	Temp (°C)	4.244	α <0.01	4.171	α <0.01	4.339	α <0.01

α =0.10, no evidence of statistical sig trend, α <0.1, possible evidence of statistical sig trend; α<0.05, strong evidence of statistical sign trend; α<0.01, very strong evidence of statistical sig trend.

percent and 75 percent of Adamawa, Bauchi, Borno, Gombe, Jigawa, Kano, Katsina, Yobe, Sokoto, and Zamfara states are seriously affected by desertification (Olawumi, 2009).

In Tables 3a-7b, the results of climatic water distributions over the Sudan savannah are presented. It can be seen that with the exception of Kano State, potential evapotranspiration and moisture demand increased during the second climate period (1978-2012) both seasonally and annually. This pattern also corresponds with a general decrease in rainfall and actual evapotranspiration during the first the climate period. In this study, the first climatic period (1945-1979) is considered as stable period before reports of confirmation

Table 2. Descriptive statistics of annual rainfall and temperature.

Climatic station	Climatic Indices	Mean	SD	SE	Min	Max	Range	Sum	CV
Yelwa Town	Rainfall (mm)	981.5	187.4	22.6	584	1566.2	982.2	67724.9	19.09
	Temperature (°C)	27.8	0.42	0.05	26.87	28.87	1.98		1.51
Sokoto Town	Rainfall (mm)	675.3	154.7	18.6	373.2	1146.7	773.5	46596.6	22.9
	Temperature (°C)	28.5	0.78	0.09	26.46	30.1	3.6		2.74
Gusau Town	Rainfall (mm)	924.8	215.2	28.2	624	1507.1	883.1	53642.6	23.4
	Temperature (°C)	26.6	0.47	0.06	25.05	27.69	2.64		1.76
Katsina Town	Rainfall (mm)	656.1	171.1	20.5	262	993.6	731.6	45267.4	26.07
	Temperature (°C)	26.49	0.67	0.08	24.5	28.1	3.6		2.53
Kano State	Rainfall (mm)	841.9	168.7	19.8	416.1	1234.1	818	60621.2	20.0
	Temperature (°C)	26.45	0.59	0.07	25.5	28.8	3.32		2.23

Table 3a. Seasonal water distribution over Yelwa Town 1943-1977.

	Jan	Feb	March	April	May	June	July	Aug	Sept	Oct	Nov	Dec	Sum
R	0.2	1.8	3.1	22.8	97.2	139.1	192.2	242.1	225.0	66.2	0.4	0.2	990.3
PET	135	148	164	170	161	150	143	140	141	146	140	133	1771
ST	0	0	0	0	0	0	49.2	125	125	45.2	0	0	344.4
∆ST	0	0	0	0	0	0	+49.2	0	0	-79.8	-139.6	-132.8	
AET	0.2	1.8	3.1	22.8	97.2	150	143	140	141	66.2	0.4	0.2	765.9
DEF	134.8	146.2	160.9	147.2	63.8	109	0	0	0	-79.8	139.6	132.8	954.5
SUR	0	0	0	0	0	0	0	102.1	84	0	0	0	186.1

R: Rainfall; PET: potential evapotranspiration; ST: soil storage; AET: actual evapotranspiration; DEF: moisture deficit; SUR: moisture surplus.

Table 3b. Seasonal water distribution over Yelwa Town 1978-2010.

	Jan	Feb	March	April	May	June	July	Aug	Sept	Oct	Nov	Dec	Sum
R	0.0	0.0	15.9	43.1	105.6	150.0	211.8	256.1	173.7	47.6	0.3	0.1	1004.2
PET	137	150	165	171	161	151	144	143	144	149	144	137	1796
ST	0	0	0	0	0	0	67.8	125	125	23.6	0	0	341.4
∆ST	0	0	0	0	0	0	+67.8	0	0	-101.4	-143.7	-136.9	-314.2
AET	0	0	15.9	43.1	105.6	150	144	143	144	47.6	0.3	0.1	793.6
DEF	137	150	149.1	127.9	55.4	1.0	0	0	0	101.4	143.7	136.9	1002.4
SUR	0	0	0	0	0	0	0	113.1	29	0	0	0	142.1

R: Rainfall; PET: potential evapotranspiration; ST: soil storage; AET: actual evapotranspiration; DEF: moisture deficit; SUR: moisture surplus.

of increase in world temperature which began in the beginning of the industrial period and an acceleration of warming since late 70s (IPCC, 2013). This period also corresponds with the period of temperature increase in Sahel region which has been traced to the anomalous large-scale sea-surface temperature (SST) warming over the Indian Ocean, tropical Atlantic SSTA, gulf of guinea and the Mediterranean Sea. It started in 1950 and became pronounced in the 1970 and has influenced the climate of Sahel region (Rowell, 2003; Bader and Latif, 2003; Archibong et al*.,* 2007; Obodo, 2008). Thus, rates of deviation were estimated by multiplying the difference

Table 4a. Seasonal water distribution over Sokoto Town 1943-1977.

	Jan	Feb	March	April	May	June	July	Aug	Sept	Oct	Nov	Dec	Sum
R	0.1	0.0	0.9	11.0	46.5	95.6	167.4	240.1	137.1	16.5	0.0	0.0	715.2
PET	131	144	166	175	174	161	150	143	148	154	145	133	1824
ST	0	0	0	0	0	0	17.4	114.5	125	0	0	0	256.9
∆ST	0	0	0	0	0	0	+17.4	+97.1	0	-137.5	-145	-133	
AET	0.1	0	0.9	11.0	46.5	95.6	150	143	148	16.5	0	0	611.6
DEF	130.9	144	165.1	164	127.5	65.4	0	0	0	137.5	145	133	1212.4
SUR	0	0	0	0	0	0	0	0	11.1	0	0	0	11.1

R: Rainfall; PET: potential evapotranspiration; ST: soil storage; AET: actual evapotranspiration; DEF: moisture deficit; SUR: moisture surplus

Table 4b. Seasonal Water Distribution over Sokoto Town 1978-2012.

	Jan	Feb	March	April	May	June	July	Aug	Sept	Oct	Nov	Dec	Sum
R	0.0	0.1	2.9	6.3	51.3	95.9	181.4	195.6	100.1	13.6	0.3	0.0	647.5
PET	138	151	169	181	178	166	154	150	154	161	152	138	1892
ST	0	0	0	0	0	0	27.4	72.4	78.5	0	0	0	178.3
∆ST	0	0	0	0	0	0	+27.4	+45	+6.1	-147.4	-151.7	-138	
AET	0	0.1	2.9	6.3	51.3	95.9	154	150	154	13.6	0.3	0	628.4
DEF	138	150.9	166.1	174.7	126.7	70.1	0	0	0	147.1	151.7	138	1263.3
SUR	0	0	0	0	0	0	0	0	0	0	0	0	0

R: Rainfall; PET: potential evapotranspiration; ST: soil storage; AET: actual evapotranspiration; DEF: moisture deficit; SUR: moisture surplus.

Table 5a. Seasonal Water Distribution over Gusau Town 1943-1977.

	Jan	Feb	March	April	May	June	July	Aug	Sept	Oct	Nov	Dec	Sum
R	0.2	0.5	4.0	22.6	71.8	139.6	202.3	279.1	179.6	29.5	0.6	0.8	930.6
PET	131	141	157	166	163	153	146	142	145	146	136	131	1757
ST	0	0	0	0	0	0	56.3	125	125	8.5	0	0	314.8
∆ST	0	0	0	0	0	0	+56.3	0	0	-116.5	-135.4	-130.2	-325.8
AET	0.2	0.5	4.0	22.6	71.8	139.6	146	142	145	29.5	0.6	0.8	702.6
DEF	130.2	140.5	153	143.4	91.2	13.4	0	0	0	116.5	135.4	130.2	1053.8
SUR	0	0	0	0	0	0	0	137.1	34.6	0	0	0	171.7

R: Rainfall; PET: potential evapotranspiration; ST: soil storage; AET: actual evapotranspiration; DEF: moisture deficit; SUR: moisture surplus.

Table 5b. Seasonal Water Distribution over Gusau Town 1978-2012.

	Jan	Feb	March	April	May	June	July	Aug	Sept	Oct	Nov	Dec	Sum
R	0.0	0.6	3.6	17.6	83.8	135.0	205.4	287.6	187.6	29.0	0.3	0.0	950.5
PET	132	146	163	174	171	157	147	143	147	150	141	133	1804
ST	0	0	0	0	0	0	58.4	125	125	4.0	0	0	312.4
∆ST	0	0	0	0	0	0	+58.4	0	0	-121	-140.7	-133	-336.3
AET	0	0.6	3.6	17.6	83.8	135	147	143	147	29	0.3	0	706.9
DEF	132	145.4	159.4	156.4	87.2	22	0	0	0	121	140.7	133	1097.1
SUR	0	0	0	0	0	0	0	144.6	40.6	0	0	0	185.2

R: Rainfall; PET: potential evapotranspiration; ST: soil storage; AET: actual evapotranspiration; DEF: moisture deficit; SUR: moisture surplus.

Table 6a. Seasonal Water Distribution over Katsina Town 1943-1977.

	Jan	Feb	March	April	May	June	July	Aug	Sept	Oct	Nov	Dec	Sum
R	0.1	0.0	0.1	7.2	51.5	85.3	182.2	268.9	123.1	9.7	0.3	0.0	728.4
PET	123	135	156	172	173	164	150	143	149	153	138	124	1780
ST	0	0	0	0	0	0	32.2	125	99.1	0	0	0	256.3
∆ST	0	0	0	0	0	0	+32.2	0	-25.9	-143.3	-137.7	-124	
AET	0.1	0	0.1	7.2	51.5	85.3	150	143	149	9.7	0.3	0	596.2
DEF	122.9	135	155.9	164.8	121.5	78.7	0	0	0	143.3	137.7	124	1183.8
SUR	0	0	0	0	0	0	0	125.9	0	0	0	0	125.9

R: Rainfall; PET: potential evapotranspiration; ST: soil storage; AET: actual evapotranspiration; DEF: moisture deficit; SUR: moisture surplus.

Table 6b. Seasonal Water Distribution over Katsina Town 1978-2012.

	Jan	Feb	March	April	May	June	July	Aug	Sept	Oct	Nov	Dec	Sum
R	0.0	0.0	1.1	20.4	34.5	74.1	154.2	161.8	90.8	14.2	0.0	0.0	551.1
PET	124	136	160	175	176	166	153	149	155	156	140	125	1815
ST	0	0	0	0	0	0	1.2	14	0	0	0	0	15.2
∆ST	0	0	0	0	0	0	+1.2	+12.8	-64.2	-141.8	-140	125	-207
AET	0	0	1.1	20.4	34.5	74.1	154	149	90.8	14.2	0	0	538.1
DEF	124	136	158.9	154.6	141.5	91.9	0	0	64.2	141.8	140	125	1277.9
SUR	0	0	0	0	0	0	0	0	0	0	0	0	0

R: Rainfall; PET: potential evapotranspiration; ST: soil storage; AET: actual evapotranspiration; DEF: moisture deficit; SUR: moisture surplus.

Table 7a. Seasonal Water Distribution over Kano Town 1943-1977.

	Jan	Feb	March	April	May	June	July	Aug	Sept	Oct	Nov	Dec	Sum
R	0.0	0.2	1.7	8.8	69.0	116.9	207.1	313.7	139.2	13.0	0.1	0.0	869.7
PET	125	138	158	173	173	167	158	159	162	167	156	145	1881
ST	0	0	0	0	0	0	49.1	125	102.2	0	0	0	276.3
∆ST	0	0	0	0	0	0	+49.1	0	-22.8	-154	-155.9	-145	-428.6
AET	0	137.8	156.3	8.8	69	116.9	158	159	139.2	13.0	0.1	0	958.1
DEF	125	137.8	156.3	164.2	104	50.1	0	0	22.8	154	155.9	145	1215.1
SUR	0	0	0	0	0	0	0	154.7	0	0	0	0	154.7

R: Rainfall; PET: potential evapotranspiration; ST: soil storage; AET: actual evapotranspiration; DEF: moisture deficit; SUR: moisture surplus.

in the indices of annual climatic value between the first and second climatic periods, and then dividing the result with annual value of the first climatic period which is considered as stable period. The percentage of deviation in this study is used to denote the extent to which distributions in the second climatic period differed from events in the first climatic period.

General patterns of deviation in PET from the first climate period were 1.4, 3.7, 2.7, 1.9% for Yelwa, Sokoto, Gusau and Katsina respectively. Deviations in climatic moisture demand (soil moisture deficit) in the second climatic period were 5.0, 4.2, 4.1 and 7.9% for Yelwa, Sokoto, Gusau and Katsina respectively. Moisture storage also decreased in the second climatic period with deviation rates of 0.87, 30.6, 0.76 and 94.1% for Yelwa, Sokoto, Gusau and Katsina respectively. Rainfall was also seen to have decreased in Sokoto and Katsina during the second climatic period with deviation rates of 9.5% (Sokoto) and 24.3% (Katsina).

In Table 8a-d, the difference and rates of deviations in climatic indices are presented. These general observations may suggest that water balance parameters during the second climatic period deviated from patterns observed in the first climatic period (1943-1977). This pattern is further buttressed in Table 9 as moisture index generally showed evidence of decreasing pattern during

Table 7b. Seasonal Water Distribution over Kano Town 1978-2012.

	Jan	Feb	March	April	May	June	July	Aug	Sept	Oct	Nov	Dec	Sum
R	0.0	0.3	0.7	20.0	64.4	136.0	240.6	297.6	138.9	13.9	0.0	0.0	912.4
PET	125	138	160	174	172	161	150	150	150	154	142	126	1802
ST	0	0	0	0	0	0	90.6	125	113.9	0	0	0	329.5
ΔST	0	0	0	0	0	0	+90.6	0	-11.1	-140.1	-142	-126	-328.6
AET	0	0.3	0.7	20	64.4	136	150	150	138.9	13.9	0	0	674.2
DEF	125	137.7	159.3	154	107.6	25	0	0	11.1	140.1	142	126	1127.8
SUR	0	0	0	0	0	0	0	147.6	0	0	0	0	147.6

R: Rainfall; PET: potential evapotranspiration; ST: soil storage; AET: actual evapotranspiration; DEF: moisture deficit; SUR: moisture surplus.

Table 8a: Differences and rate of deviation in Rainfall in the second climatic period.

Climatic station	Climatic parameter (mm)	Climatic period	Annual total (mm)	Difference (mm)	% of deviation
Yelwa	Rainfall (mm)	1st climatic period (1943-1977) 2nd climatic period (1978-2012)	990 1004.2	No indication of decrease in the second period	-
Sokoto		1st climatic period (1943-1977) 2nd climatic period (1978-2012)	715.2 647.5	67.9	9.46
Gasau		1st climatic period (1943-1977) 2nd climatic period (1978-2012)	930.6 950.5	No indication of decrease in the second period	-
Katsina		1st climatic period (1943-1977) 2nd climatic period (1978-2012)	728.4 551.1	177.3	24.3
Kano		1st climatic period (1943-1977) 2nd climatic period (1978-2012)	869.7 912.4	No indication of decrease in the second period	-

Table 8b. Differences and rate of deviation in PET in the second climatic period.

Climatic station	Climatic parameter (mm)	Climatic period	Annual total (mm)	Difference (mm)	% of deviation
Yelwa	Potential Evapotranspiration (mm)	1st climatic period (1943-1977) 2nd climatic period (1978-2012)	1771 1796	-25	1.4
Sokoto		1st climatic period (1943-1977) 2nd climatic period (1978-2012)	1824 1892	-68	3.7
Gasau		1st climatic period (1943-1977) 2nd climatic period (1978-2012)	1757 1804	-47	2.6
Katsina		1st climatic period (1943-1977) 2nd climatic period (1978-2012)	1780 1815	-35	1.96
Kano		1st climatic period (1943-1977) 2nd climatic period (1978-2012)	1881 1802	No indication of decrease in the second period	-

Table 8c: Differences and rate of deviation in Soil moisture deficit in the second climatic period

Climatic station	Climatic parameter (mm)	Climatic period	Annual total (mm)	Difference (mm)	% of deviation
Yelwa	Soil moisture deficit (mm)	1st climatic period (1943-1977) 2nd climatic period (1978-2012)	954.5 1002.4	-47.9	5.0
Sokoto		1st climatic period (1943-1977) 2nd climatic period (1978-2012)	1212.4 1263.3	-50.9	4.2
Gasau		1st climatic period (1943-1977) 2nd climatic period (1978-2012)	1053.8 1097.1	-43.3	4.1
Katsina		1st climatic period (1943-1977) 2nd climatic period (1978-2012)	1183.8 1277.9	-94.1	7.9
Kano		1st climatic period (1943-1977) 2nd climatic period (1978-2012)	1215.1 1127.8	No indication of decrease in the second period	-

Table 8d. Differences and rate of deviation in moisture storage in the second climatic period.

Climatic station	Climatic parameter (mm)	Climatic period	Annual total (mm)	Difference (mm)	% of deviation
Yelwa	Soil moisture storage (mm)	1st climatic period (1943-1977) 2nd climatic period (1978-2012)	344.4 341.4	3.0	0.87
Sokoto		1st climatic period (1943-1977) 2nd climatic period (1978-2012)	256.9 178.3	78.6	30.6
Gasau		1st climatic period (1943-1977) 2nd climatic period (1978-2012)	314.8 312.4	2.4	0.76
Katsina		1st climatic period (1943-1977) 2nd climatic period (1978-2012)	312.4 256.3	241.1	94.1
Kano		1st climatic period (1943-1977) 2nd climatic period (1978-2012)	15.2 276.3	No indication of decrease in the second period	-

the second climatic period.

These general patterns of increasing and/or decreasing water balance components are similar to observed statistically significant increases in precipitation and air temperature in the vast majority of the country (Egbinola and Amobichukwu, 2013; Akinsanola and Ogunjobi, 2014; Yaya et al., 2015). The observed evidence of increase in annual time series of temperature, potential evapotranspiration, moisture deficit and declining rainfall pattern in the second climatic period for all the synoptic stations are evidence of changing climate and this conforms with findings from other researchers that since the last century, an increase in average global temperature has been observed, and it is expected to increase further in the future (IPCC, 2001, 2007; Brunetti et al., 2009; Stocker et al., 2013). The intensity and frequency of precipitation are also expected to change, despite the trend differing with the season and the region (Gobiet et al., 2014). This will alter river-flow conditions, and in turn hydropower, which has been investigated from single catchments to a global scale (Schaefli et al., 2007; Koch et al., 2011; Majone et al., 2016). Declining

Table 9. Moisture Index over Sudan Savannah Region of Nigeria.

Climatic Year	Yelwa station			Sokoto Station			Gusau Station			Katsina station			Kano Station		
	Ia	Ih	Im	Ia	Ih	Im	Ia	Ih	Im	Ia	Ih	Im	Ia	Ih	Im
1943-1977	53.9	10.5	-22	67	0.60	-39	59.9	9.8	-26	65.5	7.1	-33	68	8.2	-31
1978-2012	55.8	7.9	-26	66.8	0.05	-40	60.8	10.3	-26	70.4	0.06	-42	63	8.2	-29

Ia : Index of aridity; Ih: Index of humidity; Im : Moisture Index.

rainfall amount is an important limiting factor for rain-fed crop production which is widely practiced in the study area. The observed decreasing rainfall amount in the extreme northern parts of the basin will exercerbate the ongoing impacts of variability, with serious implications for sustainable socio-economic lives, including decline in agricultural yeilds and farmer-herdmen crises which is already evident in the region. Studies have also linked pests attack and development of crop diseases, witting and desiccation of crops to reducing annual rainfall amount (Thompson and Amos, 2010; Obi, 2010; Aondoakaa, 2012; Singh et al., 2014). For example, Obi (2010) reported evidence of reducing pesticide sensitivity due to decreasing precipitation. His study added that pest population may increase across the northern Nigeria and threaten food production. In a simalr study, NEMA (2010) reported the outbreak of pests and diseases due to meteorological drought condition in part of Borno State, in northern Nigeria.

Evidence of rising temperature has the tendency to trigger hydo-meteorological droughts. As temperature rises, crops will loses water rapidly through transpiration thereby increasing crop water need. High potential evapotranspiration (PET) is usually observed during high temperature conditon (Audu et al., 2013). Thus, higher value of PET, means increased moisture loss, leading to deficit water balance which is unfavourable to crops. Crops growing under low soil moisture, yield little and poor quality seeds. As reported by Obi (2010), while increase in temperature is expected to elongate the growing season in temperate region, such an increase in the tropics will result in decimated agricultural output due to aggravating soil evaporation rate and invariably drought. Increasing temperature weakens plants and their leaves wither easily hence there is poor photosynthesis (Audu et al., 2013). Kim (2009) established that rising temperure will result in reduced crop quantity and quality due to the reduced growth period following high levels of temperature rise; reduced sugar content, bad coloration, and reduced storage stability in fruits; increase of weeds, blights, and harmful insects in agricultural crops; reduced land fertility due to the accelerated decomposition of organic substances. Apart from crops, animals also die in large number during prolonged drought as a result of heat stress, dehydration and attack by drought induced diseases.

CONCLUSION AND RECOMMENDATIONS

The study revealed that rainfall amount decreased from a very high value in the extreme northwest of the Sudan Savannah to a very low value in Katsina. The continuous decrease in rainfall amount in 1940s, 1950 and between 1970 and 1990 could be as a result of reversible climatic fluctuation and not climate change. This is because the 70 years of rainfall data for stations like Yelwa, Sokoto and Gusau revealed little or no evidences of statistically significant downward trends in annual rainfall distribution, but rather repeated drought periods caused by large scale shifts in the general global circulation. Repetition of drought within the present climate regime could be expected and should be planned for. Katsina and Kano however showed strong evidence of trend in rainfall distribution. For temperature, there is strong evidence of increasing trends for all the stations in the region which agrees with the global trend. The deviation in seasonal distribution of water balance components, in general may suggest a proof of changing climatic pattern towards the beginning of the 1980s, a period that coincide with intensified global and regional large-scale sea-surface temperature anomaly (SSTA) which is also reported to have affected the Sahelian climate. The region is gradually been encroached by desert from the extreme northeast. This has implications for socio-economic development of the study area especially coupled with the attendant consequences of increasing population and economic activities in the region. There is thus need to plan for and design sustainable water resources management techniques in different sectors-agriculture, irrigation and dams, water supply to adapt to the quasi-periodic patterns of rainfall fluctuation.

CONFLICT OF INTERESTS

The authors have not declared any conflict of interests.

REFERENCES

Archibong OE, Edaefinene LE, Ediang AA (2007). The teleconnection between sea surface temperature analysis from *in situ data at East Mole*, Lagos and global warming Poster S1.1-4948. 09:15 (S1.1-4947) Plenary.

Akinsanola AA, Ogunjobi KO (2014). Analysis of Rainfall and Temperature Variability over Nigeria. Global Journal of Human-Social Science 14(3):1-18.
Agabi JA (1995). Introduction to the Nigeria Environment.' In Nigerian Environment. National Conservation Foundation. Lagos. Macmillan Nigeria Publishers Limited.
Amissah-Arthur A, Jagtap SS (1999). Geographic variation in growing season rainfall during three decades in Nigeria using principal component and cluster analyses. Theatrical. Applied. Climatology. 63:107-116.
Aondoakaa SC (2012). Effects of Climate Change on Agricultural Productivity in the Federal Capital Territory (FCT), Abuja, Nigeria Ethiopian Journal of Environmental Studies and Management. 5(4):559-566.
Audu EB, Audu HO, Binbol NL, Gana JN (2013). Climate Change and Its Implication on Agriculture in Nigeria. Abuja Journal of Geography and Development 3(2):8-19.
Anyadike RNC (1987). The Linacre evaporation formula tested and compared to others in various climates over West-Africa. Agricultural and Forest Meteorology 39:111-119.
Avis CA, Weaver AJ, Meissner KJ (2011). Reduction in areal extent of high-latitude wetlands in response to permafrost thaw. Nature Geoscience 4:444-448.
Ayoade JO (1983). Introduction to Climatology for the Tropics. Spectrum Books Ltd, Ibadan.
Bader J, Latif M (2003). The impact of decadal-scale Indian Ocean sea surface temperature anomalies on Sahelian rainfall and the North Atlantic Oscillation Geophysical Research Letters 30(22):2169.
Brunetti M, Lentini G, Maugeri M, Nanni, T, Auer I, Böhm R, Schöner W (2009). Climate variability and change in the greater alpine region over the last two centuries based on multi-variable analysis. International Journal of Climatology 29:2197-2225.
Camberlin P, Diop M (2003). Application of daily rainfall principal component analysis to the assessment of the rainy season Characteristics in Senagal. Climate Research 23:159-169.
Dai A, Lamb P, Trenberth KE., Hulme M, Jones PD, Xie P.(2004). The recent Sahel drought is real. International Journal of Climatology 24:1323-1331.
Egbinola CN, Amobichukwu AC (2013). Climate Variation Assessment Based on Rainfall and Temperature in Ibadan, South-Western, Nigeria. Journal of Environment and Earth Science 3(11): 33-45.
Ekpoh IJ, Nsa E (2011). Extreme Climatic Variability in North-western Nigeria: An Analysis of Rainfall Trends and Patterns Journal of Geography and Geology 3:1.
Gobiet A, Kotlarski S, Beniston M, Heinrich G, Rajczak J, Stoffel M (2014). 21st century climate change in the European Alps—A review. Science of Total Environment 493:1138-1151.
Hamon WR (1961). Estimating potential evapotranspiration: Journal of the Hydraulics 87:107-120.
Ikhatua UJ (2010). Effect of climate change on global and national food security, Paper presented at the 34th Day Celebration of the Nigerian Institute of Food Science and Technology, held at the University of Benin, Benin City, Edo State, Nigeria, Held 5th June, 2010.
Intergovernmental Panel on Climate Change (IPCC) (2001). Climate Change 2001: Impacts, Vulnerability and Adaptation. Contribution of Working Group III to the Third Assessment Report on the Intergovernmental Panel on Climate Change. Cambridge University Press, Cambridge.
IPCC (2007). Climate Change (2007). The Scientific Basis, Summary for Policymakers – Contribution of Working Group I to the IPCC Fourth Assessment Report 2007.
IPCC (2013). The physical science basis. Contribution of working group I to the fifth assessment report of the Intergovernmental Panel on Climate Change; Cambridge University Press: Cambridge, UK and New York, USA 1535 p.
Jutla AS, Akanda AS, Griffiths JK, Colwell R, Islam S (2011). Warming oceans, phytoplankton, and river discharge: implications for cholera outbreaks. The American Journal of Tropical Medicine and Hygiene 85(2):303-308.
Kalu AE (1987): The recurrence of severe droughts in northern Nigeria. Proceedings of the 1985 Commonwealth Meteorologists Conference. Meteorological Office College, Reading.
Kamara SI (1986). The origin and types of rainfall in West Africa. Weather 41:48-56
Kim C (2009). Strategies for Implementing Green Growth in Agricultural Sector." in Proceedings in Green Korea 2009 - Green Growth and Cooperation. National Research Council for Economics, Humanities and Social Science.
Koch F, Prasch M, Bach H, Mauser W, Appel F, Weber M (2011). How will hydroelectric power generation develop under climate change scenarios? A case study in the upper Danube basin. Energies. 4: 1508-1541.
Koutroulis AG, Vrochidou AEK, Tsanis IK (2011). Spatiotemporal characteristics of meteorological drought for the island of Crete. Journal of Hydrometeorology 12:206-226.
Kwak JW, Lee SD, Kim YS, Kim, HS (2013). Return period estimation of droughts using drought variables from standardized precipitation index. Journal of Korean Water Resources. Association .46: 795-805.
Lau N, Nath MJ (2012). 'A model study of heat waves over north America: Meteorological aspects and projections for the twenty-first century', Journal of Climate 25(14):4761-4784.
Lockwood JG (1979). Causes of Climate. New York: Halsted Press, John Wiley and Sons
Lyon B (2009). 'Southern Africa Summer drought and heat waves: Observations and coupled model behaviour', Journal of Climate 22(22):6033-6048.
Majone B, Villa F, Deidda R, Bellin A (2016). Impact of climate change and water use policies on hydropower potential in the south-eastern Alpine region. Science of Total Environment 543:965-980.
National Emergency Management Agency (NEMA) (2010). Post Disaster Assessment for Nigeria.
Nicholson SE (1993). An Overview of African rainfall fluctuations of the last decade'. Monthly Weather Review 111:1646-1654.
Nicholson SE, Tucker, CJ (1998). Desertification, drought, and surface vegetation: an example from the West African Sahel. Bulletin of the American Meteorological Society, 79(5):815-829.
Obi CO (2010). Climate Change and Management of Degraded Soils for Sustainable Crop of Production. Tropical Built Environment Journal Vol. 1.
Obodo AO. (2008). Chronology of ENSO events and Teleconnection to Nigerian Weather (1978-2005), weather Bulletin.
Oguntoyinbo JS, Areola OO, Filani M (1983). A Geography of Nigerian Development. Heinemann Educational Books (Nig.) Ltd.
Olawumi A (2009). Environmental Considerations in Nigerian Agricultural Policies, Strategies, and Programs Nigeria Strategy Support Program (NSSP) Federal Ministry of Environment, Nigeria Report No. NSSP 004.
Penman HL (1948). Natural evaporation from open water, bare soil and grass. Proceedings of Royal Society A 193:120-45.
Reyburn R, Kim DR, Emch M, Khatib A, von Seidlein L, Ali M (2011). Climate variability and the outbreaks of cholera in Zanzibar, East Africa: a time series analysis. American Journal of Tropical Medical Hygiene 84(6):862-869.
Romero-Lankao P, Smith JB, Davidson DJ, Diffenbaugh NS, Kinney PL, Kirshen P, Kovacs P, Villers LR (2014). North America. In: Climate Change (2014): Impacts, Adaptation, and Vulnerability. Part B: Regional Aspects. Contribution of Working Group II to the Fifth Assessment Report of the Intergovernmental Panel on Climate Change [Barros VR, Field CB, Dokken DJ, Mastrandrea MD, Mach KJ, Bilir TE, Chatterjee M, Ebi KL, Estrada YO, Genova RC, Girma B, Kissel ES, Levy AN, MacCracken S, Mastrandrea PR, White LL (eds.)]. Cambridge University Press, Cambridge, United Kingdom and New York, NY, USA pp. 1439-1498.
Rowell DP (2003). The impact of Mediterranean SSTs on the Sahelian rainfall season, Journal of Climate 16:849-862.
Schaefli B, Hingray B, Musy A (2007). Climate change and hydropower production in the Swiss Alps: Quantification of potential impacts and related modelling uncertainties. Hydrology of Earth System Science 11:1191-1205.
Singh SK, Singh KM. Singh RK Kumar P, Kumar U (2014). Impact of Rainfall on Agricultural Production in Bihar: A Zone-Wise Analysis. Environment and Ecology 32(4A):1571-1576.
Stocker TF, Qin D, Plattner GK, Tignor M, Allen SK, Boschung J, Nauels A, Xia Y, Bex V, Midgley PM (2013). The Physical Science

Basis; IPCC: Cambridge, UK; New York, NY, USA.
Thompson OA, Amos TT (2010). Climate Change and Food Security in Nigeria. In Journal of Meteorology and Climate Science 8(2): 92-95.
Thornthwaite CW (1953). The Water Balance of Arid and Semi-Arid climates, in Desert Research. Proceedings, International symposium held in Jerusalem pp. 112-120.
UNGC (2009). Climate Change and the Global Water Crisis: What Businesses Need to Know and Do? Pacific Institute. http://www2.pacinst.org/publication/climate-change-and-the-global-water-crisis-what-businesses-need-to-know-and-do/
USAID (2012). Famine Early warning systems Network: Nigerian security outlook, www.fews.net/west-africa/Nigeria
Van Asselen S, Verburg PH (2013). Land cover change or landuse intensification: simulating land system change with a globalscale land change model, Global. Change Biology 19:3648-3667.
Vicente-Serrano SM Beguería S, López-Moreno JI (2010). A multiscalar drought index sensitive to global warming: The standardized precipitation evapotranspiration index. Journal of Climate 23:1696-1718.
Westerling AL, Swetnam TW (2003). Interannual to decadal drought and wildfire in the Western United States. EOS 84:545-560.
Whitman E, Batllori E, Parisien MA, Miller C, Coop JD, Krawchuk MA, Chong GW, Haire SL (2015). The climate space of fire regimes in north-western North America. Journal of Biogeography 42(653):1736-1749.
Yaya OS, Gil-Alana LA, Akomolafe AA (2015). Long Memory, Seasonality and Time Trends in the Average Monthly Rainfall in Major Cities of Nigeria. CBN Journal of Applied Statistics 6(2):39-58.

Vol. 13(12), pp. 481-509, December 2019
DOI: 10.5897/AJEST2019.2757
Article Number: DC24E0062334
ISSN: 1996-0786

http://www.academicjournals.org/AJEST

African Journal of Environmental Science and Technology

Full Length Research Paper

Future evolution of surface temperature extremes and the potential impacts on the human health in Senegal

Sarr A. B., Diba I., Basse J., Sabaly H. N. and Camara M.*

Laboratoire d'Océanographie, des Sciences de l'Environnement et du Climat (LOSEC), UFR Sciences et Technologies, Université Assane SECK de Ziguinchor, Sénégal.

Received 19 September, 2019; Accepted 4 November, 2019

Climate change impacts negatively vulnerable regions such as West African countries like Senegal, through an increase of climate extremes. The objectives of this study is to analyze the future evolution of the extreme temperature events and their impacts on human health in Senegal during the cold (DJF), hot (MAM) and wet seasons (JAS) under the greenhouse gas scenarios RCP4.5 and RCP8.5 using Climate projections of five (5) regional climate models (RCMs) of the Coordinated Regional Climate Downscaling Experiment (CORDEX) program. The results show that the biases of the RCMs are globally low especially their ensemble mean of the RCMs. This ensemble mean was afterwards considered in the analysis of the climate extremes in the near (2021-2050) and far future (2071-2100). When considering the near future, the frequency of the hot nights (Tn90p) increases under the scenario RCP8.5 (up to 90%) during the rainy season in the south of the country. As for the percentage of the hot days (Tx90p), it may reach approximately 70% under the scenario RCP8.5 in DJF over the majority of the country. Moreover, a strong increase of Tn90p and Tx90p is also diagnosed during the far future with values exceeding 80% over most parts of the country. Concerning the evolution of the heat wave magnitude index-daily, the ensemble mean of all models shows that the heat waves are more severe in MAM and JAS under both scenarios during the near and the far future over most parts of the country. To estimate the potential impacts of this heat stress on the human health, the heat index and the humidex are used. The analysis of the heat index shows that the sanitary risks are more perceptible over the whole country during the rainy season with values reaching the symptom band II for both scenarios during the far future. As for the humidex, it is characterized by a gradual increase from the historical period to the far future. This analysis highlights the fact that appropriate adaptation measures should be considered to tackle efficiently the increase of temperature extremes which may impact negatively the human health.

Key words: Regional climate models, CORDEX, climate indices, heat stress, climate scenarios, Senegal.

INTRODUCTION

The knowledge of extreme events of temperatures is of a key importance for several economic sectors,

*Corresponding author. E-mail: moctar.camara@univ-zig.sn or moctar1sn@yahoo.fr.

particularly for agriculture. Indeed, these extreme events can impact strongly the West African populations. Agriculture, which is the main source of income for the populations of this region, and particularly those of Senegal, is the most sensitive sector to these extreme changes in temperature. Indeed, very large increases in temperature can inhibit the growth of certain plants (Salack et al., 2015; Basak et al., 2013). Thus, yields of some crops such as wheat, rice, maize or groundnuts can be greatly reduced by extremely high temperatures at the key stage of their development. These temperature increases can also have negative impacts on human health as some studies have shown (Campbell et al., 2018; Hass et al., 2016; Garland et al., 2015). According to Kotir (2011), the African continent is generally considered as warm and dry continent with current trends showing warmer heat waves than those that prevailed 100 years ago. The mean temperatures observed show an increase in global warming since 1960 (IPCC, 2013).

Recent studies led by Moron et al. (2016), Ly et al. (2013) and New et al. (2006) showed an increase in heat waves and a decrease in cold days over West Africa. In addition, the minimum temperature increases more rapidly than the maximum temperature, thus involving a reduction of the diurnal variation in temperature. The predictions of models based on greenhouse gas emissions scenarios showed that the global warming continues to increase (Ceccherini et al., 2017; Sylla et al., 2016; Giorgi et al., 2014; Boko et al., 2007). However, these temperature changes are not uniform. Indeed, the climate change scenarios used in West Africa showed that the greatest temperature rises are recorded in semi-arid areas such as the Sahara and the Sahel and the lowest in the lower latitudes, especially in the Guinean zone (Hulme et al., 2001). At the beginning, these climate change scenarios were done with global climate models (IPCC, 2013). However, these global climate models (GCMs) face enormous difficulties in representing the climate at the regional scale because of their low spatial resolution (200 to 300 km). Certainly, these GCMs do not take into account certain surface processes such as topography or heterogeneities of the Earth's surface. To remedy it, regional climate models (RCMs) are increasingly being used to dynamically disaggregate GCMs (Giorgi et al., 2014; Laprise et al., 2013; Camara et al., 2013).

In this paper, we analyze the future evolution of temperature extremes and perceived heat indices (humidex and heat index) in Senegal using regional climate models of the Coordinated Regional Climate Downscaling EXperiment (CORDEX programme) during the future under the scenarios RCP4.5 and RCP8.5. This program is described in detail by Giorgi et al. (2009). The CORDEX is an international program led by a number of research centers to provide the scientific community with reliable climate change scenarios for impact assessment and research adaptation. Two types of simulations are considered: those concerning the present time and the climate projections. The first category of simulations (present time) consists of evaluating the performance of RCMs to reproduce the present climate (1989-2008). Studies led in this context (Gbobaniyi et al., 2014;, Kim et al., 2014; Nikulin et al., 2012; Camara et al., 2013) have shown that these CORDEX RCMs represent well enough the spatial distribution of rainfall and temperature and also the ensemble mean of the models outperforms the regional climate models taken individually.

The second series of simulations (climate projections, period 2006-2100) aims to analyze the future evolution of the climate. In this context, several studies have been carried out (Sarr and Camara, 2017; Diallo et al., 2016; Sylla et al., 2016; Mariotti et al., 2014; Giorgi et al., 2014; Laprise et al., 2013) to identify the future evolution of the precipitation and the mean surface temperature. However, few research works have been devoted in studying the future evolution of extreme temperature events and its impact on human health in West Africa and particularly in Senegal. Then, the main purpose of this study is to analyze the seasonal evolution of temperature extremes and their impacts on human health in Senegal by focusing on greenhouse gas concentration scenarios RCP85 and RCP4.5.

DATA AND METHODS

Description of the study area

Senegal is an African country located in the westernmost part of the continent (Figure 1). It extends in longitude between 12° W and 17° W and in latitude between 12° N and 16.5°N in the so-called Sudano-Sahelian region. This latter is considered by the Intergovernmental Panel on Climate Change (IPCC) experts as an area vulnerable to climate change due to its low capacity adaptation (Boko et al., 2007; IPCC, 2013). The climate in Senegal is characterized by a single rainy season (roughly from June to October) followed by a longer dry season (November to May). During the rainy season, rainfall decreases from South to North; this translates into a semi-arid type climate in the North and a tropical one in the South (Sagna, 2000).

Climate change scenarios and climate indices

A study based on daily temperature data is done using high resolution simulations (0.44°) of five (5) regional climate models (RCMs) of the CORDEX program. These models are: CCLM4, RCA4, HIRHAM5, RACMO22T and REMO. The institutions of these models and their references are presented in Table 1. The RCMs outputs are available from this website: https://www.cordex.org/output.html. These models are described in details by Nikulin et al. (2012). The RCMs RACMO22T, HIRHAM5 and REMO are forced by the outputs of the GCM EC-EARTH; while models RCA4 and CCLM4 are forced by the outputs of the GCM CNRM-CM5. The climate projections were obtained by forcing these RCMs through the outputs of these GCMs under the greenhouse gas scenarios RCP4.5 (medium scenario) and RCP8.5

Figure 1. Map of Africa. The study area (Senegal) is in red color.

Table 1. Description of the regional climate models.

Name	GCM forcing	Institution	References
CCLM4	CNRM-CM5	CLM-community	Baldauf et al. (2011)
RACMO22T	EC-EARTH	KNMI, The Netherlands	Van Meijgaard et al. (2008)
RCA4	CNRM-CM5	SMHI, Sweden	Samuelsson et al. (2011)
HIRHAM5	EC-EARTH	DMI, Denmark	Christensen et al. (2006)
REMO	EC-EARTH	MPI, Germany	Jacob et al. (2007)

Table 2. Description of the climate indices

Indices	Descriptive name	Definition	Unit
Tn90p	Frequency of warm nights	Percentage of nights with daily minimum temperatures Tn > 90th percentile of the reference period (1976-2005)	%
Tx90p	Frequency of warm days	Percentage of days with daily maximum temperatures Tx > 90th percentile of the reference period (1976-2005)	%

(severe scenario), corresponding respectively to an emission of 4.5 and 8.5 W/m^2 by 2100 (Moss et al., 2010). To study the future evolution of temperature extremes in Senegal, we considered the periods 1976-2005 (reference period), 2021-2050 (near future) and 2071-2100 (far future). Some climate indices relevant for the characterization of the temperature extremes are analyzed (Table 2).

In addition to these indices presented in Table 2, we also used

the heat waves magnitude index- daily (HWMId) (Russo et al., 2015). The HWMId is defined as the maximum of all heat wave magnitudes for a given year, where heat wave is the period of 3 or more consecutive days with maximum temperature above the daily threshold for the reference period 1976-2005. The threshold is defined as the 90th percentile of daily maxima, centered on a 31-day window. This index is designed to take into account both the severity of temperature extremes and the duration of a heat wave. The magnitude of a heatwave is defined as the sum of the daily magnitude (Md) within a heatwave. Md is given by:

$$M_d = \begin{cases} \frac{T_d - T_{75p}}{T_{75p} - T_{25p}}, T_d > T_{25p} \\ 0, T_d \leq T_{25p} \end{cases} \quad (1)$$

where Td is the daily maximum temperature, T_{75p} and T_{25p} are respectively the 75 and 25th percentile values of the yearly maximum temperature during the reference period (1976-2005).

To assess the heat stress, we considered the two main standard heat indices used in numerous studies (Garland et al., 2015; Anderson et al., 2013; Willett and Sherwood, 2012; Hayhoe et al., 2010): the heat index (HI) developed by the US National Weather Service and the humidity-index commonly called humidex (HUM) developed by the Canadian meteorologists. The HI measures the combined effect of heat and humidity on human physiology while the HUM was used to describe the impacts of humidity on human comfort.

The heat index (HI) and the humidex (HUM) are respectively defined by the Equations 2 and 3:

$$HI = -42{,}379 + 2{,}04901523T + 10{,}14333129R - 0{,}22475541TR - 6{,}83783 \times 10^{-3}T^2 - 5.481717 \times 10^{-2}R^2 + 1{,}22874 \times 10^{-3}T^2R + 8{,}5282 \times 10^{-4}TR^2 - 1{,}99 \times 10^{-6}T^2R^2 \quad (2)$$

where HI is the heat index (in °F), T is the 2 m air temperature (in °F) and R is the 2 m relative humidity (in %). In this study, the HI values were afterwards converted into °C.

$$HUM = T + 5/9\,(e - 10) \quad (3)$$

where $e = 6.112 \times 10^{7.ST/\,(237.7+T)}.R/100$. T and HUM are respectively the 2 m air temperature (°C) and the humidex (°C)

The analysis of these climate indices is carried out during the hot (March-April-May, MAM), cold (December-January-February, DJF) as well as the rainy (July-August-September, JAS) seasons.

RESULTS

Validation of the surface temperature

Figure 2 shows the evolution of the mean surface temperature during DJF (average from December to February), MAM (average from March to May) and JAS (average from July to September) periods from 1989 to 2008 for the Climate Research Unit (CRU) observation data and the deviation from CRU of the ensemble mean of the models. The CRU data shows that the lowest temperatures (around 24°C) are observed during the DJF period and especially in the northwestern part of Senegal. During the MAM period, temperatures are relatively high through Senegal compared to other seasons. In addition, CRU climatology has a zonal gradient with higher temperatures observed towards the east of the country during this period. However, during the rainy season (JAS), it has a decreasing north-south gradient over Senegal. This is due to the fact that during this season, the rainfall in this country is characterized by a latitudinal gradient with intensities much stronger in the south causing a considerable temperature declines in this part of the country. When considering the deviation from CRU of the ensemble mean of the models, weak warm biases (less than 1.5°C) are recorded in DJF over the country especially in the southern and north-eastern parts over the western part of the country and weak cold bias over the coastal zone. The deviation from CRU of the ensemble mean during the summer period (JAS) shows that the ensemble mean of all models reproduces well the spatial pattern of the temperature over the country with an underestimation over the southern part where it has a very low underestimation (less than 1°C). When comparing the performance of individual models with the ensemble of all models (Figure not shown), we found that biases are weaker for the latter; in coherence with Gbobaniyi et al. (2014) and Kim et al. (2014) works which showed that the ensemble mean of the models better reproduces the spatial distribution of surface temperature (Appendix Figures 1-4). These small biases also confirm that the ensemble mean of all models has a more robust signal.

This validation study allowed us to confirm that the ensemble mean of the models improves the performance of the models taken individually as shown in the previous studies (Gbobaniyi et al., 2014; Kim et al., 2014). That is why it will be considered to diagnose the future evolution of temperature and some extreme temperature indices in Senegal.

Future evolution of the mean surface temperature

The spatial distribution of the mean surface temperature difference between the near future (2021-2050) and the reference period (1976-2005) shows that the ensemble mean of the models shows an increase of the mean temperature during all three considered seasons (Appendix Figures 5). These increases are generally higher during the cold season (DJF) and can exceed 1.5°C, over large parts of the country under the severe scenario (RCP8.5). The east-west gradient during the MAM season is materialized by increases which are stronger towards the eastern part of the country. This warming could exceed 1°C under the medium scenario and 1.3°C under the severe one. Temperature increases are relatively lower during the rainy season (JAS) compared to the other seasons. The largest increases are in the northeastern part of the country and do not exceed 1.2°C under the severe scenario. Senegal could experience a very strong rise in temperatures during the far future compared to the near future. The highest

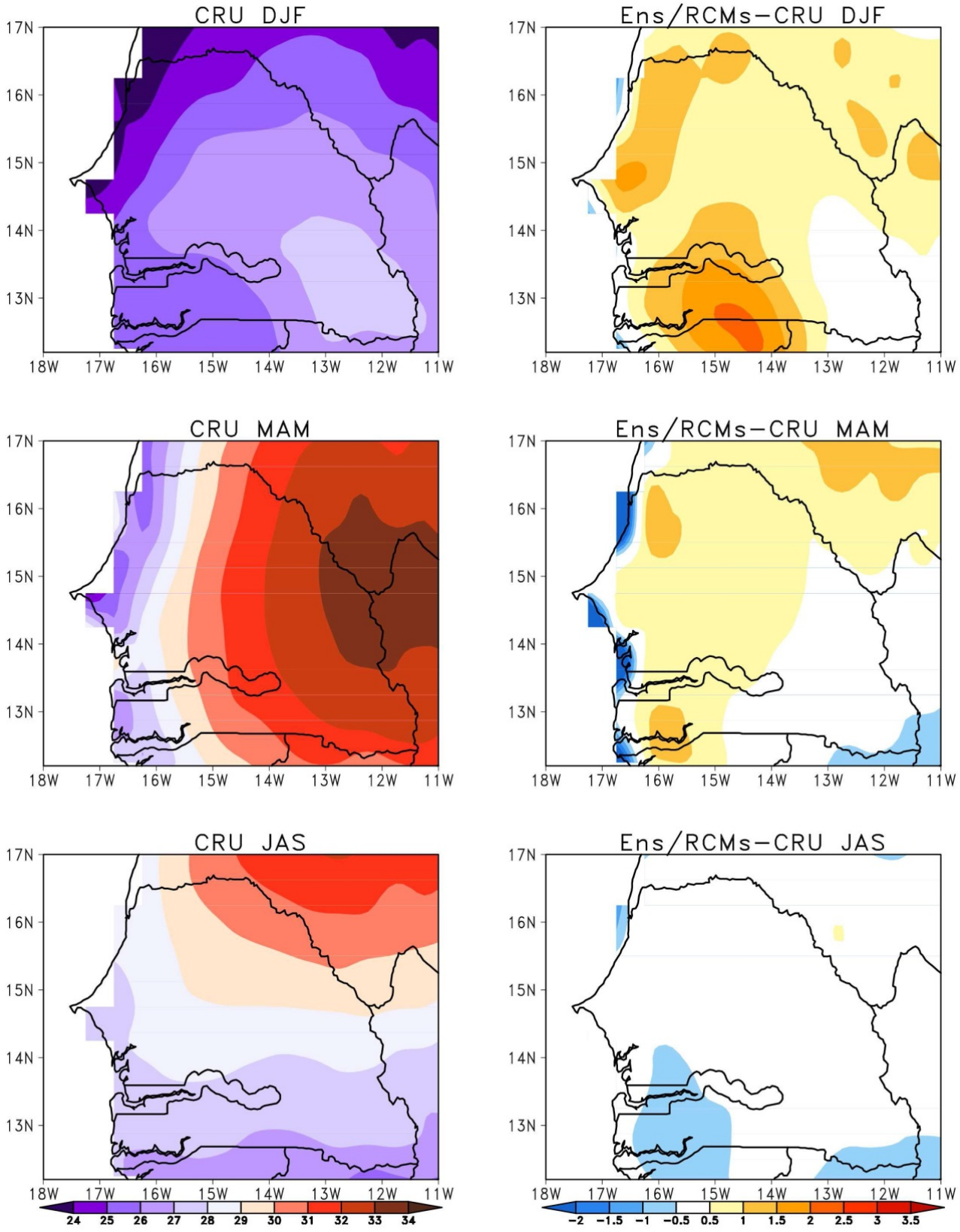

Figure 2. Mean temperature in DJF, MAM and JAS seasons from 1989 to 2008 for CRU data and deviation from CRU observations of mean DJF, MAM and JAS temperature averaged from 1989 to 2008 of the ensemble mean of regional climate models (RCMs).

increases are still observed in DJF in the center of the country and can exceed 2°C under the medium scenario and 4.4°C under the severe one. These temperature increases are relatively low in the north and the south of the country. In MAM, the ensemble mean of the models under the RCP4.5 and RCP8.5 scenarios simulates temperature increases of up to 2 and 4.2°C, respectively in the eastern part of the country. As for the near future, the highest temperature increases in JAS are still recorded in the north-east and can exceed 2.3 and 4°C, respectively under the scenarios RCP4.5 and RCP8.5 during the far future. These strong temperature increases observed in the semi-arid countries of Sahel and particularly in Senegal may lead to an increase in evaporation phenomena and consequently a strengthening of rainfall extreme events such as floods as pointed by Ly et al. (2013).

Future evolution of temperature extremes

Figure 3 shows the frequency of days during the near future with minimum temperature warmer than the 90th percentile of the reference period (1976-2005) threshold for the three seasons considered (DJF, MAM, JAS). The ensemble mean of the models under both scenarios shows a strong percentage of warm night (Tn90p) in DJF over the center of the country with values exceeding 70%. During the MAM and JAS seasons, the ensemble mean of the models presents a north-south gradient with values exceeding 90% during the JAS season over the south of the country for both scenarios. The Tn90p spatial evolution during the far future (2071-2100) (Figure 4) shows that the ensemble mean of the models predicts a stronger change during the far future compared to the near future. In fact, during the cold season (DJF), its projects Tn90p values of the order of 80% under the medium scenario (RCP4.5). Under the severe scenario (RCP8.5), it envisages very strong changes especially over the coastal zone (greater than 98%). In MAM, large increase in the percentage of warm nights during the far future are recorded in the south of the country and can exceed 99% under the RCP8.5 scenario. This increase in warm nights is consistent with the larger surface temperature in the MAM season known as the hottest one. Moreover, the greenhouse gas concentration in the atmosphere tends to increase during the far future under the severe scenario RCP8.5 which in turn may increase surface temperature and thermal extremes. The frequency of warm nights is generally higher during the JAS season through Senegal, especially under the RCP8.5 scenario with values close to 100% by 2100. The larger increase in the percentage of warm nights (Tn90p) is consistent with the faster strengthening of minimum temperatures compared to maximum temperatures in the Sudano-Sahelian region as suggested by New et al. (2006), Ly et al. (2013) and CEDEAO-ClubSahel/OCDE/CILSS (2008).

The percentage of days with maximum temperature greater than the 90th percentile (Tx90p) of the reference period during the near future is as shown in Figure 5. The ensemble mean of the models, under both scenarios, projects a frequency of Tx90p of the order of 70% over a large part of the country in DJF. During the hot season (MAM), it projects small changes in hot days (Tx90p). The highest values of Tx90p recorded in the country are of the order of 60% for the severe scenario (RCP8.5). The changes are generally lower in the coastal zone for both scenarios. This result suggests some possible sea effects as this latter may decrease the surface temperature which in turn may impact temperature extremes. Tx90p changes by 2050 are generally low in JAS compared to the cold season (DJF) and hot season (MAM). Indeed, the highest values are obtained with the RCP8.5 scenario (less than 60%) over a large part of the country. Stronger values of Tx90p are recorded when considering the far future (Figure 6). In DJF, the ensemble mean of the models presents a north-south gradient of Tx90p with a hot day frequency reaching 94% under the RCP4.5 scenario and 98.5% under the RCP8.5 scenario in the south of the country. On the other hand, during the hot season (MAM), the ensemble mean of the models has an east-west gradient with an important increase in the occurrence of hot days (up to 97%) towards the west during this period under the severe scenario (RCP8.5). Projected changes during the far future of Tx90p in JAS under the medium scenario are relatively low with values not exceeding 70% over a large part of the country. However, under the severe scenario, it predicts very strong changes (above 93%) over Senegal. This could translates into negative consequences for the socio-economic activities such as agriculture and the human health. Projected changes during the far future of Tx90p in JAS under the medium scenario are relatively low with values not exceeding 70% over a large part of the country. But, under the severe scenario, it predicts very strong changes (above 93%) over the country.

To go deeper in the analysis of thermal extremes, Figure 7 shows the heat waves magnitude index-daily (HWMId) during the near future (2021-2050). In DJF, the ensemble mean of the models under both scenarios presents heat waves with magnitude of the order of 35 over a large part of the country. Values reaching 55 are located over the north-western part of the country. High values of HWMId are also diagnosed during the hot season (MAM) for both scenarios. During the rainy season, the ensemble mean of the models projects very strong values of HWMId over a large part of the Senegal especially under the RCP8.5 scenario. The analysis shows that the strongest values of HWMId are expected during the far future (2071-2100) in the country (Figure 8). In fact, during the DJF season, the HWMId values

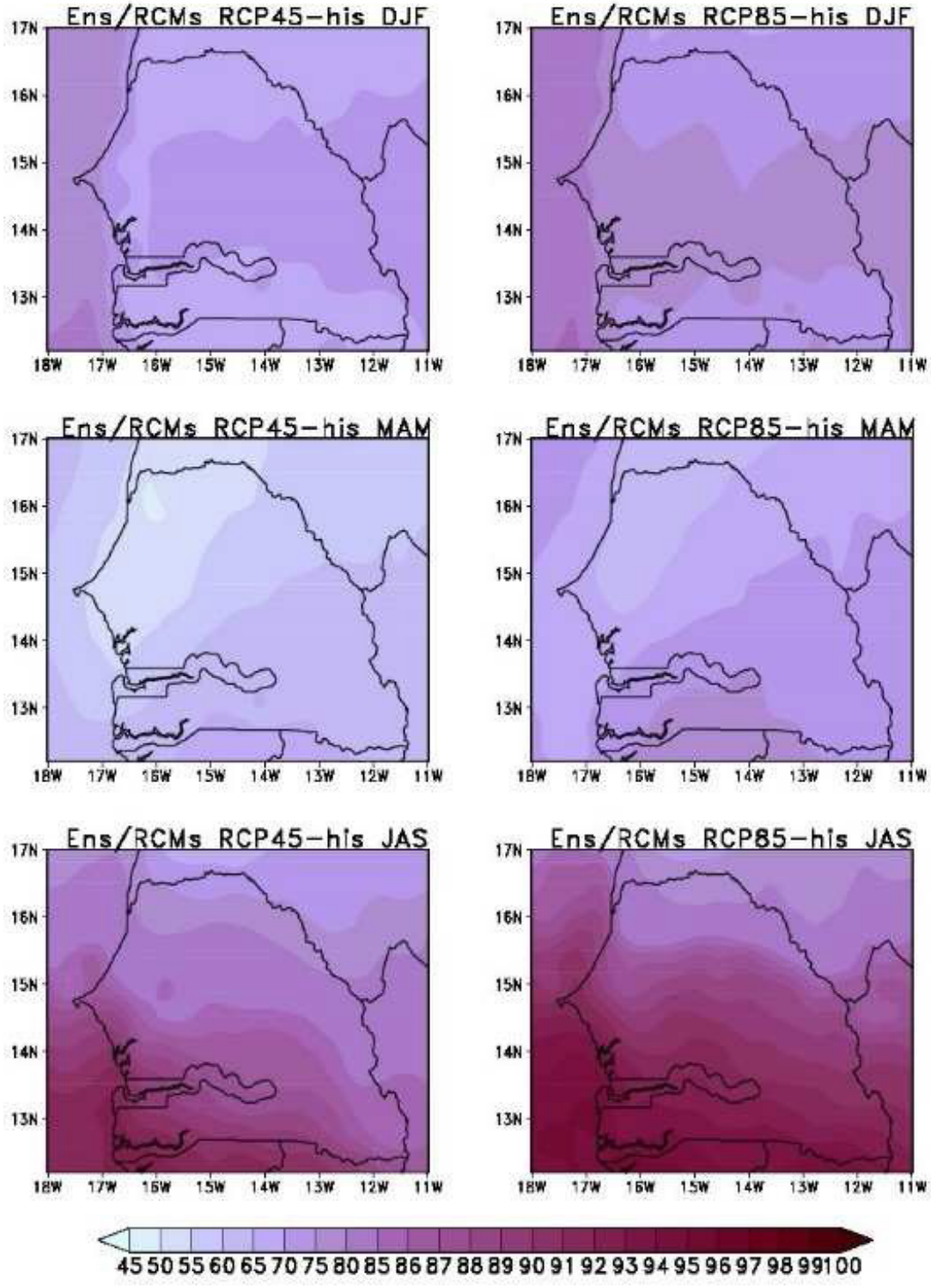

Figure 3. Percentage of days in the near future (2021-2050) with minimum temperature warmer than the 90th percentile of the reference period (1976-2005) during the DJF, MAM and JAS seasons.

can reach 50 and 60, respectively under the RCP4.5 and RCP8.5 scenarios over the north-western part of the country. These heat waves are relatively important during the hot season for both scenarios with magnitude

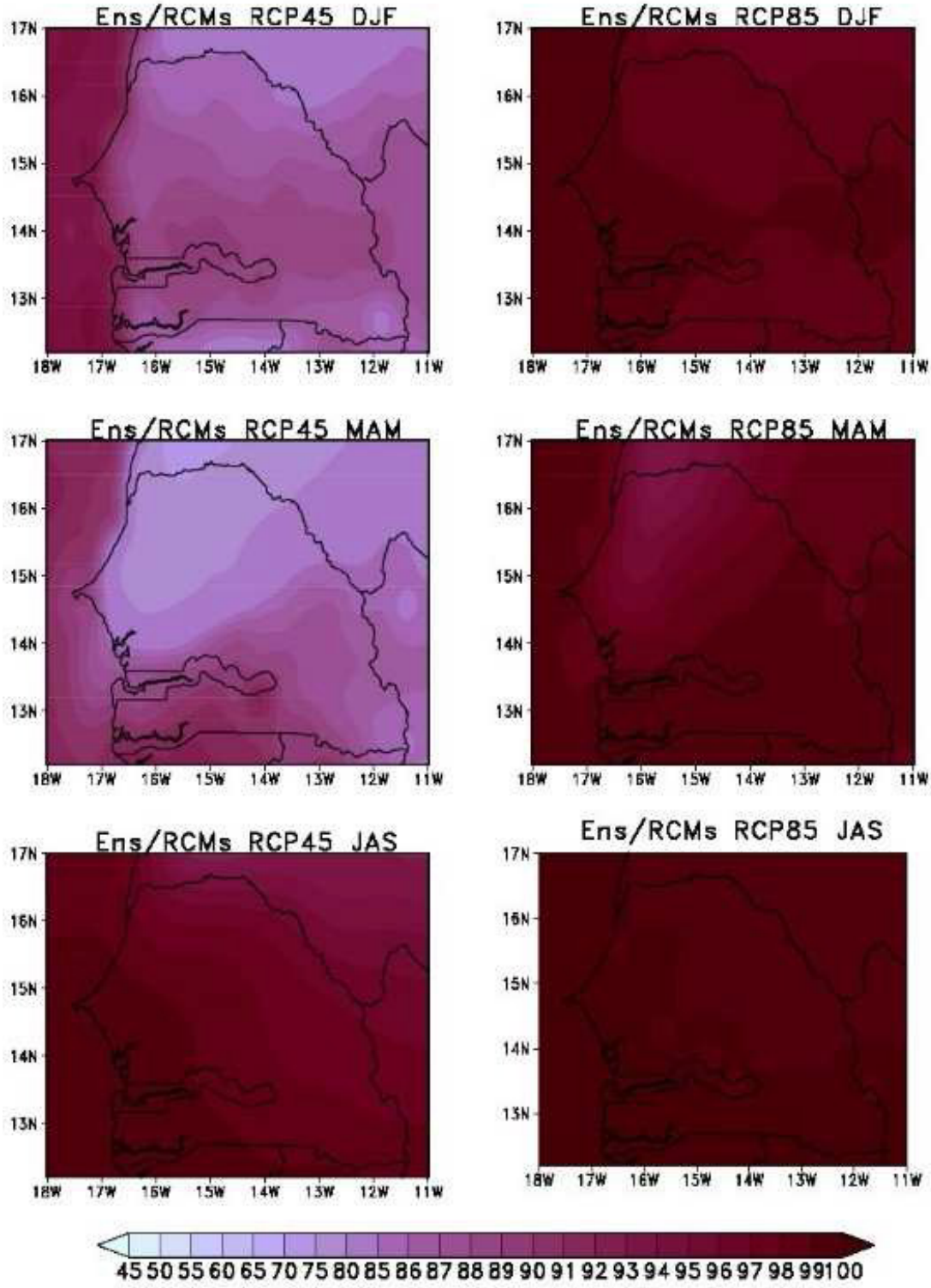

Figure 4. Percentage of days in the far future (2071-2100) with minimum temperature warmer than the 90th percentile of the reference period (1976-2005) during the DJF, MAM and JAS seasons.

exceeding 60 in the western part of the country. The projections obtained with the ensemble mean of the models during the rainy season (JAS) show that Senegal could be affected by heat waves episodes with

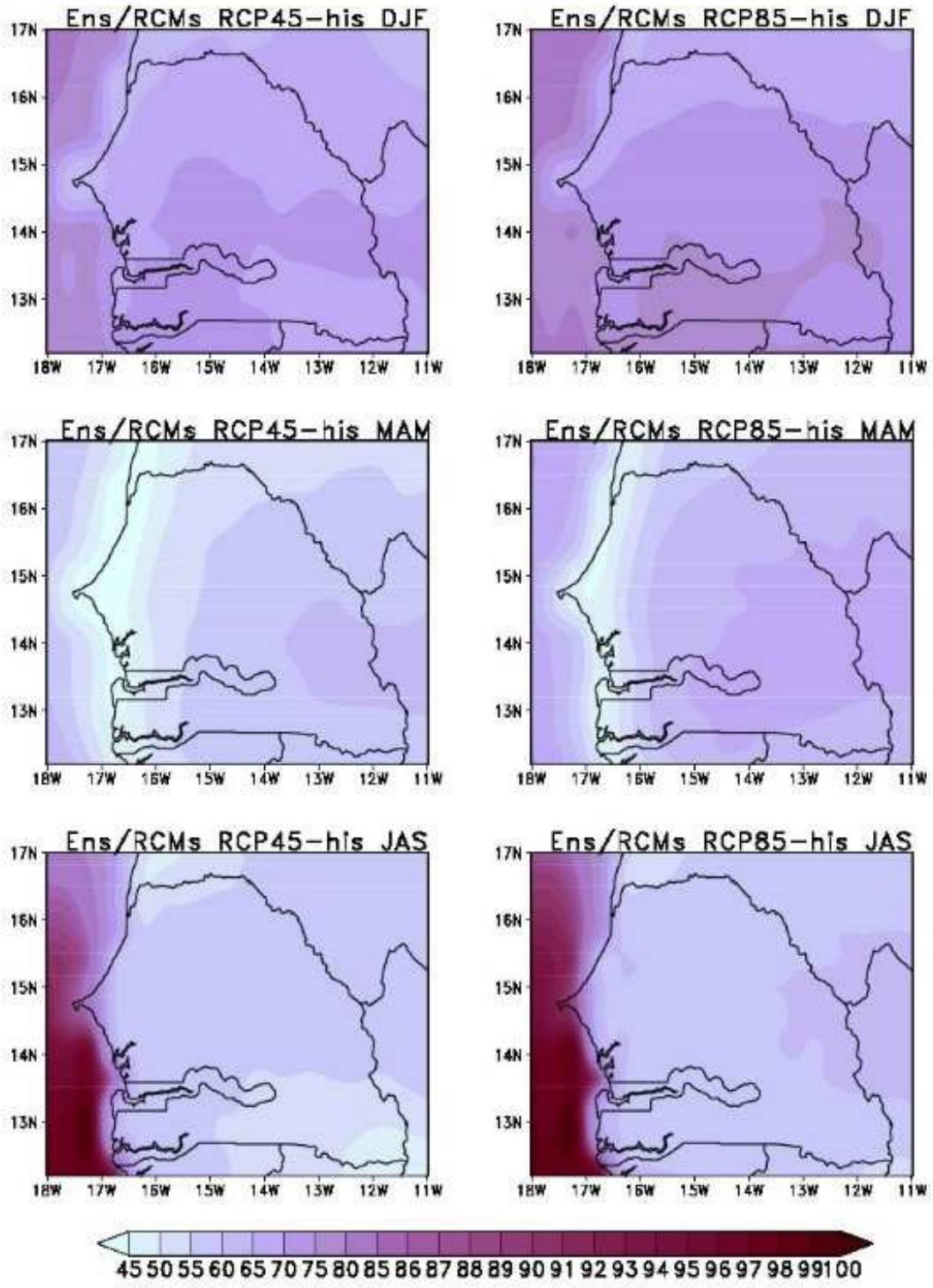

Figure 5. Percentage of days in the near future (2021-2050) with maximum temperature warmer than the 90th percentile of the reference period (1976-2005) during the DJF, MAM and JAS seasons.

magnitudes that could exceed 65 under the severe scenario. This increase of heat waves is consistent with Dosio et al. (2017) studies. This strong increase in HWMId predicted by the ensemble mean of all models during the rainy season (JAS) could be detrimental for agricultural yields during the far future (Sarr and

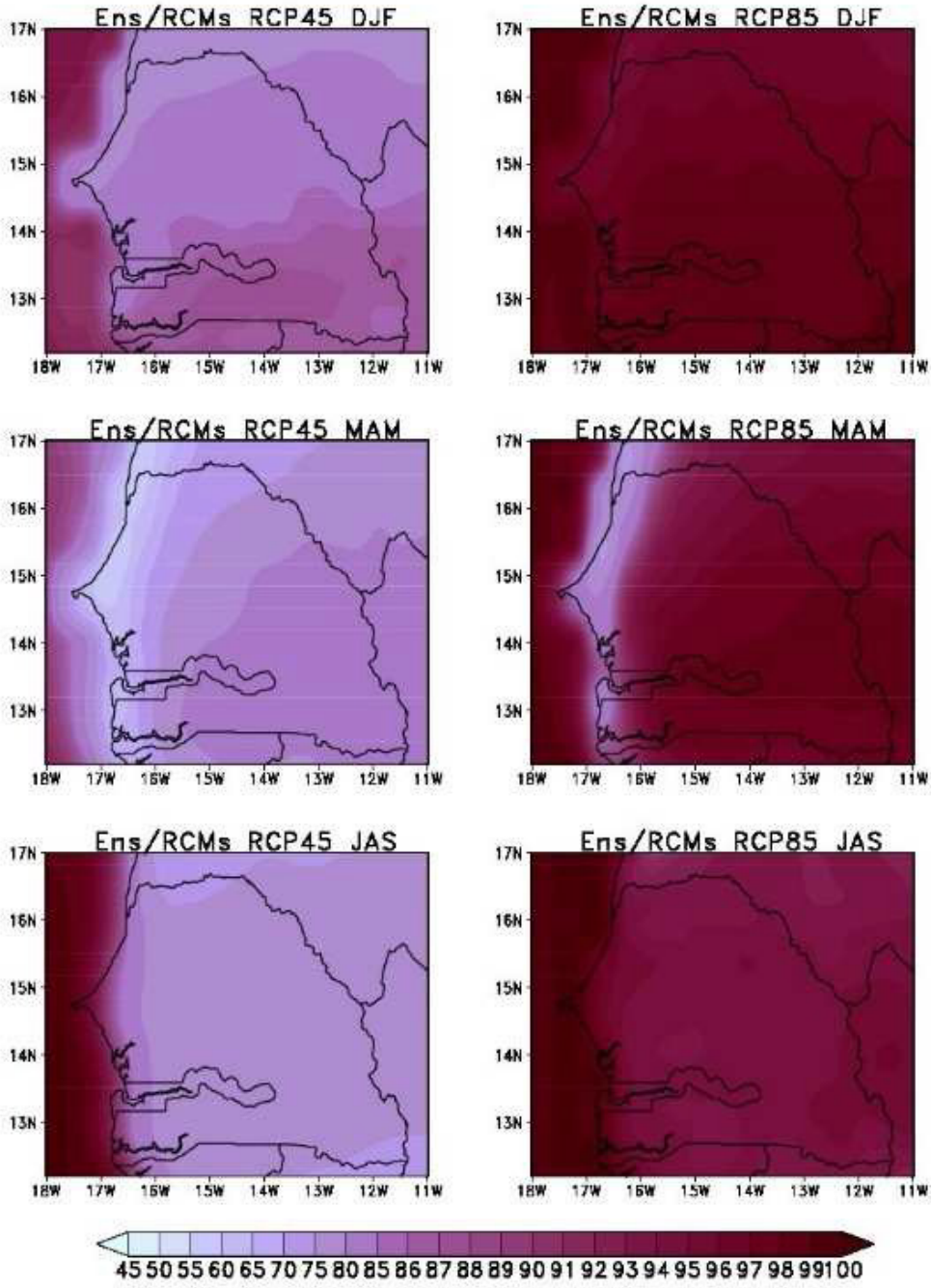

Figure 6. Percentage of days in the far future (2071-2100) with maximum temperature warmer than the 90th percentile of the reference period (1976-2005) during the DJF, MAM and JAS seasons.

Camara, 2018) as well as the health of populations.

The associated health risks

Rising heat waves can negatively impact human health, according to some authors (Campbell et al., 2018; Hass et al., 2016; Garland et al., 2015). In fact, the combination of temperature and relative humidity increases could have negative impacts on human health. When considering the spatial distribution of the heat index during the reference period (Figure 9), the ensemble mean of the models shows low heat index (HI) values during the cold period (DJF) compared to

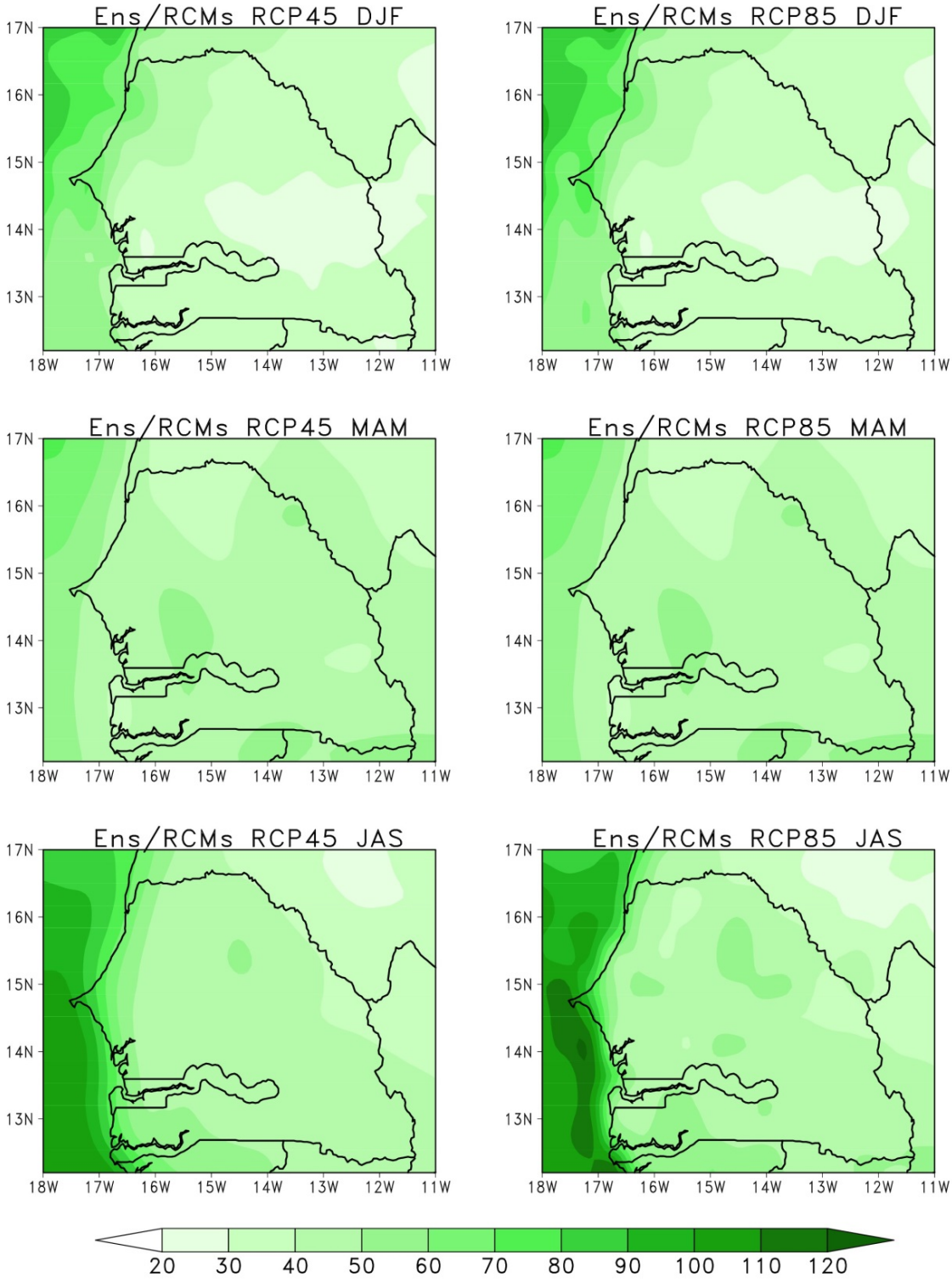

Figure 7. Heat waves magnitude index-daily (HWMId) during the near future (2021-2050) for the DJF, MAM and JAS seasons.

other seasons. The HI is relatively stronger during the hot season (MAM) with values reaching 28°C in Central and Southern Senegal. The reinforcement of the HI during the hottest season (MAM) may due to the increase in

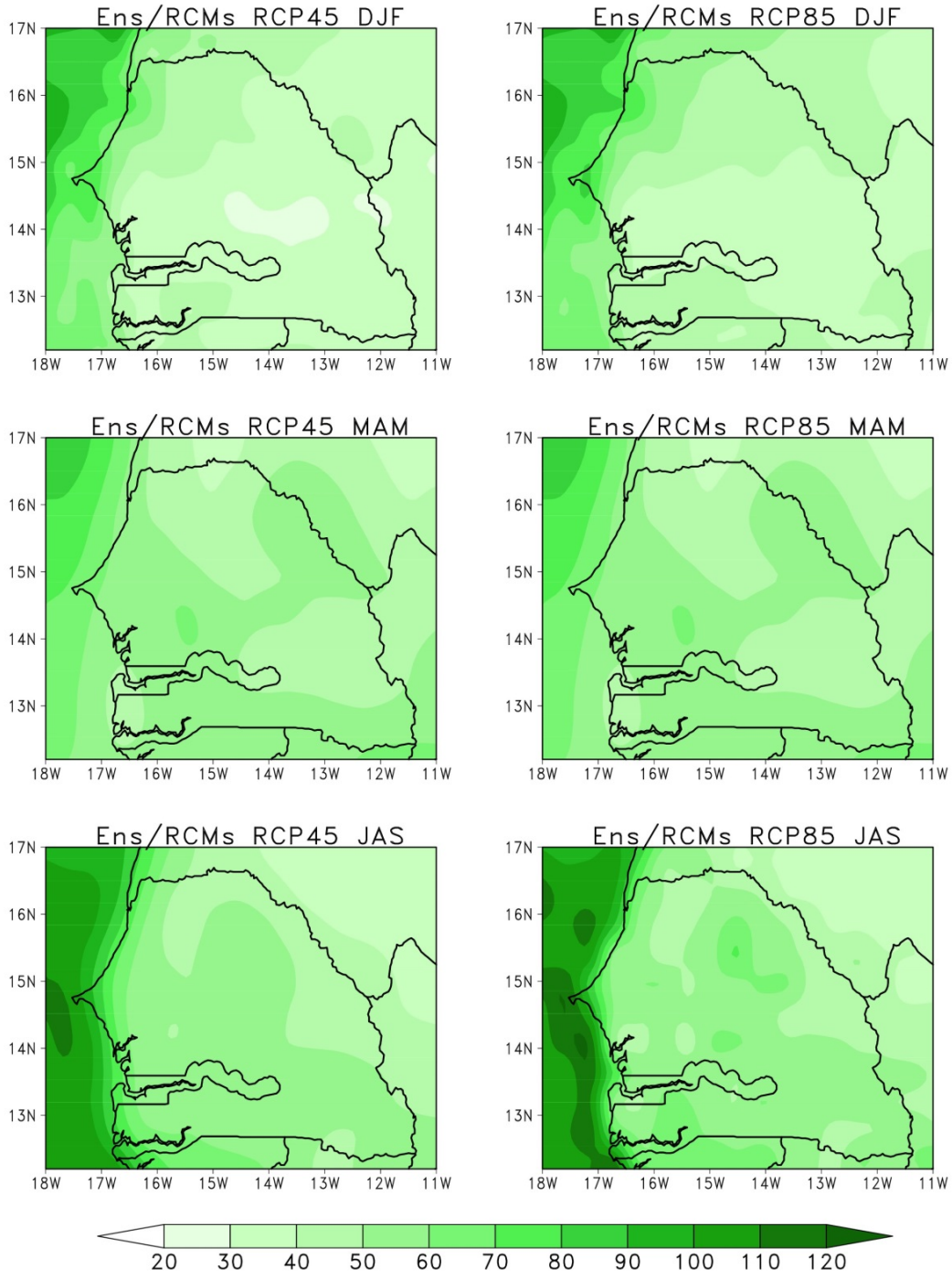

Figure 8. Heat waves magnitude index-daily (HWMId) during the far future (2071-2100) for the DJF, MAM and JAS seasons.

surface temperature. During the rainy season (JAS), the ensemble mean of the models has a North-South gradient with strong HI values located in the north of the country (up to 30°C) as for the surface temperature. This result suggests that the temperature is the main factor controlling the HI spatial variability. These high HI values obtained during the hot and the rainy seasons correspond to the symptom band I (Table 3). The strong HI values recorded during the rainy season could be due to the increase of the relative humidity during this period. The projections obtained on the heat index during the near future (2021-2050) (Figure 10) show that the

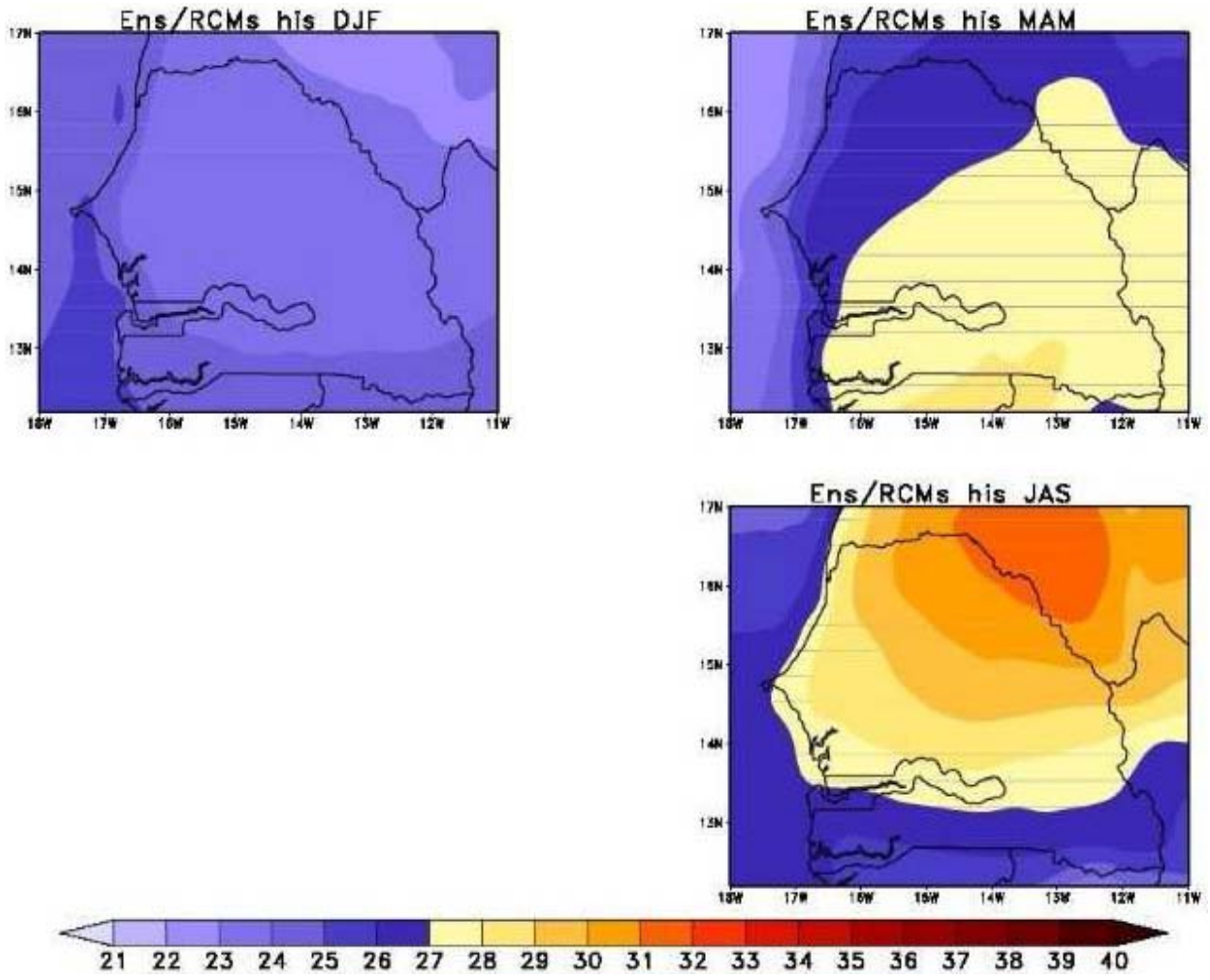

Figure 9. Evolution of heat index (°C) during the reference period (1976-2005) in DJF, MAM and JAS seasons.

Table 3. Heat index threshold and potential health impact.

Symptom band (SB)	US NWS Classification	Heat index (°C)	Possible adverse effect
SBI	Caution	27-32	Fatigue possible with prolonged exposure and/or physical activity
SBII	Extreme caution	32-39	Heat stroke, heat cramps, or heat exhaustion possible with prolonged exposure and/or physical activity
SBIII	Danger	39-51	Heat cramps or heat exhaustion likely, and heat stroke possible with prolonged exposure and/or physical activity
SBIV	Extreme danger	> 51	Heat stroke highly likely

Source: OHSCO (2008); http://ggweather.com/101/hi.html.

ensemble mean of the models presents slight changes during the cold season.

However during the warm season, an increase is noted especially in the south of the country with HI values

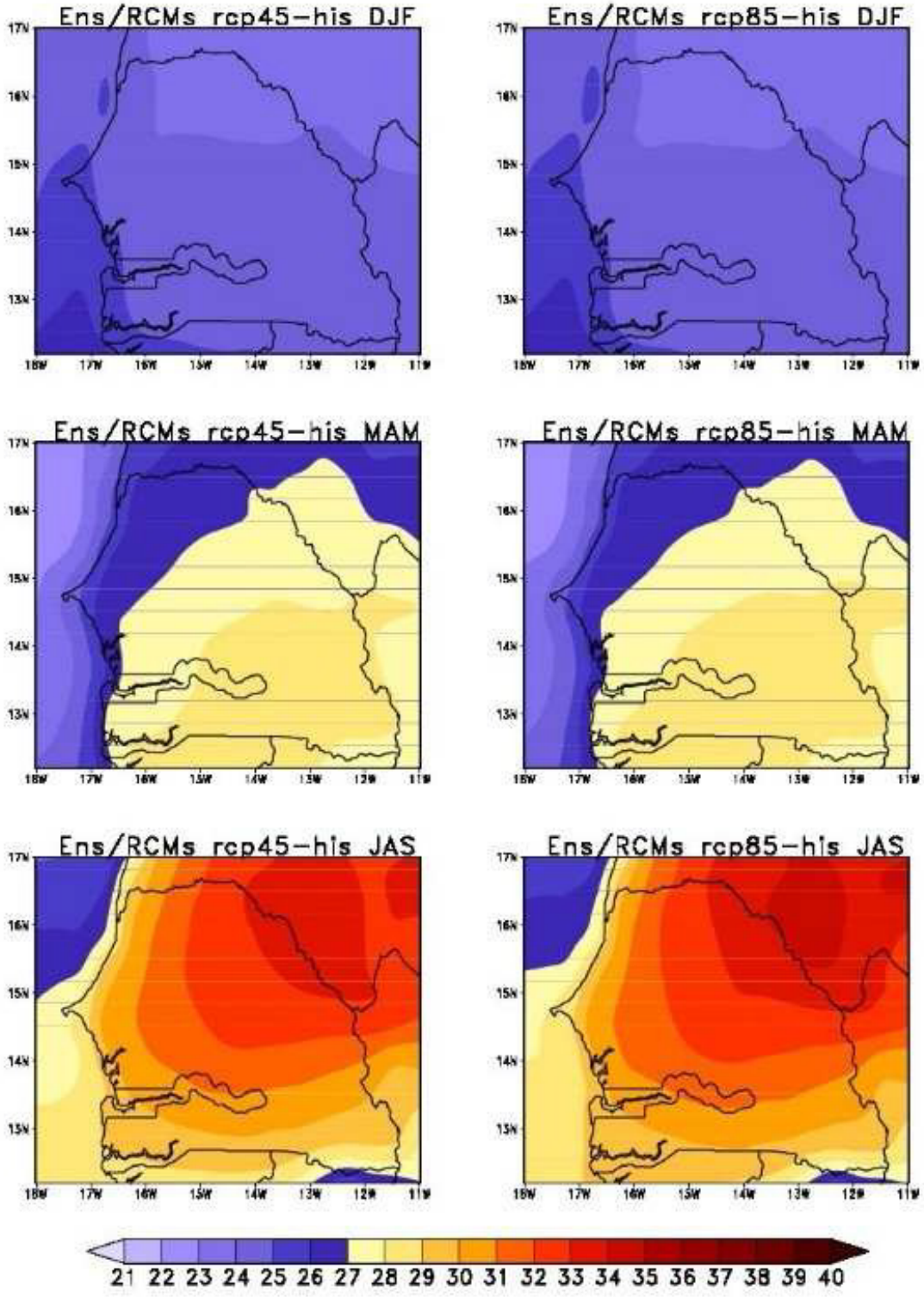

Figure 10. Evolution of the heat index (°C) during the near future (2021-2050) in DJF, MAM and JAS seasons.

greater than 31°C under both scenarios. During the reference period, the highest values are still recorded in JAS season during the near future (2021-2050). However, the ensemble mean of the models under both

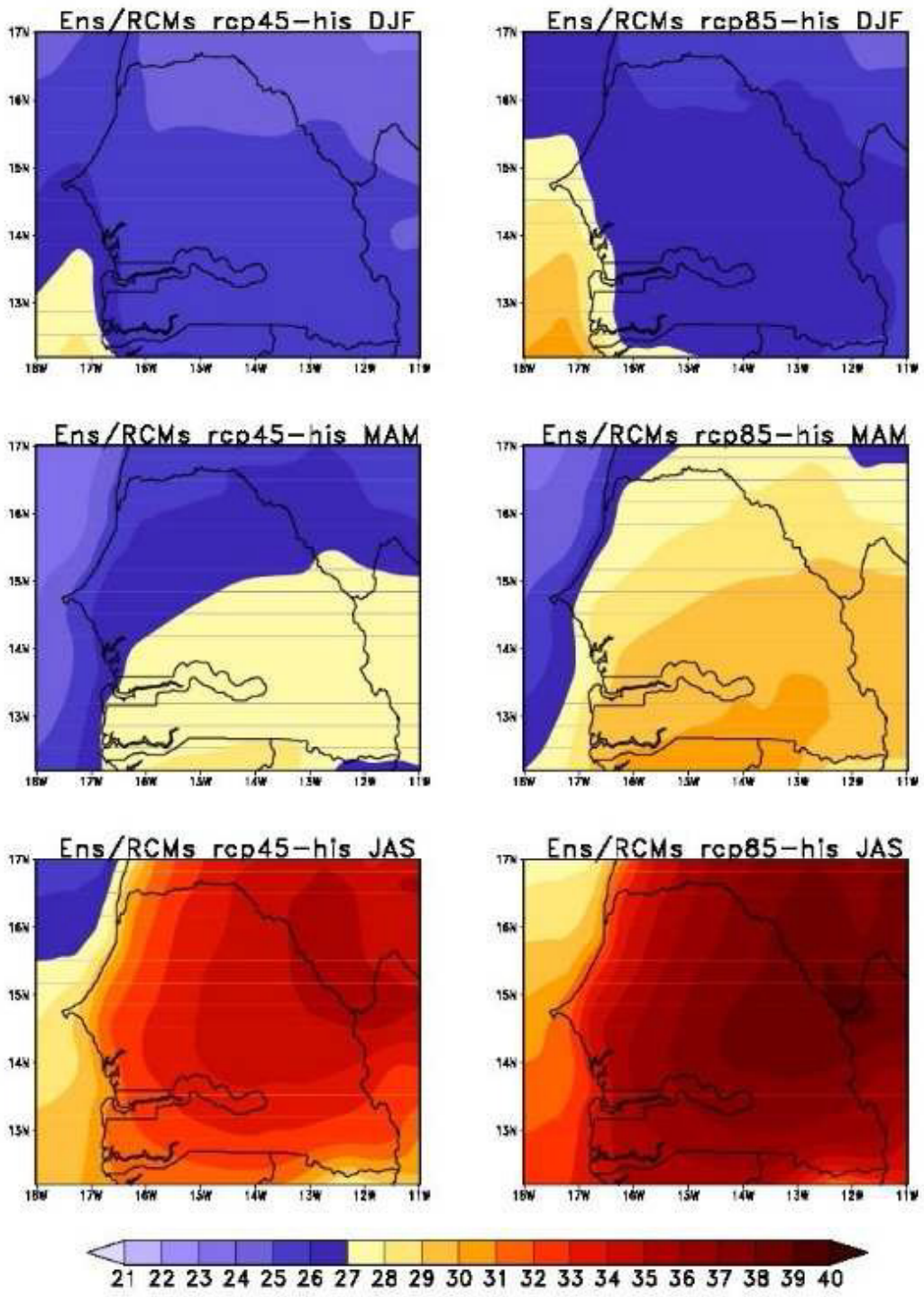

Figure 11. Evolution of the heat index (°C) during the far future (2071-2100) in DJF, MAM and JAS seasons.

scenarios simulates an increase of HI (up to 33°C) in the northeastern part of the country highlighting the presence of the symptom band II (SBII). It should also be noted that this increase in HI values is not always due to an increase in temperature. In fact, relative humidity also plays a fairly important role, as some studies have shown (Suparta and Yatim, 2017; Hass et al., 2016). Figure 11 shows the projections during the far future (2071-2100) of the heat index. A gradual increase is simulated during this period compared to the reference

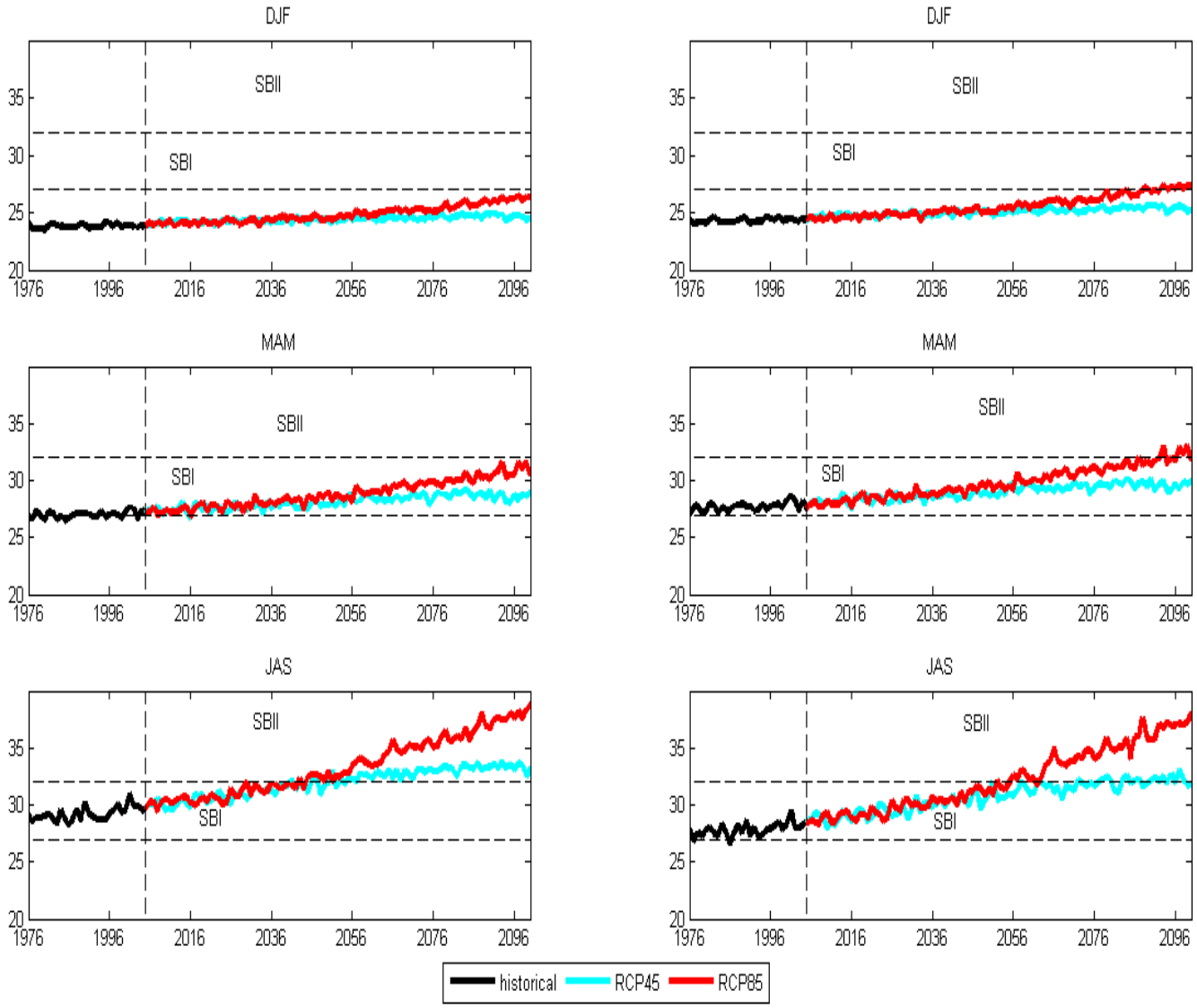

Figure 12. Temporal evolution of the heat index (°C) during the cold (DJF), hot (MAM) and wet seasons (JAS) in the north (left panel) and in the south (right panel) of Senegal.

period and the near future. However, this increase is generally less than the threshold value (27°C) in DJF. It is only on the southwest coast of Senegal that HI values of around 27°C are recorded under the RCP8.5 scenario.

In MAM, the ensemble mean of the models simulates a slight decrease under the RCP4.5 scenario compared to the near future. However, under the RCP8.5 scenario, it simulates an important increase compared to the near future (2021-2025) with values greater than 32°C corresponding to the symptom II band (32°C<SBII<41°C). The situation could be much more alarming during the rainy season (JAS) due to the strong increase of humidity. In fact, the projections obtained with the ensemble mean of the models by 2100 shows HI values which are generally above 27°C under both scenarios across the country. Under the RCP4.5 scenario, it highlights the presence of symptom band I in the western part of the country and the presence of symptom band II in the south-east of the country. However, under the RCP8.5 scenario, a large increase in symptom band II is expected almost all over Senegal, causing serious discomfort (fatigue, heat stroke, heat cramps, etc.) for local populations.

The temporal evolution of the seasonal heat index in Northern (17°W-12°W, 14.4°N-16.8°N) and Southern (17°W-12°W, 12.7N-14.4N) Senegal from 1976 to 2100 is as shown in Figure 12. The heat index has increased in almost all parts of Senegal. However, this increase is relatively low during the cold season (DJF). However, the HI values may reach the SBI at the end of the

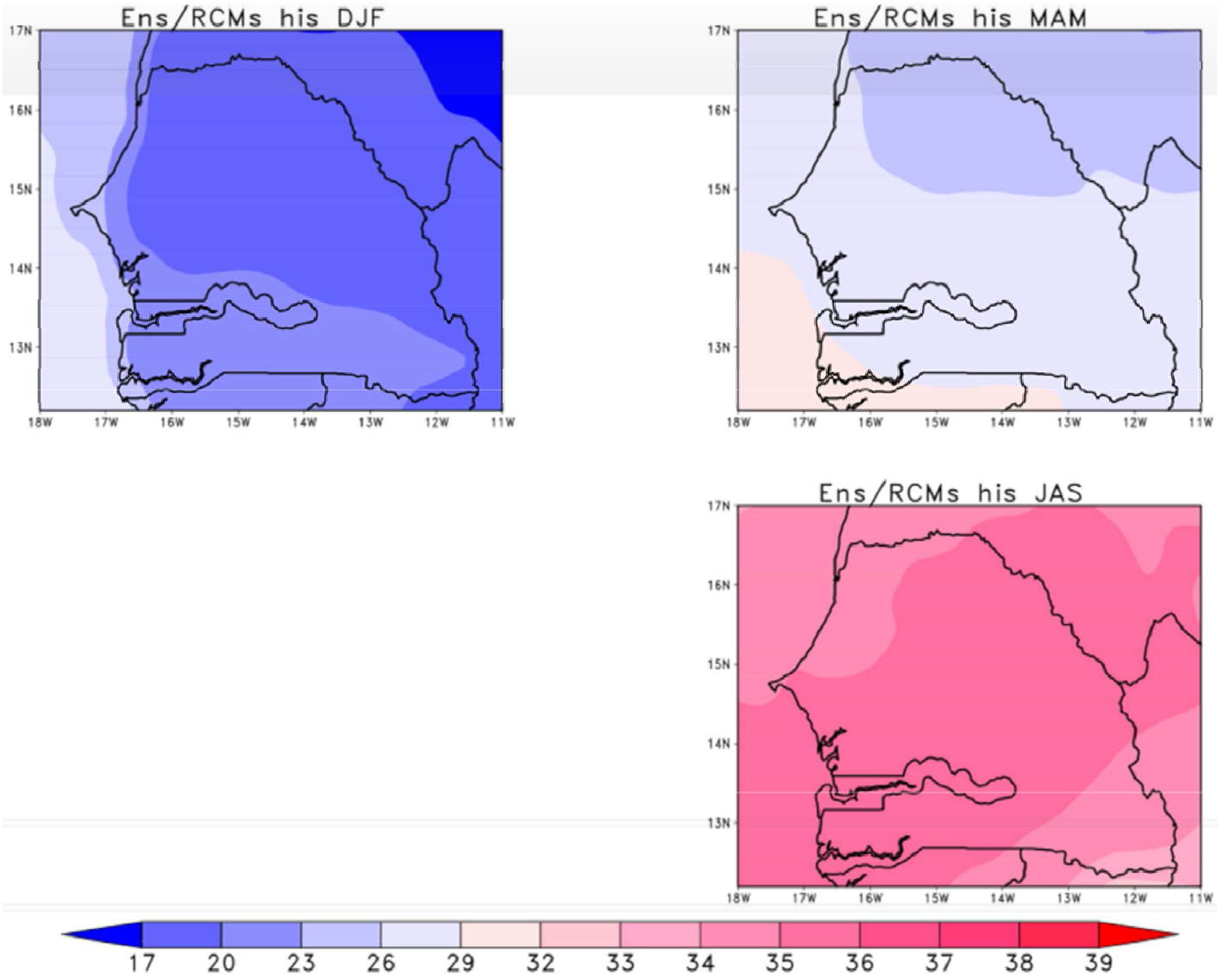

Figure 13. Evolution of the humidex (°C) during the reference period (1976-2005) in DJF, MAM and JAS seasons.

century under the RCP8.5 scenario in coherence with the temperature rise in the far future Appendix Figures 6 and 7. During the hot season (MAM), the ensemble mean of the models shows that the HI values are relatively stronger compared to cold season. The HI values are also stronger in the south and can reach the SBII under the RCP8.5 scenario. A strong increase of HI values is recorded during the rainy season compared to other seasons causing serious discomfort to the local populations. The presence of SBII is highlighted by the ensemble mean of the models in the north and the center of country from 2050 for both scenarios. This increase is relatively low in the south of the country. It reaches the SBII from 2070 only for the RCP8.5 scenario. This large increase in the heat index could be harmful for those working or exercising physical activity.

As for the heat index, the evolution of humidex during the reference period (Figure 13) shows that the cold season (DJF) is the more comfortable season followed by the hot season (MAM). However, some discomfort (category B) is observed during this season particularly in the south-west of the country. In fact, some discomfort are observed in all the country. The projections during the near future (2021-2050) of the humidex are as shown in the Figure 14. The results show a slight increase of the category B during the hot season in the south of the country and in all the country during the rainy season under both scenarios. Compared to heat index, the results obtained during the hot season (MAM) show that when we consider the humidex the heat stress would not affected the human health during this season. Figure 15 shows the evolution of the

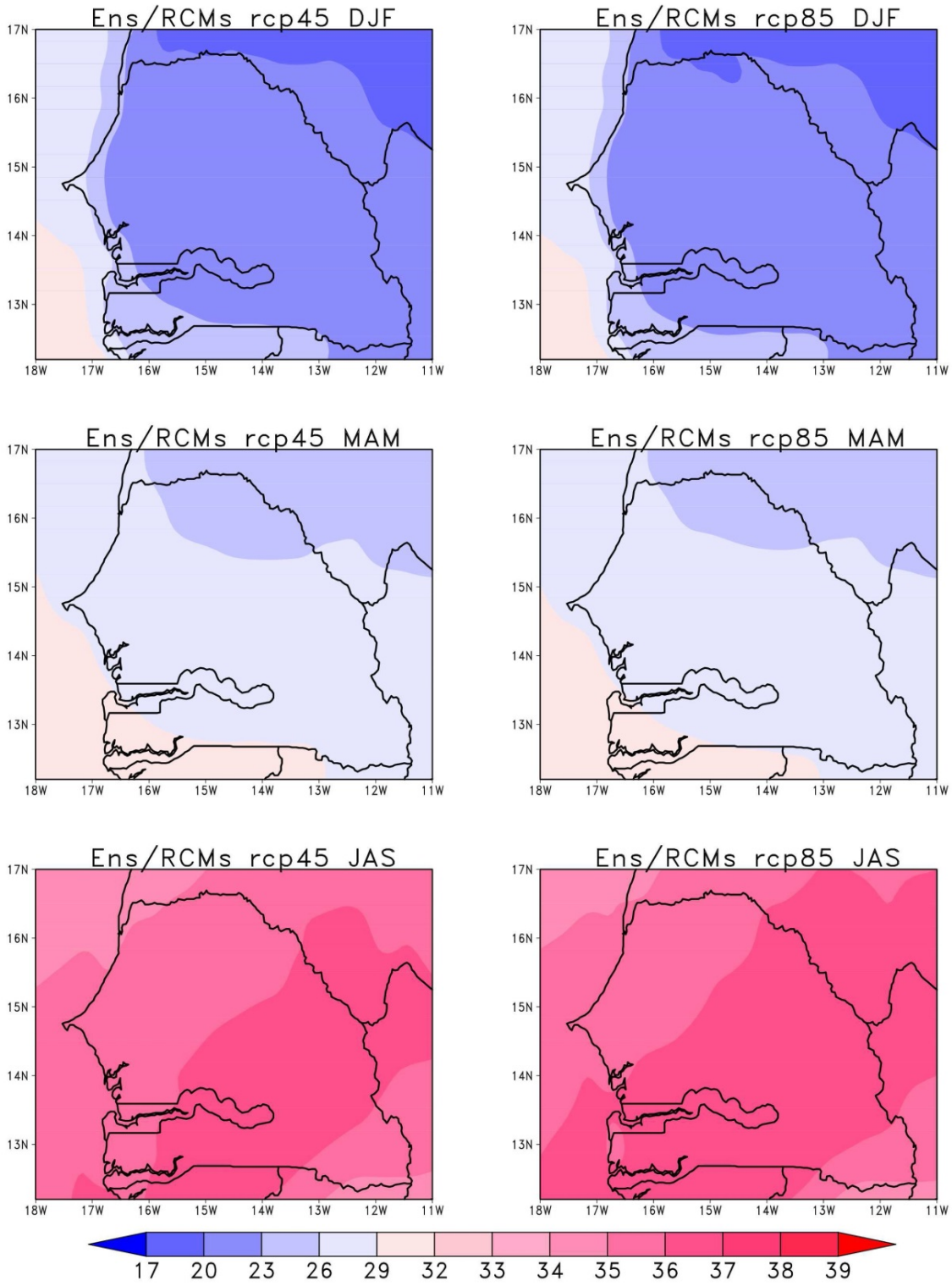

Figure 14. Evolution of the humidex during the near future (2021-2050) in DJF, MAM and JAS seasons.

humidex during the far future (2071-2100). Results show that the human discomfort during this period is imminent. In fact, the category B continues to increase and its presence is noted during the cold season in the south of the country particularly under the RCP8.5 scenario. Admittedly, the acclimatization capacity of

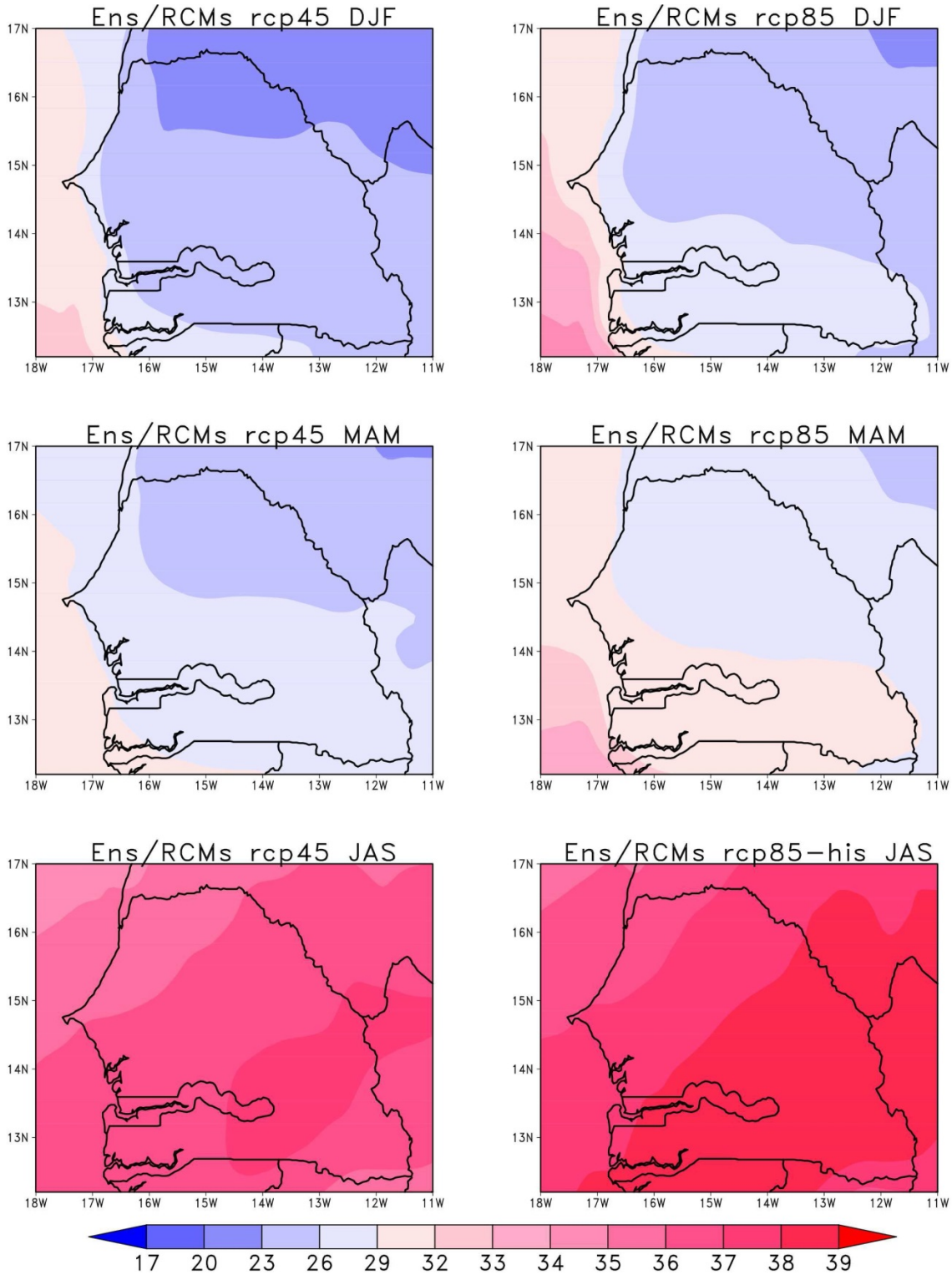

Figure 15. Evolution of the humidex during the far future (2071-2100) in DJF, MAM and JAS seasons.

the human body in the country of residence to global warming is not well studied, especially in the countries of the world. However, in Sahel regions for example, large temperature increases combined with strong humidity could be mortal particularly for the sick, the small children and the elderly persons.

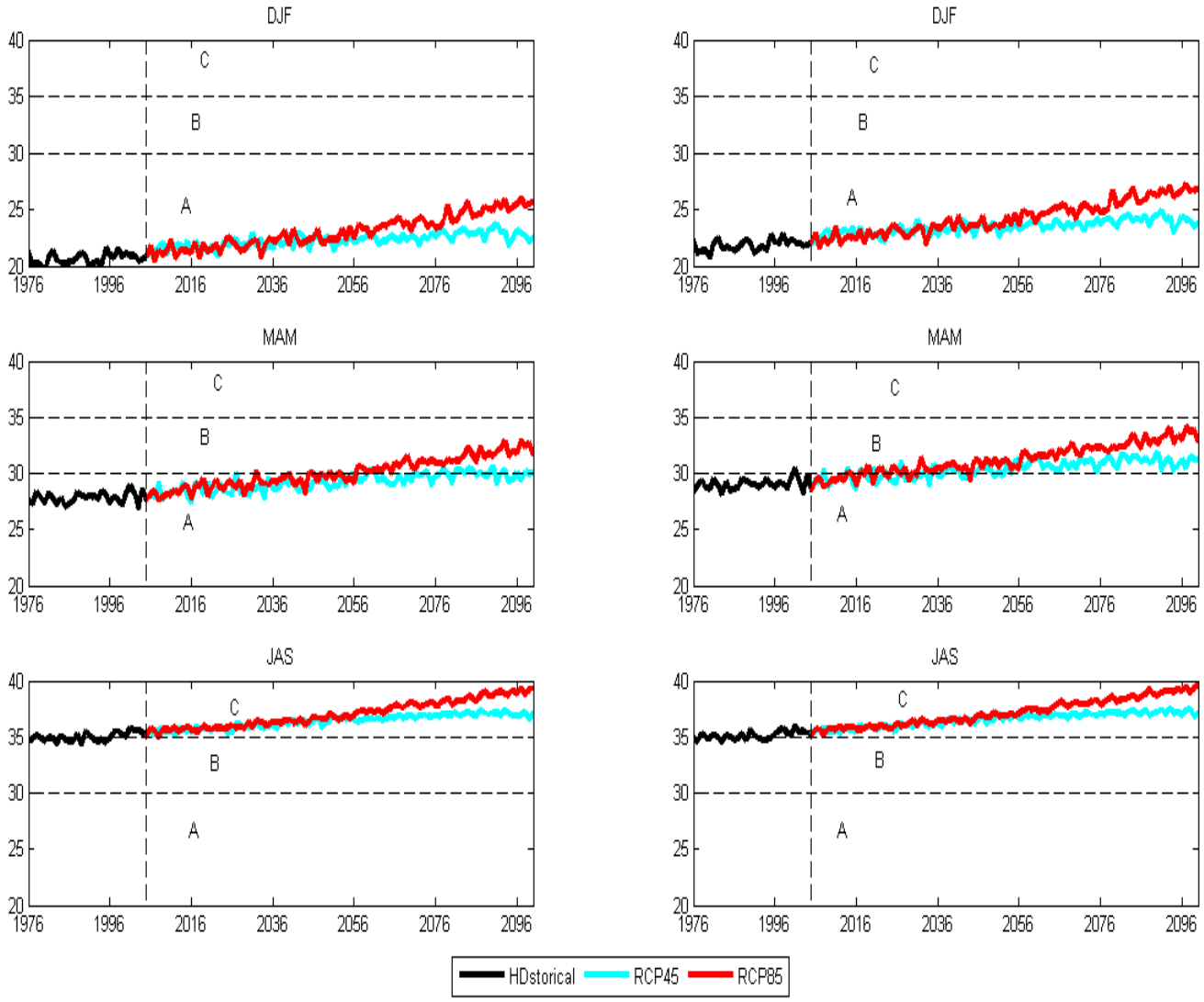

Figure 16. Temporal evolution of the humidex (°C) during the cold (DJF), hot (MAM) and wet seasons (JAS) in the north (left panel) and in the south (right panel) of Senegal.

The temporal evolution of the seasonal humidex in Senegal from 1976 to 2100 are shown in Figure 16 for the north (17°W-12°W, 14.4°N-16.8°N) and the south (17°W-12°W, 13.7°N-14.4°N). The results show that the presence of category A during the cold season (DJF) which is characterized by a little or no discomfort in the south and the north of the country. However, the humidex values are stronger in the south with values which can reach 27°C for RCP8.5 scenario. During the hot season (MAM), the ensemble mean of the models shows the presence of the category B, characterized by some discomfort from 2060 in the north for only the RCP8.5 and in the south for both scenarios. The strong humidex values are recorded during the wet season (JAS) in the north and south of the country highlighting the development of the category C Table 4.

CONCLUSION AND PERSPECTIVES

In this study, the ensemble mean of 5 CORDEX RCMs was considered to analyze the seasonal evolution (DJF, MAM and JAS) of the mean temperature as well as some extreme temperatures such as Tn90p (percentage of warm nights), Tx90p (percentage of hot days) and heat waves during the near future (2021-2050) and the far future (2071-2100). The biases of the ensemble mean of the models considered were first assessed. The validation step results highlight the good performance of the ensemble mean of the models. The latter was then considered in the study of the future evolution of temperature and extreme temperature events. An increase in temperature is predicted by the ensemble mean of the models across the country. The

Table 4. Humidex threshold and potential health impacts.

Categories corresponding to the rising thermal discomfort conditions	Humidex (°C)	Impacts
A	30	Little or no discomfort
B	30-34	Noticeable discomfort
C	35-39	Evident discomfort
D	40-45	Intense discomfort; avoid exertion
E	54	Real dangerous; heat stroke probable

Source: NIOSH (1992); http://www.hpc.ncep.noaa.gov/html/heatindex.shtml.

highest increases are recorded during the DJF season and can reach 1.5°C under the RCP8.5 scenario over most of the country soon. During the far future, increases can reach 2 and 4.5°C, respectively under the scenarios RCP4.5 and RCP8.5. The warming is relatively lower during the rainy season (JAS) compared to DJF and MAM.

For extreme temperature events, the largest increases in warm nights are located during the DJF season in the south of the country for both scenarios with Tn90p occurrences higher than 70% by 2050. During the far future, the increase is above 80% over a large part of the country. These increases are more significant during the JAS season under the RCP8.5 scenario with Tn90p values close to 100% over a large part of the country and this could have negative consequences on the agriculture of our country. Changes in the percentage of hot days (Tx90p) are relatively lower than those of Tn90p almost nationwide. The largest increases in Tx90p in the near future are recorded in DJF under the RCP8.5 scenario and are less than 70%. By 2100, the Tx90p maxima recorded during the DJF season in the southern zone of the country can reach 94 and 98.5% respectively under the RCP4.5 and RCP8.5 scenarios. The heat wave magnitude index-daily analysis (HWMId) shows that the magnitude of the heat waves are stronger during the hot and the rainy season with values exceeding 50 over most parts of the country during the far future.

To study the impact of this heat stress on human health, we analyzed the heat index and the humidex. The results obtained show that maxima of heat index corresponding to symptom band II are recorded in JAS over the south-east of the country during the near future and over most part of the country during the far future for both scenarios. In addition, the frequency of the symptom band II is higher during this season. The analysis of the humidex shows an increase of the discomfort which is more pronounced during the rainy season.

Finally, these results show that temperatures could become stronger in Senegal in the future, resulting in longer and more frequent heat waves. This warming could have negative consequences for the natural ecosystem and local populations. In perspective, it would be important to conduct additional studies to better quantify the impact of this future warming on socio-economic activities of the population in order to put in place appropriate adaptation measures.

ABBREVIATIONS

DJF, Average from December to February; **MAM,** average from March to May; **JAS,** average from July to September; **CORDEX,** Coordinated Regional climate Downscaling Experiment (CORDEX) program; **CRU,** Climate Research Unit.

CONFLICT OF INTERESTS

The authors have not declared any conflict of interests.

REFERENCES

Anderson GB, Bell ML, Peng R (2013). Methods to Calculate the Heat Index as an Exposure Metric in Environmental Health Research. Environmental Health Perspectives 121(10):1111-1119.

Baldauf M, Seifert A, Förstner J, Majewski D, Raschendorfer M, Reinhardt T (2011). Operational convective-scale numerical weather prediction with the COSMO model: description and sensitivies. Monthly Weather Review 139(12):3887-3905.

Basak JK, Titumir RA, Biswas JK, Mohinuzzaman M (2013). Impacts of Temperature and Carbon dioxide on Rice yield in Bangladesh. Bangladesh Rice Journal 17(1-2):15-25.

Boko M, Niang I, Nyong A, Vogel C, Githeko A, Medany M, Osman-Elasha B, Tabo R, Yanda P (2007). Africa Climate Change: impacts, adaptation and vulnerability. In ML Parry, OF Canziani, JP Palutikof, PJ van der Linden, & CE Hanson (Eds.), Contribution of Working Group II to the Fourth Assessment Report of the Intergovernmental Panel on Climate Change. Cambridge, UK: Cambridge University Press, pp. 433-467.

Camara M, Diedhiou A, Sow BA, Diallo MD, Diatta S, Mbaye I, Diallo I (2013). Analyse de la pluie simulée par les modèles climatiques régionaux de CORDEX en Afrique de l'Ouest. Science et changements planétaires/Sécheresse 24(1):14-28.

Campbell S, Remenyi TA, White CJ, Johnston FH (2018). Heatwave and health impact research: A global review. Health and Place 53:210-218.

Ceccherini G, Russo S, Ameztoy I, Marchese AF, Carmona-Moreno C (2017). Heat waves in Africa 1981–2015, observations and reanalysis. Natural Hazards and Earth System Sciences 17(1):115-125.

CEDEAO-ClubSahel/OCDE/CILSS Climate and Climate Change (2008). The Atlas on Regional Integration in West Africa Environment

Series, p.13. “http://www.oecd.org/fr/csao/publications/40121057.pdf”
Christensen OB, Drews M, Christensen JH (2006). The DMI-HIRHAM regional climate model version 5, Denmark: DMI Tech. Rep. 06-17.
Diallo I, Giorgi F, Deme A, Tall M, Mariotti L, Gaye AT (2016). Projected changes of summer monsoon extremes and hydroclimatic regimes over West Africa for the twenty-first century. Climate dynamics 47(12):3931-3954.
Dosio A (2017). Projection of temperature and heat waves for Africa with an ensemble of CORDEX Regional Climate Models. Climate Dynamics 49(1-2):493-519.
Garland R, Matooane M, Engelbrecht F, Bopape MJ, Landman W, Naidoo M, Merwe J, Wright C (2015). Regional projections of extreme apparent temperature days in Africa and the related potential risk to human health. International Journal of Environmental Research and Public Health 12(10):12577-12604.
Gbobaniyi E, Sarr A, Sylla MB, Diallo I, Lennard C, Dosio A, Dhiédiou A, Kamga A, Klutse NA, Hewitson B, Nikulin G (2014). Climatology, annual cycle and interannual variability of precipitation and temperature in CORDEX simulations over West Africa. International Journal of Climatology 34(7):2241-2257.
Giorgi F, Jones C, Asrar G (2009). Addressing climate information needs at the regional level. The CORDEX framework. WMO Bulletin, July 2009 issue.
Giorgi F, Coppola E, Raffaele F, Diro GT, Fuentes-Franco R, Giuliani G, Mamgain A, Llopart MP, Mariotti L, Torma C (2014). Changes in extremes and hydroclimatic regimes in the CREMA ensemble projections. Climatic Change 125(1):39-51.
Hass A, Ellis K, Reyes Mason L, Hathaway J, Howe D (2016). Heat and humidity in the city: neighborhood heat index variability in a mid-sized city in the southeastern United States. International Journal Of Environmental Research and Public Health 13(1):117.
Hayhoe K, Sheridan S, Kalkstein L, Greene S (2010). Climate change, heat waves, and mortality projections for Chicago. Journal of Great Lakes Research 36:65-73.
Hulme M, Doherty R, Ngara T, New M, Lister D (2001). African climate change: 1900-2100. Climate research 17(2):145-168.
IPCC (2013). Climate Change. The Physical Science Basis. In TF. Stocker, Qin D, Plattner GK, M. Tignor, SK. Allen, J. Boschung, A. Nauels, Xia Y, Bex V & Midgley PM (Eds.), Contribution of Working Group I to the Fifth Assessment Report of the Intergovernmental Panel on Climate Change (p. 1535). Cambridge, United Kingdom and New York, NY, USA: Cambridge University Press.
Jacob D, Bärring L, Christensen OB, Christensen JH, De Castro M, Deque M, Giorgi F, Hagemann S, Hirschi M, Jones R, Kjellström E (2007). An inter-comparison of regional climate models for Europe: model performance in present-day climate. Climatic Change 81(1):31-52.
Kim J, Waliser DE, Mattmann CA, Goodale CE, Hart AF, Zimdars PA, Crichton DJ, Jones C, Nikulin G, Hewitson B, Jack C (2014). Evaluation of the CORDEX-Africa multi-RCM hindcast: systematic model errors. Climate dynamics 42(5-6):1189-11202.
Kotir JH (2011). Climate change and variability in Sub-Saharan Africa: a review of current and future trends and impacts on agriculture and food security. Environment, Development and Sustainability 13(3):587-605.
Laprise R, Hernández-Díaz L, Tete K, Sushama L, Šeparović L, Martynov A, Winger K, Valin M (2013). Climate projections over CORDEX Africa domain using the fifth-generation Canadian Regional Climate Model (CRCM5). Climate Dynamics 41(11-12):3219-3246.
Ly M, Traoré SB, Alhassane A, Sarr B (2013). Evolution of Some Observed Climate Extremes in the west African Sahel. Weather and Climate Extreme 1:19-25.
Mariotti L, Diallo I, Coppola E, Giorgi F (2014). Seasonal and intraseasonal changes of African monsoon climates in 21st century CORDEX projections. Climatic Change 125(1):53-65.
van Meijgaard E, van UlftL L, van de Berg WJ, Bosveld FC, van den Hurk B, Lenderink G, Siebesma AP (2008). The KNMI regional atmospheric climate model RACMO version 2.1, Tech. Rep. 302.
Moron V, Oueslati B, Pohl B, Rome S, Janicot S (2016). Trends of mean temperatures and warm extremes in northern tropical Africa (1961-2014) from observed and PPCA-reconstructed time series. Journal of Geophysical Research: Atmospheres 121(10):5298-319.
Moss RH, Edmonds JA, Hibbard KA, Manning MR, Rose SK, van Vuuren DP, Carter TR, Emori S, Kainuma M, Kram T, Meehl GA, Mitchell JF, Nakicenovic N, Riahi K, Smith SJ, Stouffer RJ, Thomson AM, Weyant JP, Wilbanks TJ (2010). The next generation of scenarios for climate change research and assessment. Nature 463:747-756.
New M, Hewitson B, Stephenson DB, Tsiga A, Kruger A, Manhique A, Gomez B, Coelho CAS, Masisi DN, Kululanga E, Mbambalala E, Adesina F, Saleh H, Kanyanga J, Adosi J, Bulane L, Fortunata L, Mdoka ML and Lajoie R (2006). Evidence of Trends in Daily Climate Extremes over Southern and West Africa. Journal of Geophysical Research 111:1-11.
Nikulin G, Jones C, Giorgi F, Asrar G, Büchner M, Cerezo-Mota R, Christensen OB, Déqué M, Fernandez J, Hänsler A, van Meijgaard E (2012). Precipitation climatology in an ensemble of CORDEX-Africa regional climate simulations. Journal of Climate. 25(18):6057-6078.
Niosh (1992). Recommendations for occupational safety and health: compendium of policy documents and statements. Department of Health and Human Services, Public Health Service, Centers for Disease Control and Prevention, National Institute for Occupational Safety and Health, DHHS (NIOSH) Publication No. 92–100. http:// www.hpc.ncep.noaa.gov/html/heatindex.shtml.
Occupational Health and Safety Council of Ontario (OHSCO) (2008). http://ggweather.com/101/hi.htm.
SAGNA P (2000) : 0A P.y.ificer.com/101/h*in Atlas du Sénégal,* Paris, s du Saris, , 101/hi.htm./101
Salack S, Sarr B, Sangare SK, Ly M, Sanda IS, Kunstmann H (2015). Crop-climate ensemble scenarios to improve risk assessment and resilience in the semi-arid regions of West Africa. Climate Research 65:107-121.
Samuelsson P, Jones CG, Will´ En U, Ullerstig A, Gollvik S, Hansson UL, Jansson E, Kjellstro¨ M C, Nikulin G, Wyser K (2011). The Rossby Centre Regional Climate model RCA3: model description and performance. Tellus A: Dynamic Meteorology and Oceanography 63(1):4-23.
Sarr AB, Camara M (2017). Evolution des indices pluviométriques xtrêmes par l’analyse de modèles climatiques régionaux du programme CORDEX: Les projections climatiques sur le Sénégal. European Scientific Journal 13:17.
Sarr AB, Camara M (2018). Simulation of the impact of climate change on peanut yield in Senegal. International Journal of physical Sciences 13(5):79-89.
Suparta W, Yatim AN (2017). An analysis of heat wave trends using heat index in East Malaysia. In Journal of Physics: Conference Series 852(1):012005. IOP Publishing.
Sylla MB, Nikiema PM, Gibba P, Kebe I, Klutse NA (2016). Climate change over West Africa: Recent trends and future projections. InAdaptation to climate change and variability in rural West Africa, Springer, Cham, pp. 25-40.
Willett KM, Sherwood S (2012). Exceedance of heat index thresholds for 15 regions under a warming climate using the wet-bulb globe temperature. International Journal of Climatology 32(2):161-177.

APPENDIX FIGURES

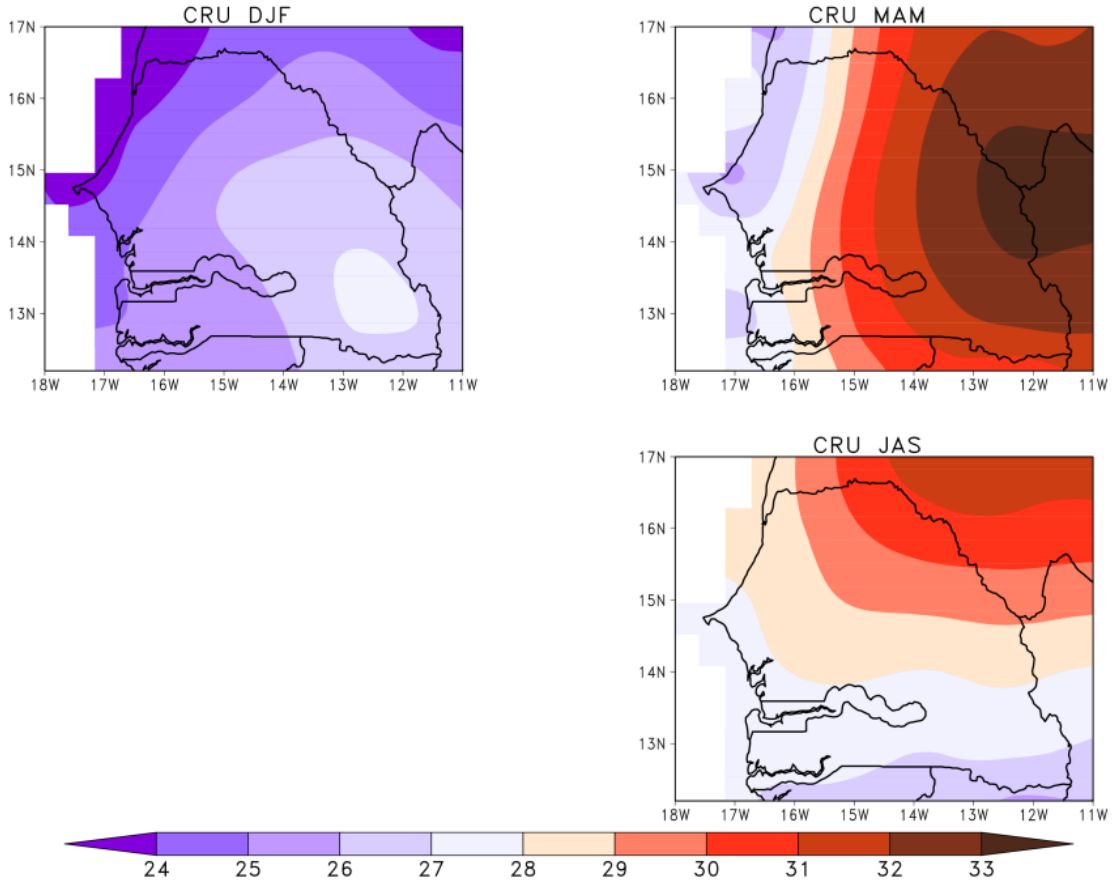

Figure 1. Mean temperature in DJF, MAM and JAS seasons from 1989 to 2008 for CRU data.

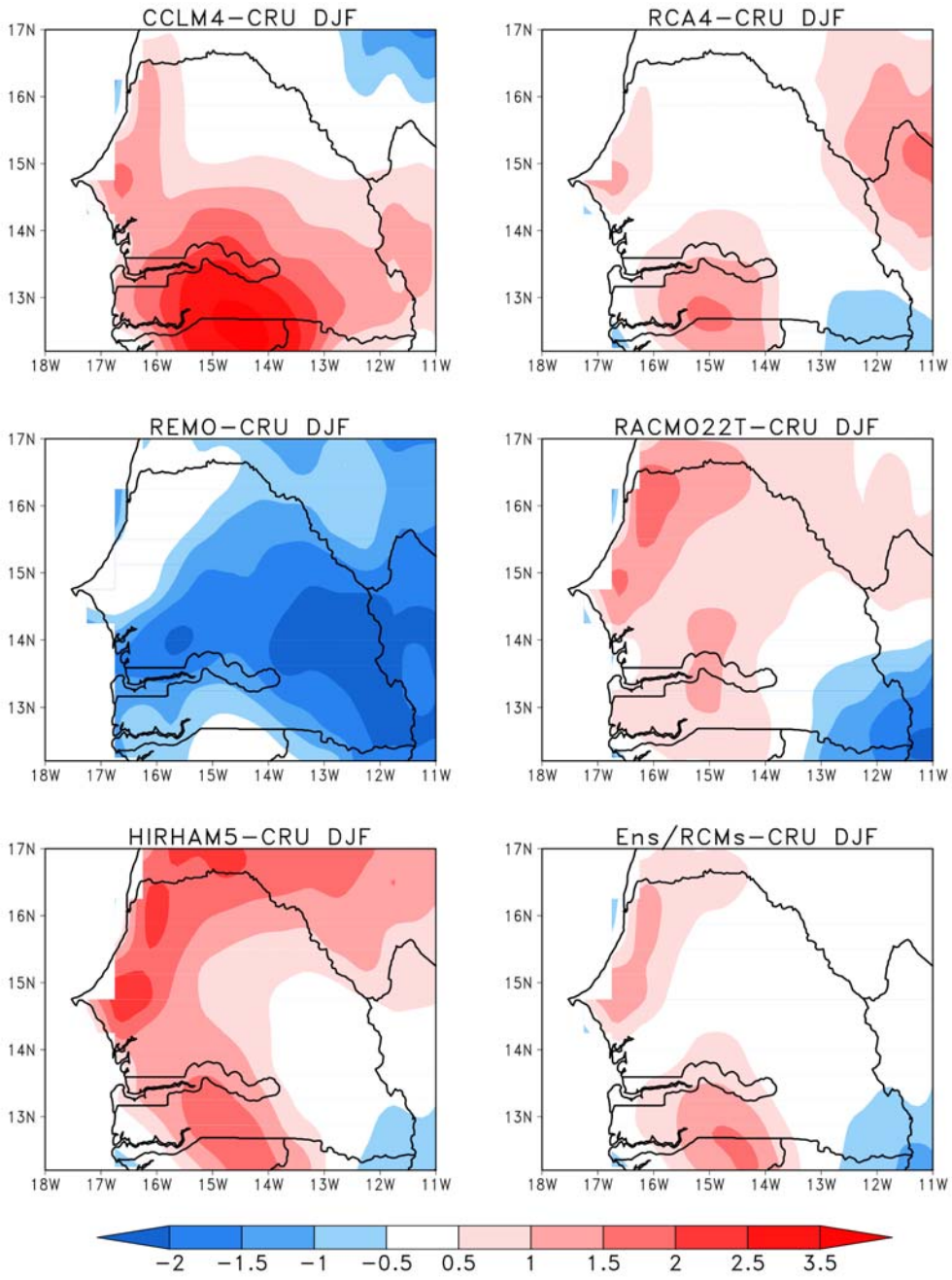

Figure 2. Deviation from CRU observations of mean DJF temperature averaged from 1989 to 2008 of the RCMs and their ensemble mean.

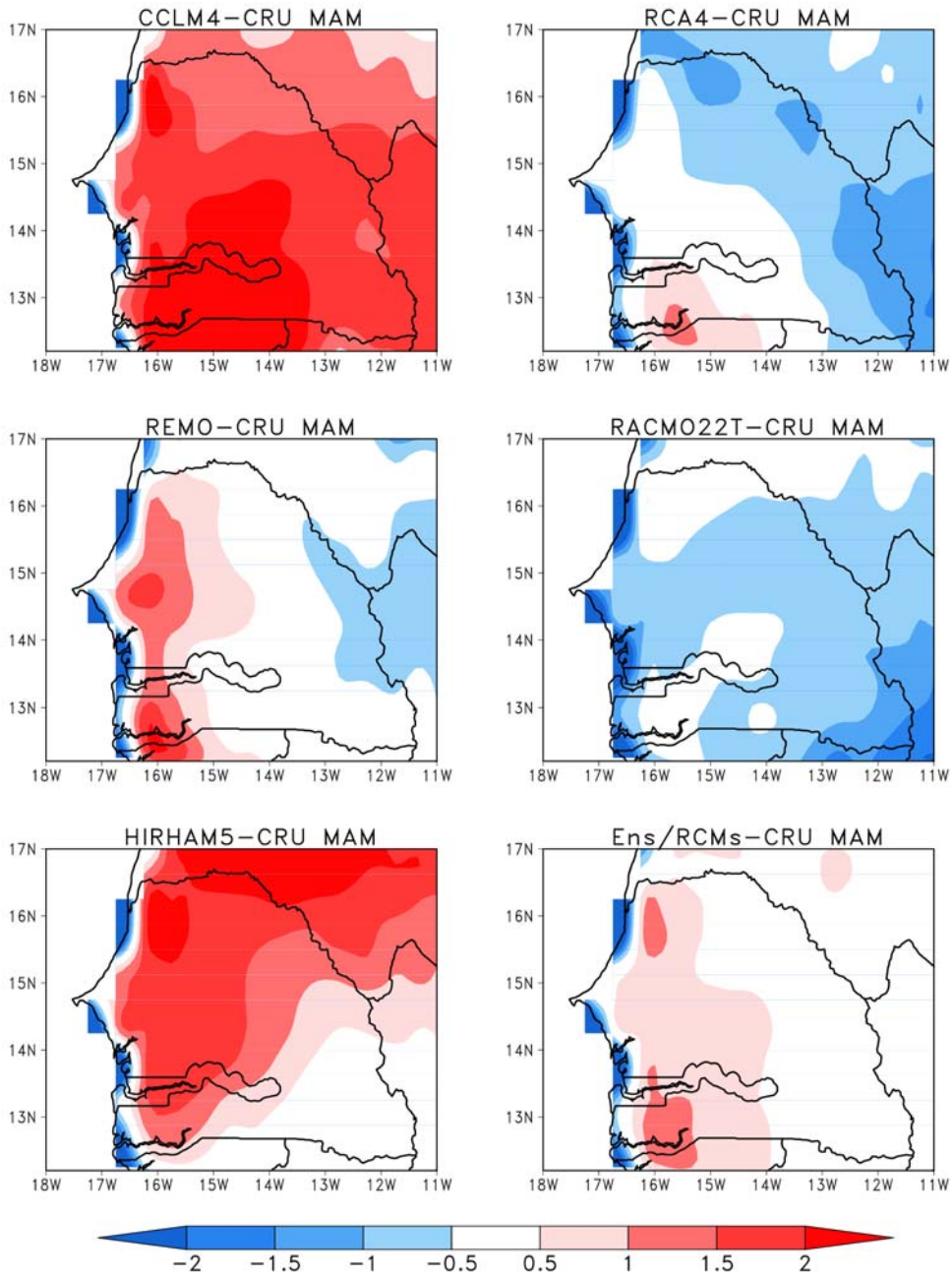

Figure 3. Deviation from CRU observations of mean MAM temperature averaged from 1989 to 2008 of the RCMs and their ensemble mean.

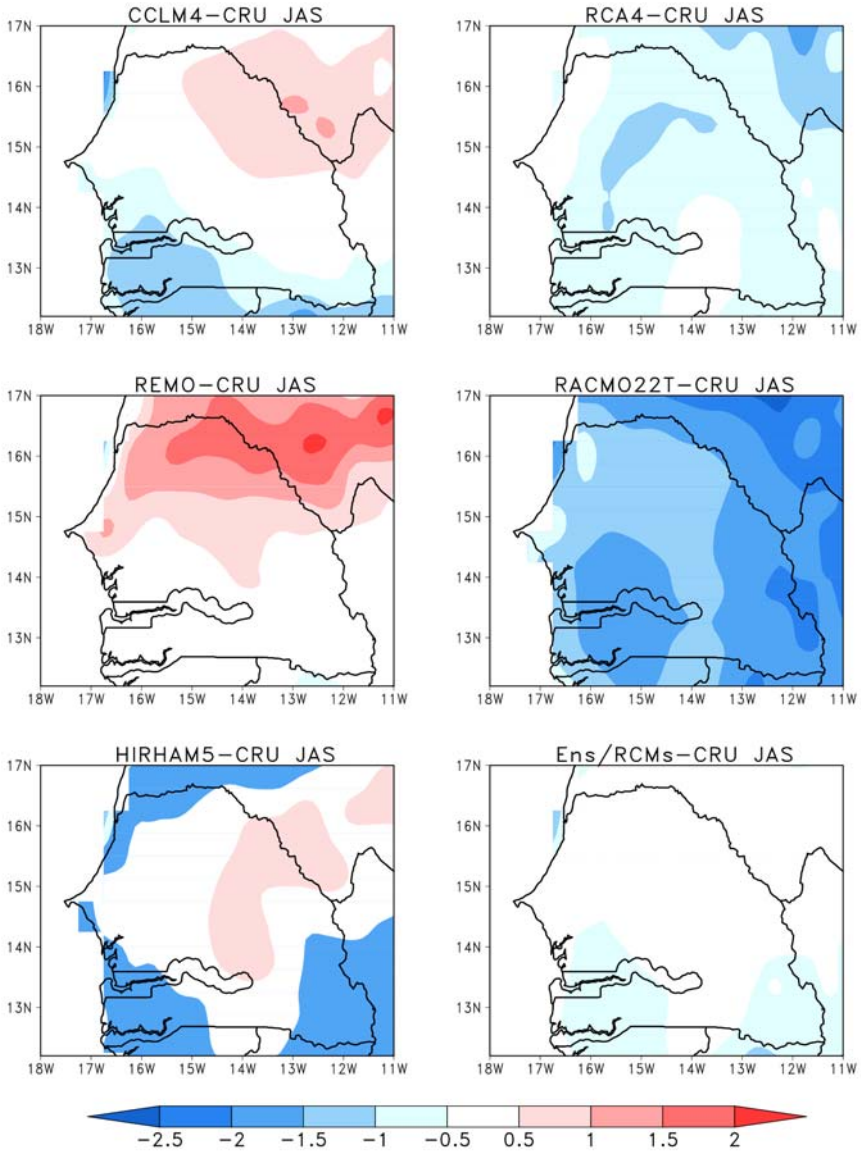

Figure 4. Deviation from CRU observations of mean JAS temperature averaged from 1989 to 2008 of the RCMs and their ensemble mean.

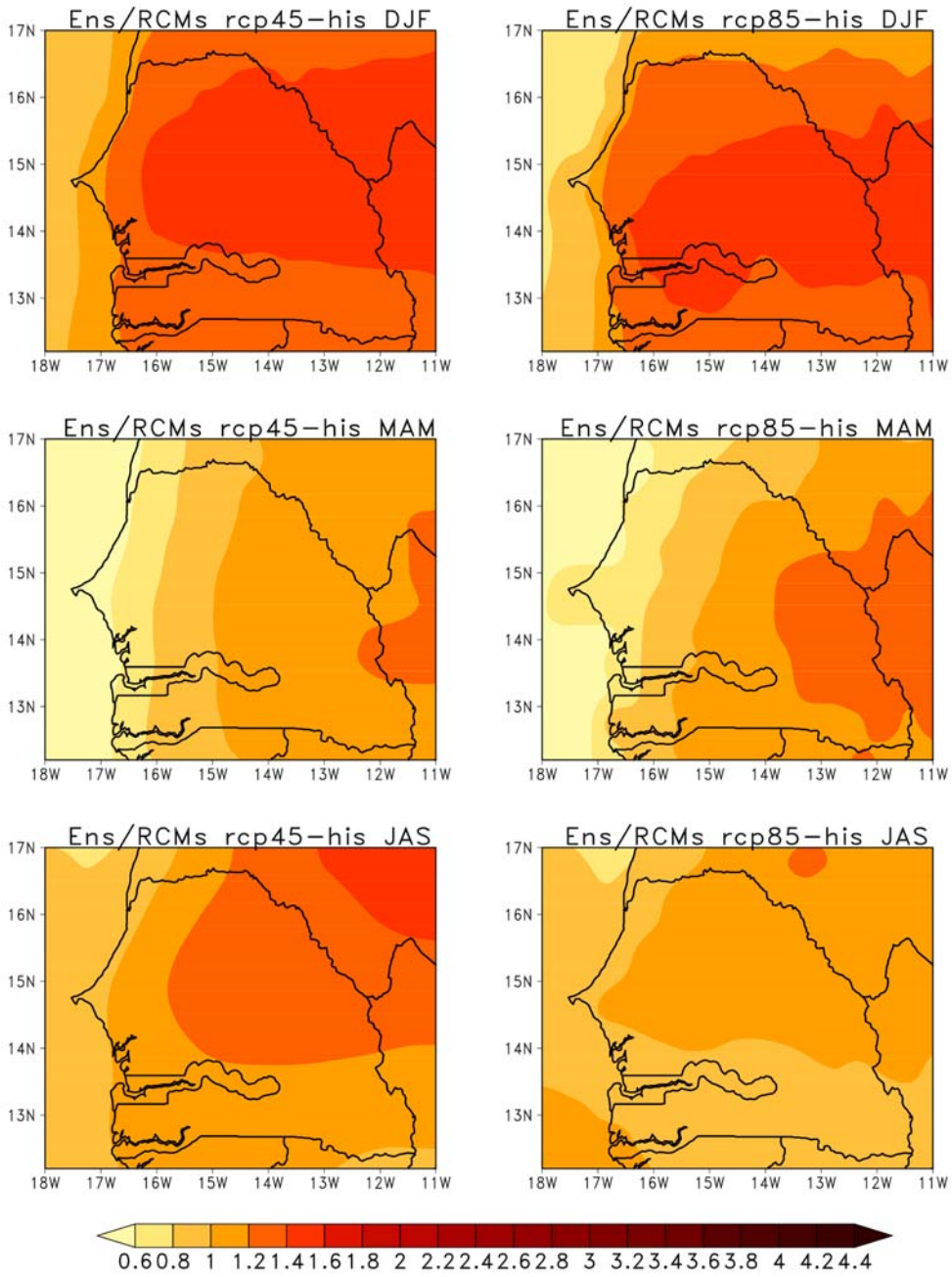

Figure 5. Spatial distribution of the mean surface temperature difference between the near future (2021-2050) and the reference period (1976-2005).

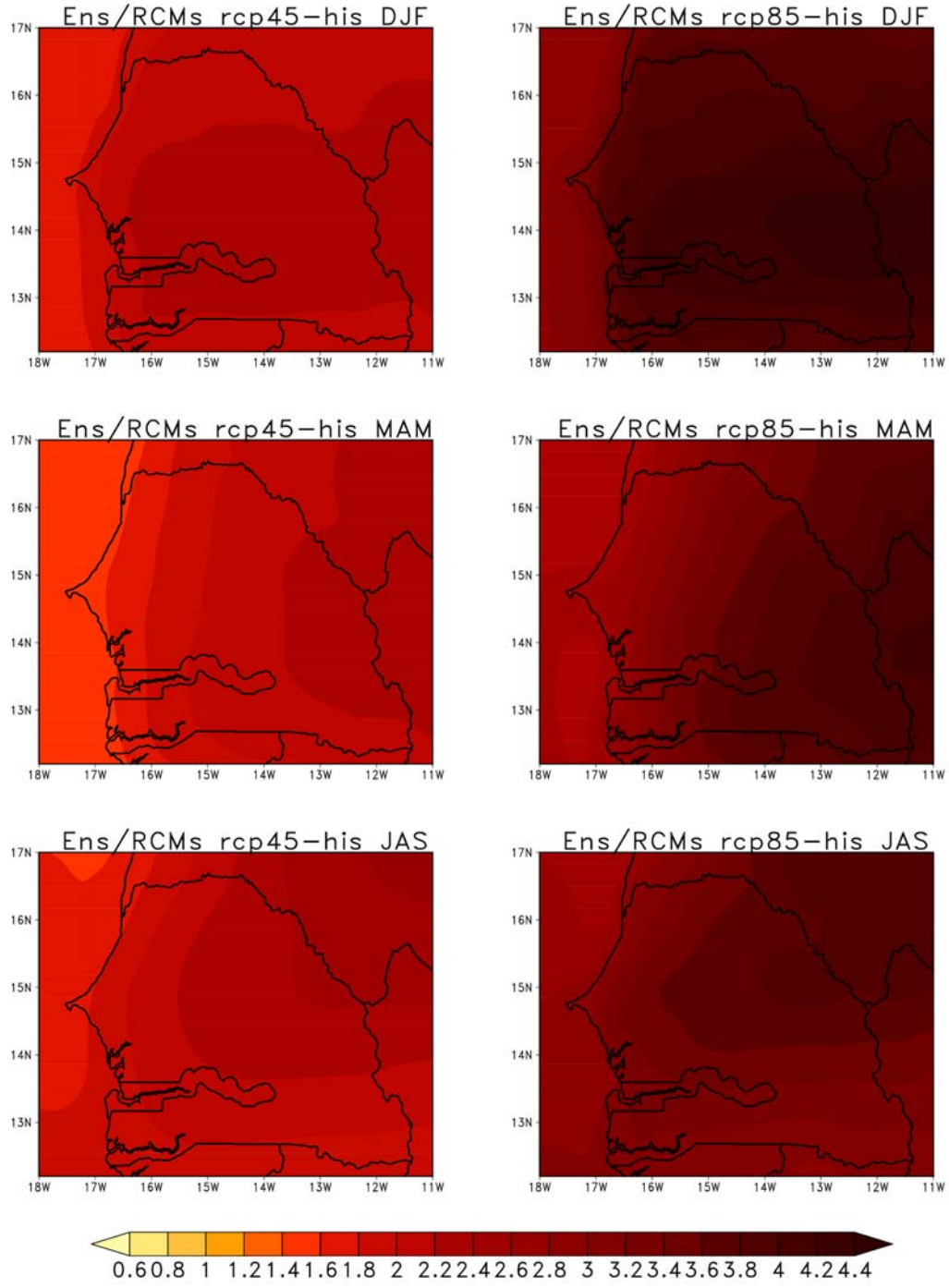

Figure 6. Spatial distribution of the mean surface temperature difference between the far future (2071-2100) and the reference period (1976-2005).

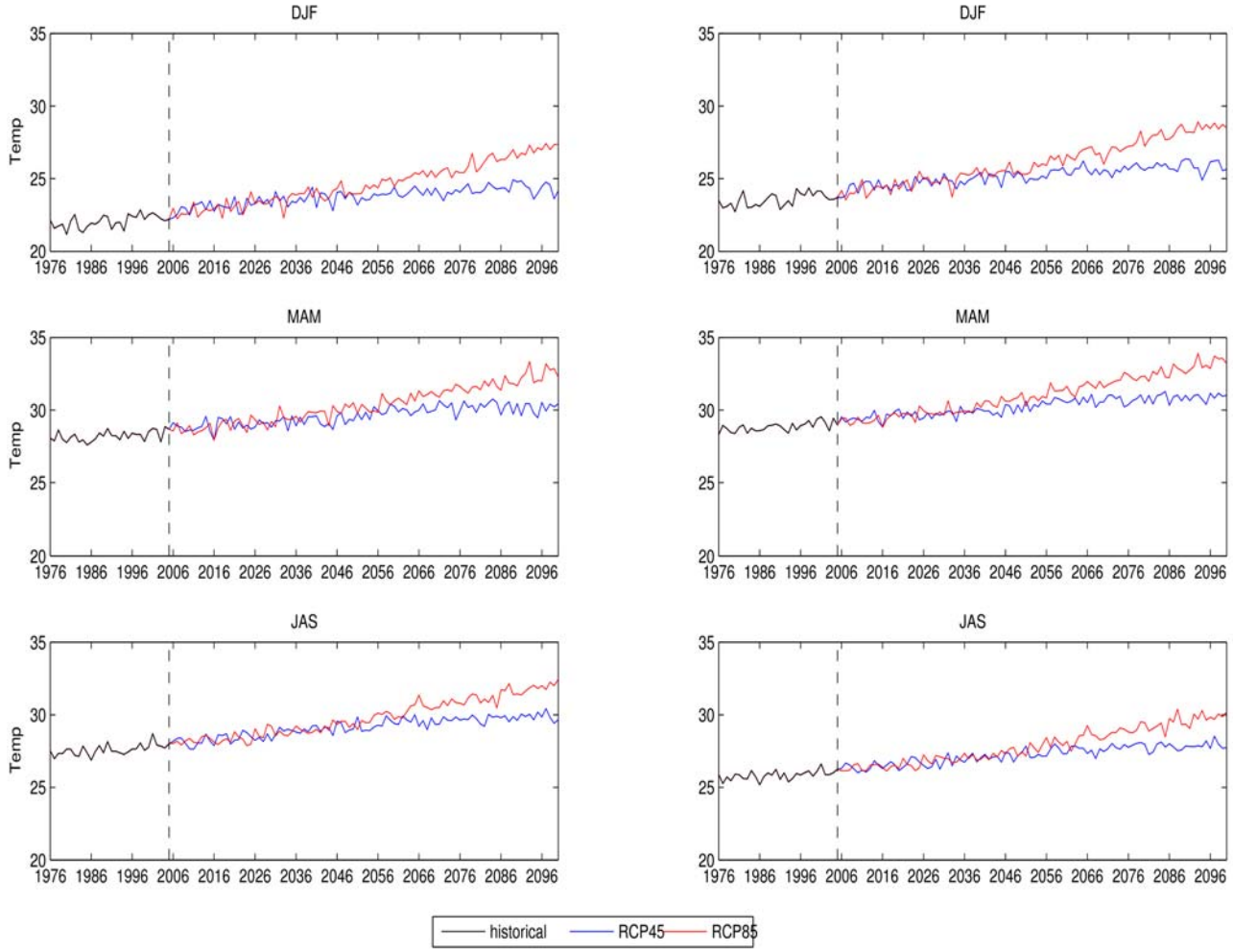

Figure 7. Temporal evolution of the surface temperature (°C) during the cold (DJF), hot (MAM) and wet seasons (JAS) in the north (left panel) and in the south (right panel) of Senegal.

Vol. 13(12), pp. 511-523, December 2019
DOI: 10.5897/AJEST2019.2780
Article Number: 7E7059E62411
ISSN: 1996-0786

http://www.academicjournals.org/AJEST

African Journal of Environmental Science and Technology

Full Length Research Paper

Assessment of hydrological pathway and water quality of the songor wetland, Ghana

Klubi Emmanuel*, Addo Samuel and Akita Lailah Gifty

Marine and Fisheries Sciences Department, School of Biological Sciences, College of Basic and Applied Sciences, P. O. Box LG 99, Legon, Ghana.

Received 16 October, 2019; Accepted 19 November, 2019

Wetlands regulate sediment accumulation, minimize pollution load and act as a buffer against coastal erosion. However, the overflow of seawaters into closed lagoons and wetlands could cause an excessive build-up of solutes through evaporation and could threaten the health of the aquatic life. This study examined hydrological regime, water quality and spatial distribution of flora within the Songor Wetland, Ghana using standard methods. The results indicate hyperhaline (46‰) condition at the west and limnetic [freshwater] (≤ 0.5‰) at the east with mesohaline (±18 - ± 5‰) and oligohaline (±5 - ±0.5‰) in between the east and the west. Natural and anthropogenic barriers are impeding the hydrological connectivity and are creating hyperhaline water conditions that are flowing in the eastward direction. High levels of nitrate (3.5 mg/L) and ammonia (0.25 mg/L) suggested possibilities of toxicity of TDS (41 g/L) and sulphate (4245 mg/L) effect on the biota at the west. While levels of phosphate (1.71 mg/L) and silicate (24.3 mg/L), indicated anthropogenic contamination at the east. Principal Component Analysis (PCA) displayed salinity as the major environmental variable contributing to the spatial variation of the water quality in the wetland. The flow of hypersaline waters in the west-east direction is also confirmed by perfect second-order polynomial relationship between conductivity, salinity and sulphate levels. There exist significant ($p<0.01$, $p<0.05$) correlation among the environmental variables.

Key words: Wetland, salinity, sulphate, water quality, principal component analysis (PCA), Songor.

INTRODUCTION

Wetlands are fragile ecosystems yet vital components of the hydro-biological cycles of the global aquatic ecosystem. They provide a wide range of functions that cumulates to overall well-being and integrity of the aquatic ecosystems and human dependency (McCartney et al., 2010). Wetlands of any form are useful habitats that attract adaptation and modification for food crop and aquaculture development. It is believed that more than billions of world populations depend on wetland resources. Artificial wetlands are also designed and

*Corresponding author. E-mail:efo.emma@gmail.com.

constructed to augment the treatment of wastewaters and effluents (Carter, 1991; Xu and Mills, 2018). The occurrences of natural coastal wetlands in the contiguous zones of oceans and seas provide a defence mechanism for shoreline stabilization against erosive forces of floodwaters and storm runoff from land to sea. As such the built sand bars; mostly separating coastal wetland and the sea provides the seaward and the landward barriers that absorbed wave force at the seaside and floodwaters at the land side. However, these sand bars are becoming targets for sand wining (Amekudzie et al., 2011; Morton, 2003). The sand bars are also intentional breached to allow inflows of seawaters into wetland for salt extraction in addition to mangrove deforestation and exploitation of fisheries resources (Dankwa et al., 2004: Bojang and Ndeso-Atanga, 2009).

Coastal wetlands and their immediate ecotopes are considered as transitional zones unique for protection of coastline and transformation of contaminants. They are formed in close associations with the continental shelves, seas and oceans of which the wetlands are located in low lying coastal plains next to the ocean (Biney, 1990). Some of the coastal wetlands are results of interaction and modification of coastal landscape by tidal and river discharges (Morton, 2003). This placed majority of coastal wetlands as a precarious environment and subjected to destruction and erosion when least disturbed. In contrast, well-established wetlands are remarkable ecosystems that function in improving water quality and stabilization of the coastal sand bars and dunes (Kadlec and Wallace, 2009).

The wetland's vegetation cover together with the sediment and the soils demonstrate severally as an important component of the hydrological network of the wetland ecosystems (Bojang and Ndeso-Atanga, 2009; Helfield and Diamond, 1997). A well maintained and developed hydrological pathways are closely associated with established vegetation cover and improved water quality (Carter, 1991). These place interconnected roles between the vegetation cover and the hydrological connectivity of wetland ecosystems. Natural and anthropogenic modification create biologogical or physical imbalance leading to depletion of the wetland. Therefore, there is a need for a safe guiding of the hydrological networks of wetland ecosystems to maintain the vegetation cover in order to protect coastal wetlands from destruction. The biogeochemical characteristics of wetland are primarily reflections of water balance, quality of water inflow, vegetation cover and human impacts. (Xu and Mills, 2018). Wetland's hydrology dominated by surface water inflow and outflow reflects the chemistry of the associated water bodies. As such wetlands that receive surface waters, groundwater recharge and limited by outflow and loses water mainly by evapotranspiration, turn to have high solutes content (Carter, 1991). Tidal wetlands dominated by intrusion of saline waters influences plant and animal community and species diversity. Whereas in freshwater wetlands, pH and nutrients influence the abundance and species diversity. Therefore, the understanding of wetland community structure and their hydrological network, physical, and biological processes facilitate the management and protection of wetland and their associated basins (Allersma and Tilmans, 1993).

Remarkable importance of wetland's vegetation cover is their ability to reduce gully erosion by stabilizing sediments and absorbing and dissipating water current and energy (Hammer, 1992; Morton, 2003). The capacity of wetlands to stabilize and offer protection against flood and storm runoffs depends on their ability to reduce the erosive forces of water current. This is ascribed to submerge and emerged vegetation that impedes water flow through bouncing off rushing waters. This generates upfront wave surges and causes a reduction in the incoming water current and thereby induces sedimentation in shallow water areas and flood plain of the wetlands (Carter, 1991; Allersma and Tilmans, 1993). Thus, the erosive forces of the waters are considerably dissipated leading to the build-up of natural levees. It is therefore well noted that when wetland vegetation covers are removed, streambanks collapse and channels widen and deepens, turning sediment sinking wetland to sediment sources (Carter, 1991).

In West Africa coastal zones, there are many wetlands in diverse settings from the coastal savanna deserts of Mauritania to dense tropical rainforests of Cameroon (Bojang and Ndeso-Atanga, 2009). The wetlands form semi-continuous chains of water bodies crisscrossing sections of the Africa coastal zones and might be built during the ice formation periods as a result of the lowing of sea level and then separated from the sea by sand bars or formed from wave and tidal interactions (Carter, 1991). The occurrence of wetlands on the low flat plains and hardwood forest, and swampy lands of Cameroon, Nigeria, Ghana and Cote d'Ivoire and other coastal zones could be ascribed as the main stabilization mechanism for coastal land and the seafronts (Bojang and Ndeso-Atanga, 2009).

In recent times, wetlands dominance in coastal zones are declining (Bojang and Ndeso-Atanga, 2009; Oteng-Ababio et al., 2011; Tano et al., 2018). The wetlands losses have been linked to the siltation, expansion of human settlement and extending of bad farming practices (Addo et al., 2011). Pollution and destruction of wetland and their vegetation cover may weakening coastal sand bars and make them vulnerable to wind, current and wave erosions. The Songor wetland located in the west section of the Ada community (Finlayson et al., 2000), is an important economic ecosystem but inadequately studied. Songor lagoon with a mean salinity of 60% could trigger the physiological constraints of the living resources (Dankwa et al., 2004). The sandbar is periodically breached allowing seawater inflow into the Songor lagoon at a higher rate than usual (Dankwa et al.,

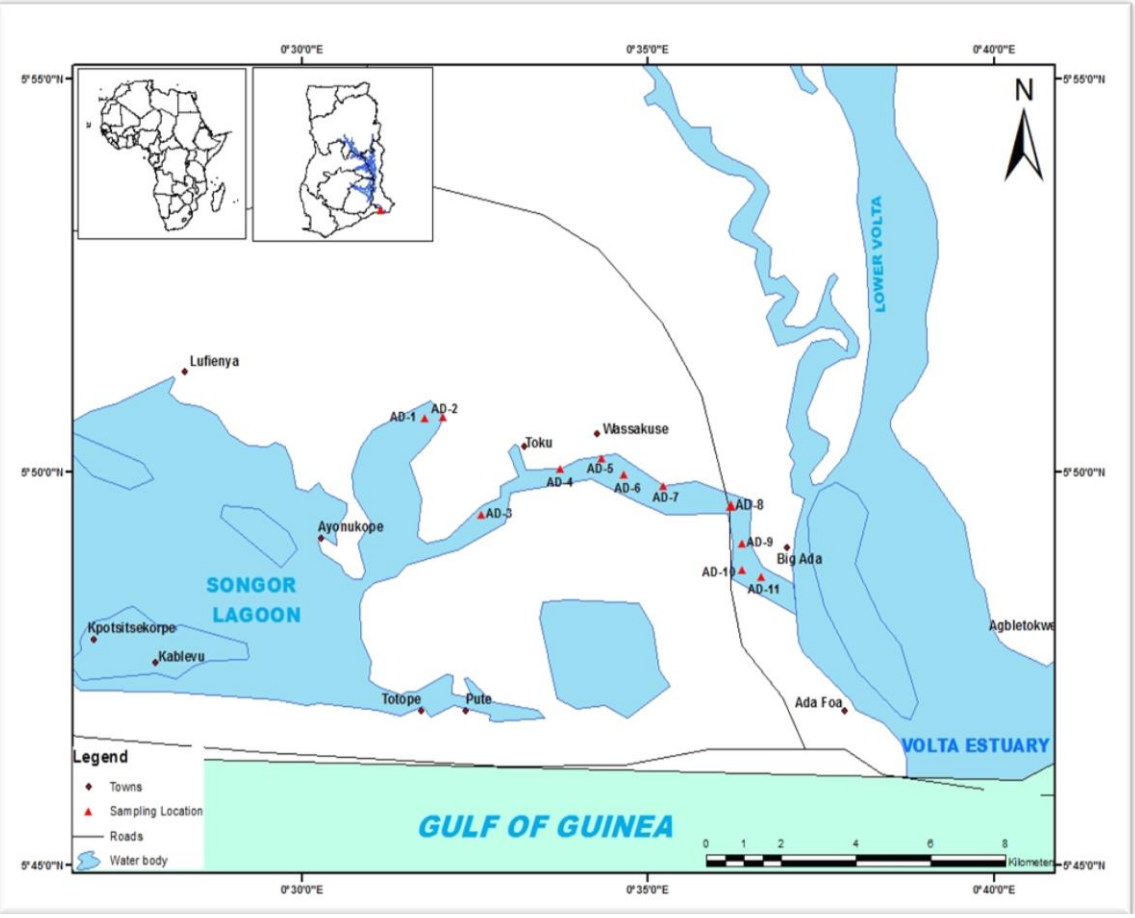

Figure 1. Map of Africa inserted Ghana geographical location indicating the Songor Wetland and the sampling sites.

2004). The study assessed the surface water pathways and its implication through characterisation of the water quality and relative descriptive assessment of flora distribution in the Songor Wetland.

MATERIALS AND METHODS

Study area and sampling strategy

Data collection for the study was done in August 2017. Field samples were done between the Big-Ada (05°48′ 25″ N, 00°37′ E), Wassakuse (05° 49′ 15″ N, 00° 34′ 05″ E), Toku (05° 49′ 15″ N, 00° 33′ E) and the Lufienya (05° 51′ 35″ N, 00° 31′ E) cross-section of the Songor Wetland in the Ada East District of the Greater-Accra Region, Ghana (Figure 1). The Songor wetland covers about 1100 ha of land and forms part of the Volta deltaic system. The wetland is connected to the Songor River at north-east that runs parallel to the lower section of the Volta River. The inflow from the Songor River is limited and only have impacts during the raining season in Ghana. However, the main inflow is the Volta River. The wetland is connected to the Volta River at the east by two canals allowing freshwater inflow with the rising tides from the Volta estuary near Ada Foah. The canals connecting the river formed a network of smaller channels feeding the low lying plains of the wetland. The freshwater inflow has been considered reduced due to upstream dams built on the Volta River at Akosombo and Kpong in 1964 and 1982 respectively (Bollen et al., 2011; Nyarko et al., 2016; Finlayson et al., 2000). As such the volume of freshwater inflow currently depends on the rainfall patterns and the tidal surges through the estuary that “pushes” diverted waters into the wetland. There is also possible surface water runoffs as well as groundwater recharges into the wetland from the northern and the far west sections. It is believed that seawater is also overflowing the strip of sand bar separating Songor Lagoon and the Atlantic Ocean into the wetland at spring and high tide periods (Dankwa et al., 2004).

The sediment types of the Songor Wetland could be relatively described as sand mud texture forming an undulating and isolated strip of parallel sand bars and sand dunes. An earthwork done in other to aid water supply to Wasakuse and Toku communities revealed a long strip of oyster shells. This suggested a possible dump of oyster shells which has been covered by sediments possible during the formation of the deltaic system. This indicates possible occurrences of oysters in the Volta deltaic now replaced by clam (*Galatea paradoxa*) in the sections of the estuary. According to Dankwa et al. (2004), the oyster fishery was ones the main shell fishery of the Keta lagoon a twin water body of Songor Wetland but collapsed due to dam and insufficient inflow of freshwater into the lagoon.

Though the vegetation cover was not assessed for statistical interpretation, crude description of the flora could be that of

transition between freshwater, brackish and none existence in the east to the western direction of the wetland. The elevated sand bar strips and sand dunes are dotted with thicket of semi-deciduous coastal savanna plants. The aquatic plants were of freshwater-brackish water origins (*Nymphaea* sp., *Typha* sp., *Cyperussp.* and *Paspalum* sp.). The hardwood mostly mangrove species (*Avicennia nitida*, *Rhizophora mangle*, and *Acrostichum aureum*) clusters within the east and mid-sections of the wetland. While poorly developed white mangrove (*A. nitida*) were more restricted to mid-section with *Sesuvium portulacastrum* extensions at the extreme end and finally replaced by stunted *Typhae sp*. at the west section. The relatively high sand dunes are dominated by coastal savanna plants species (*Phoenix dactulifera*, *Panicum maximum* and *Digitaria insularis)*. Coconut plants form the vegetation cover of the narrow sand bars between the Atlantic Ocean and the wetland at the south. The north-west sections, however, have *Cyperus sp.* that terminates in the uplands farms and the grazing fields.

Sampling design

Data for assessment of hydrological pathway of the Songor wetland were collected at 1 km intervals within the channel at east and traced the watercourse as far as possible to connect to the Songor lagoon at the west (Figure 1). This approach is modified and adopted sampling strategy for physical and isotopic characteristics of the lower Volta River Basin, Ghana (Gampson et al., 2017). The physicochemical parameters and water samples collections were made possible by a fibreglass boat and trekking at the eastern section (near Big-Ada), mid (Wassakuse) and western sections (Toku and Lufienya) respectively. The sample locations (GPS coordinates) were marked using Garmin GPS (extrex) receiver while the distances between sampling locations were tracked and estimated using the tracking mode of the GPS. The coordinates of the sampling sites were recorded and coded from the west (Songor Lagoon) AD-1 to the east (Big-Ada) AD-11 (Figure 1).

Water quality assessment

The environmental parameters such as pH, conductivity, total dissolved solids (TDS), salinity, temperature, dissolved oxygen (DO) and turbidity were collected *in situ* using a multi-parameter probe (Horiba 52U) with a depth sensor. For best results, three readings were taken and the average values were recorded for each sample locations. Water samples for nutrient analysis were also collected into a cleaned acid-washed and distilled water rinsed 250 high-density polystyrenes (HDPE) bottles. The water samples were placed in thermally insulated container with ice packs to minimize biological activities and transported to the Laboratory of Department of Marine and Fisheries Sciences, University of Ghana. In the Laboratory, the samples were allowed to attain room temperature and analysed for nitrate, phosphate, silicate, sulphate, and total alkalinity levels using spectrophotometer (HACH, DR 2800) adopting APHA (1989) and the WHO, GEMS/WOG (1987) methods. Zero solutions (using distilled water) and sample blanks were prepared for assessing trueness of levels of the measured nutrients. The levels of total suspended solids (TSS) of the sampled waters were determined at 630 nm wavelength after vigorous homogenisation (HACK, 1992).

Summary of chemical analysis procedures

1. Nitrate; cadmium reduction method. 10 ml samples were transferred into a vial and NitrVerfive (5) reagent containing cadmium was added and shake vigorously. The cadmium reduced nitrate to a brownish nitrite and measured at 550 nm: **2**. Phosphate; ascorbic acid method. 10 ml samples were transferred into a vial and PhosVer 3 reagent containing molybdate and ascorbic acid were added and mix gently. Mixed complexes of phosphate and molybdate were formed and the ascorbic acid then reduces the complex into molybdenum blue and measured at 880 nm: **3**. Silicate; Silicomolydate method. 10 mL samples were transferred into a vial and Silicate Reagent Set (Molybdate, Acid Reagent and Citric Acid) were added in turns. Molybdate ions react with silicate and phosphate in the sample to form a yellow complexes silicomolybdic and phosphomolybdic acids. Addition of citric acid destroys phosphate complexes leaving the silicomolybdaic acid and measured at 452 nm: **4**. Sulphate; USEPA Method 375.4. 10 ml samples were transferred into a vial and SulfaVer 4 reagent containing barium was added and mix gently. The barium ion react with sulphate ions to form white precipitate and was measured at 450 nm.

Data analysis

Pearson correlation analysis with two significance levels ($p<0.05$ and $p<0.01$) were employed to establish linear relationships between the measured physicochemical parameters. Cluster Analysis and Principal Component Analysis (PCA) were also conducted to established associations and sources of variation in water quality using Plymouth Routines in Multivariate Ecological Research (PRIMER)vz. 6 computer software. The data was square-root transformed and standardized to obtain a normalized distribution. A resemblance matrix of Euclidean distance was applied and used to plot the contour lines and subsequently overlaid on the PCA chart. The critical linkages distance used to distinguish the various clusters were based on the similarity profile test (SIMPROF). The clusters obtained were then used to explain the site-specific characteristics of the water quality of the wetland. Bar graphs were also used for graphical representation of physicochemical parameter levels using OriginPro 10.35 and Excel computer software. Linear graphs were also generated using second polynomial plots.

RESULTS

Water quality parameters

The water quality parameters (TDS, salinity, conductivity, sulphate and alkalinity) measured at the sampling stations of the Songor Wetland (Table 1) indicates decreasing trend from the west to the east. Water temperature levels were quite uniform with arithmetic mean of 28 ± 1°C. The conductivity of the waters ranges between 0.43 and 68.4 mS/cm with arithmetic mean of 11 ± 19 mS/cm. There is a remarkable association with conductivity (68.4 mS/cm), salinity (46.6‰), TDS (41 g/L) and sulphate (4245 mg/L) at AD-1 (at the western section of the study area) (Figure 1 and Table 1) indicating seawater intrusion. Whereas the low levels of conductivity (between 0.43 to 4 mS/cm), salinity (0.2 to 2.1‰), and TDS (0.28 and 2.56 g/L) and sulphate (60 to 70 mg/L) at locations AD-11, AD-10, AD-9 and AD-8 (Table 1 and Figure 2) of the eastern section could be related to freshwater inflow from the lower section of the Volta River. However, this is slightly above the physicochemical parameters (salinity [0.02-0.03 PSU], TDS [27-35 mg/L] and conductivity [52-70 µS/cm[)

Table 1. Physicochemical parameters of the sampling point, Songor Wetland, Ada.

SID	Temp. (°C)	pH	Turb (mg/L)	DO (mg/L)	TDS (g/l)	Salinity (ppt)	Cond ($mScm^{-1}$)	ORP (mV)	Depth (m)
AD-1	29.42	8.26	19	3.23	41	46.6	68.4	-42	0.2
AD-2	27.5	7.79	15.1	6.87	3.19	2.7	5.07	91	0.45
AD-3	25.55	7.21	57	7.7	9.3	8.7	15	-104	0.25
AD-4	28.17	7.84	34	11.11	6.51	6.1	10.7	-55	0.3
AD-5	27.72	7.03	22.6	6.51	3.57	3.1	5.66	131	0.6
AD-6	28.18	6.8	24.2	6.03	3.57	3.1	5.67	143	0.75
AD-7	27.8	6.65	14.2	1.45	3.63	3.1	5.74	-1	2.45
AD-8	28.69	6.93	37	1.76	2.56	2.1	4	30	0.5
AD-9	27.28	7.23	248	7.4	2.04	1.7	3.19	131	0.4
AD-10	27.97	7.41	72.7	10.92	1.82	1.5	2.84	165	0.95
AD-11	27.42	7.33	33.4	9.06	0.28	0.2	0.43	185	1.4
Mean ± SD	28 ± 1	7.32 ± 0.49	52 ± 67	7 ± 3	7 ± 12	7 ± 13	12 ± 19	61 ± 100	0.8 ± 7
Minimum	25.55	6.65	14.2	1.45	0.28	0.2	0.43	-104	0.2
Maximum	29.42	8.26	248	11.11	41	46.6	68.4	185	2.45

SID, Sampling point; Temp, Temperature; Turb; Turbidity,TDS, Total dissolved solids; ORP, Oxidation reduction potential; mV, Millivolts; ppt, Part per thousand (‰).

reported for the lower Volta River Basin (Obirikorang et al., 2013), and are indication of the mixing of fresh water from the Volta River at the east with infiltrated saline water from the west of the wetland. The measured TDS, salinity and sulphate levels at location AD-1 were above the average seawater value [salinity (35‰)] (Carter, 1991; Karikari et al., 2009) due to limited inflows of freshwater into the wetland at the west. The salinity at location AD-1 was higher than the salinity range (34.6- 35.4‰) recorded for the near offshore coastal waters of Ghana (Karikari et al. 2009). However, the level of conductivity (5.07 $mScm^{-1}$), salinity (2.7‰), TDS (3.19 g/L) and sulphate (550 mg/L) at AD-2 close to AD-1 were low. On the contrary, the levels of conductivity, salinity, TDS and sulphate were surprisingly high at AD-3 and AD-4 than at AD-2 (Table 1) which are eastward of AD-1 and AD-2 respectively. This suggests inflow of saline water from AD-1 towards the eastern section of the Songor Lagoon despite a physical separation between location AD-1 and AD-2.

Alkalinity ranged between 60 and130 mg/L $CaCO_3$ with arithmetic mean value of 83 ± 22 mg/L $CaCO_3$ (Figure 2). The slightly alkaline (pH 8.26) nature of waters at AD-1 could be associated with seawater. While about neutral (pH 7.03 and 7.79) (Table 1) could be related to freshwater from the lower Volta River and mixing of seawater by surface runoffs from the northern section of the wetland. The slight acidity (pH between 6.93 and 6.65) of the waters at the mid-section (AD-6, AD-7 and AD-8) could be results of the breakdown of organic matter from litter falls of white mangroves. The oxidation-reduction potential (ORP) levels (between -104 and 185 mV) (Table 1) assumed more positive values than negative values and could be interpreted as oxidation reactions are favoured in the wetland. This can be related to high levels of oxygen recorded across the wetland (Table 1). Turbidity levels were erratic and ranges between 14.2 and 248 mg/L with arithmetic mean value of 52 ± 67 mg/L (Table 1). The relative high turbidity levels at the eastern section (AD-11 [33.4 mg/L], AD-10 [72.7 mg/L], AD-9 [248 mg/L] and AD-8 [37 mg/L] (Table 1)) could be results of physical interaction of fast-moving waters exiting the wetland due to ebbing tides at the Volta estuary. While the high turbidity at AD-3 (57 mg/L) and AD-4 (34 mg/L) could be attributed to wave-induced turbulence.

Nitrate and ammonia levels were relative high at AD-1 (Figure 2A and B) and decrease to relatively uniform levels at the eastern section of the study area. The relatively high levels of nitrate (3.5 mg/L) and ammonia (0.25 mg/L) at AD-1 also corresponded to high levels of sulphate, salinity, TDS and conductivity. Reactive phosphate and silicate levels, on the other hand, were

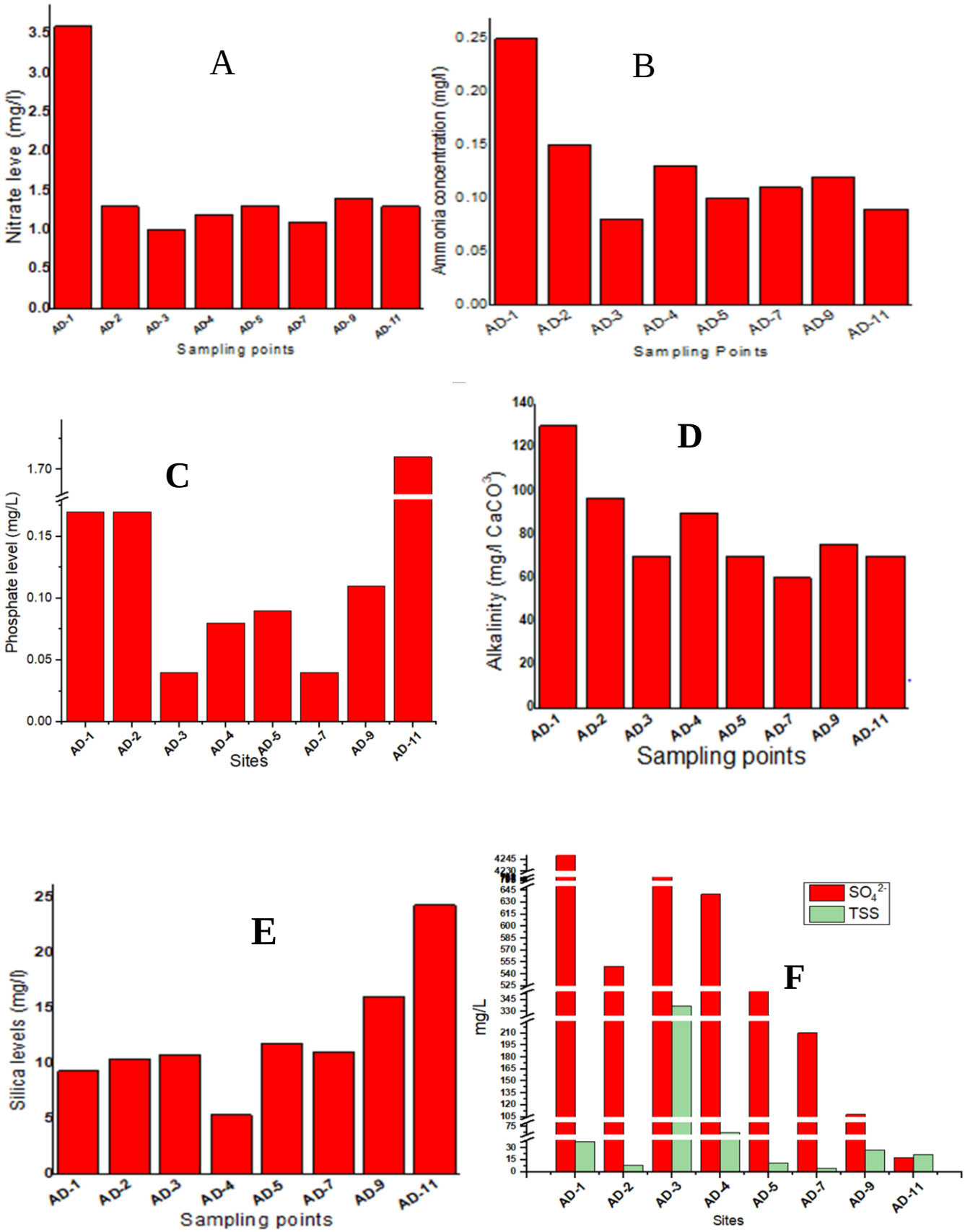

Figure 2. Nutrient, alkalinity and TSS levels within cross section of Songor Wetland.

exceptionally high at AD-11 and decreases towards the western section of the study area (Figures 1, 2C, 2E). Total suspended solids (TSS) levels were erratic and varied between 4 (AD-7) and 337 mg/L (AD-3) (Figure 2F). The levels of TSS were in the same ranges (16.6 – 361.16 mg/L) as those measured for the Can Gio estuary (Thanh-Nho et al., 2018) (Table 1). However, the relatively high levels of TSS measured at locations AD-3 and AD-4 could be attributed to disturbance of bottom sediment due to wind-induced wave interactions with the bottom bed. The high level of the TSS measured at location AD-3 were lower than the range of the World Rivers (10 – 1,700 mg/L) (Berner and Berner, 1987; Cang et al., 2007).

Multivariate analysis

Pearson coefficient analysis

The result of the multivariate analysis using Pearson Coefficient Analysis is reported in Table 2 indicates that there are significant correlations between the physico-chemical parameters as was expected. Temperature levels displayed moderate correlation with TDS (r = 0.59), conductivity (r = 0.59), salinity (r = 0.61) and sulphate (r = 0.61) while the relation between TSS assumed negative correlation (r = -0.71) (Table 2). There were strong and significant ($p < 0.01$) correlations between conductivity and salinity (r = 1.00), TDS (1.00), sulphate (1.00) and alkalinity (0.84) (Table 2). The perfect correlation between conductivity and the other parameters displayed a linear relationship between points of high and low concentrations (this could be passed for a calibration curve for serial dilution solutions). There were also a strong and significant ($p < 0.01$) correlation between alkalinity and pH (r = 0.93), conductivity (r = 0.84), TDS (r = 0.84), salinity (r = 0.85) and sulphate (r = 0.88) (Table 2). Moderate to strong relation and significant ($p < 0.05$ and $p < 0.01$) correlation also existed between pH and conductivity (r = 0.67), TDS (r = 0.67), salinity (r = 0.67), sulphate (r = 0.71) and alkalinity (r = 0.93) (Table 2).

Principal component analysis

Principal Component Analysis (PCA) was performed by excluding conductivity, TDS, sulphate and alkalinity data for salinity and pH respectively base on the Pearson Correlation Coefficient values (Table 2). This is because highly correlated variables are believed to have similar effect and direction and any of such variables could be substituted (Kendall, 1975). The plot of PC1 and PC2 with overlaid cluster chart (Figure 3) show significant groupings of water quality parameters and associated sample locations. Salinity is displayed as the greatest discriminant variable (-0.935) (Table 3) and could be considered as the main water quality parameter affecting the spatial distribution of the water quality within the wetland. This by extension includes conductivity, TDS, sulphate and alkalinity together with salinity are the main indicators of the hydrological pathways of the wetland. Turbidity and dissolved oxygen (DO) levels also contributed significantly to the variabilities of water quality parameters within the wetland. For visual inspection, Euclidean distances (contour marks) were used for clarity (Figure 3). This placed location AD-1 as an outlier with salinity as the discriminating factor (that is, salinity, conductivity, TDS, sulphate, and partly pH [that is, pH and alkalinity] and temperature), followed by AD-3 and AD-4; AD-2, AD-5, AD-6 and AD-8; and AD-11.

The five principal components (PC1, PC2, PC3, PC4 and PC5) computed, four are contributing 100% of the total variabilities while the fifth PC loaded by pH and temperature formed zero per cent (Table 3). This is indicating that pH and temperature contributions to the spatial water quality distribution within the wetland are less significant (pH and temperature levels across the study area could be considered as constant (Table 1)). PC1 formed 60.1% of the variabilities with salinity as the main factor; including conductivity, TDS and sulphate (Tables 2 and 3).These variables have a high score for location AD-1 and followed by AD-3, AD-4, and the AD-11 the least (Tables 3 and 4). As such this is confirming location AD-1 as an area of high saline water environment and reduces in the eastward direction with AD-11 the least impacted with salinity. PC2 assumed 26.9% of the total variabilities with turbidity as the main factor having high scores for location AD-9 and followed by AD-3, AD-10 and AD-4 (Table 4). This placed turbidity variability as erratic and could be due to localized effect like wind and water current as illustrated in section 3.1. PC3 formed 9% of the total variabilities with water depth and dissolved oxygen (DO) the most dominating factor. The water depth has a high score for locations AD-7 and AD-9 (Table 4) indicating these areas are the lowest (deeper) section of the wetland. PC4, 4% of the total variability loaded by DO and have a high score for locations AD-10, AD-11 and AD-4 (Tables 3 and 4). PC5 accounted for zero per cent of the variability and loaded by pH (Table 4). This suggested that the levels of pH within the study area are similar and are not significantly different between sample locations.

In-situ and *ex-situ* measurements and relating them to the Pearson Correlation Coefficient and the PCA: salinity, conductivity, TDS and sulphate levels and their trend displayed a stepwise gradient across the study area. This is demonstrated in Figure 4A and B by a plot of a second-order polynomial curve between salinity and sulphate; salinity and conductivity respectively. This has confirmed the linearity of conductivity (TDS) and salinity and salinity. It should be noted that conductivity is one of the basic water quality parameters and the basis for calculating TDS and salinity (Carter, 1991). As such this study has

Table 2. Pearson correlation between the physicochemical parameters within the Songor Wetland, Ada.

	Temp.	pH	Cond	DO	TDS	Salinity	Silicate	Sulphate	TSS	Alkalinity
Temp.	1.00									
pH	0.53	1.00								
Cond	0.59	0.67	1.00							
DO	-0.33	0.23	-0.41	1.00						
TDS	0.59	0.67	1.00**	-0.41	1.00					
Salinity	0.61	0.67	1.00**	-0.42	1.00**	1.00				
Silicate	-0.23	-0.32	-0.35	0.13	-0.36	-0.33	1.00			
Sulphate	0.61	0.71	1.00**	-0.39	1.00**	1.00**	-0.36	1.00		
TSS	-0.71	-0.05	0.07	0.24	0.08	0.05	-0.18	0.04	1.00	
Alkalinity	0.67	0.93*	0.84*	-0.12	0.84*	0.85*	-0.39	0.88*	-0.15	1.00

Level of significance: *P < 0.05 **P < 0.01 (Pearson's rank of correlation).

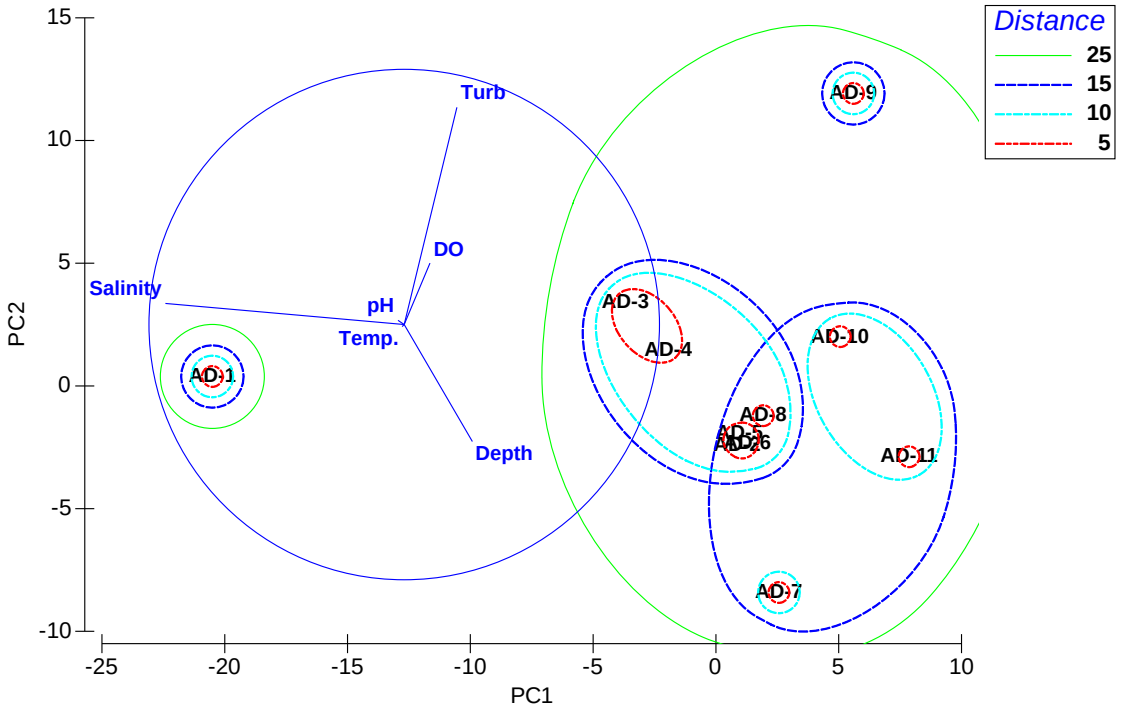

Figure 3. PCA overlay with cluster analysis showing sampling points by Euclidean distance.

Table 3. Factor loading matrix for principal component (PC) axes.

Factor	PC1(60.1)	PC2 (26.9)	PC3 (9)	PC4 (4)	PC5 (0)
Temperature	-0.008	-0.008	-0.009	-0.008	0.515
pH	-0.024	0.016	0.039	0.044	0.856
Turbidity	0.207	0.851	-0.477	0.07	0.008
DO	0.101	0.241	0.584	0.766	-0.043
Salinity	-0.935	0.083	-0.219	0.263	-0.027
Depth	0.267	-0.458	-0.617	0.581	0.01

Table 4. Scores loading matrix for the variables that determine principal component.

Locations	SCORE1	SCORE2	SCORE3	SCORE4	SCORE5
AD-1	-20.52	0.38	-1.85	0.80	0.14
AD-2	0.88	-2.42	3.50	-1.24	0.21
AD-3	-3.68	3.43	1.33	-0.12	-0.41
AD-4	-1.94	1.46	3.82	1.08	0.10
AD-5	0.97	-1.95	1.91	-0.56	-0.15
AD-6	1.26	-2.31	0.95	-0.23	-0.21
AD-7	2.57	-8.42	-5.84	0.70	-0.06
AD-8	1.93	-1.21	-0.86	-4.69	0.11
AD-9	5.60	11.92	-3.67	-0.44	0.06
AD-10	5.06	2.01	0.12	2.66	0.08
AD-11	7.87	-2.89	0.60	2.05	0.12

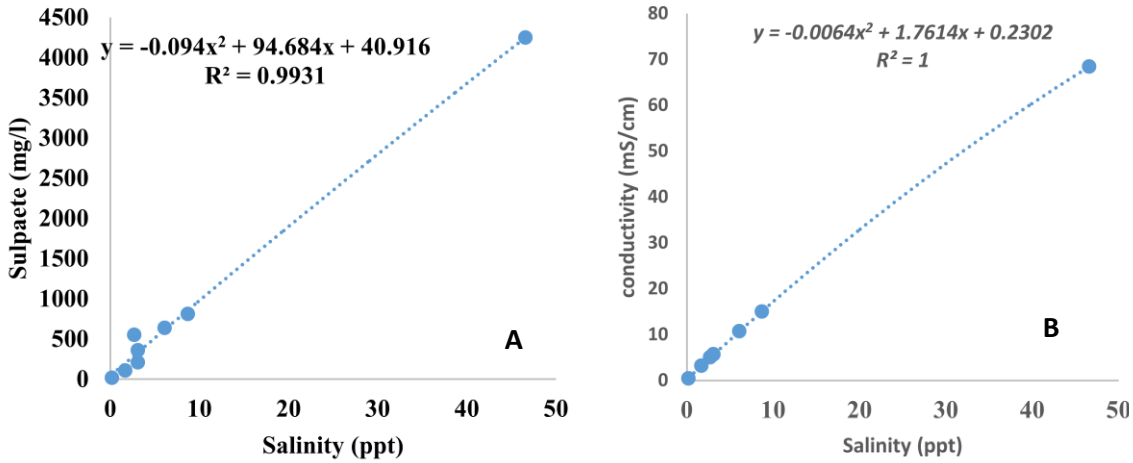

Figure 4. Second order polynomial relationship between salinity and sulphate (A) and conductivity (B) within the studied sites of the Songor Wetland, Ada ppt; part per thousand.

also established that conductivity could be used to estimate sulphate levels through salinity (Figure 4B).

DISCUSSION

The hydrological network of the study area is composed of freshwater at the east, north-west and seawater at the south-west corner. The waters of the study area can be classified as limnetic (freshwater) [salinity ≤ 0.5‰], oligohaline (salinity ± 0.5 - ± 5‰), mesohaline (salinity ± 5 - ± 18‰) and hyperhaline (salinity ≥ ±40‰) (Venice System, 1959). This is demonstrated copiously by low values of the physicochemical parameters (salinity, conductivity sulphate, TDS and alkalinity) at the east and

high values, at the west (Table 1 and Figure 2D respectively). The remarkable differences in the water quality parameter in the Songor Wetland are due to freshwater inflows from the lower section of the Volta River Basin through the Ada community at the east and seawater inflow from the south-west corner near Totope. The high levels of conductivity, salinity TDS and sulphate at AD-1 compared to AD-2 and AD-3 and AD-4 (Table 1) could be assigned to human interference with the natural hydrological connectivity and the topography of the wetland. According to Dankwa et al. (2004), there were periodical breaching of sand bar near Totope to allow seawater into the Songor Lagoon for extraction of salt together with the observed remnant of a dike between AD-1 and AD-2 are the causes of the sharp differences in the water quality parameters at the west of the study area. However, the measured parameter levels were above the average seawater values [salinity (35‰)] (Carter, 1991), especially at location AD-1. The extremely high levels of conductivity, TDS, salinity and sulphate could be due to evaporation resulting in concentrating of solute fractions of the introduced seawater at the western section of the Songor Wetland. The relatively high levels of conductivity, salinity, TDS and sulphate at AD-3 and AD-4 than at AD-2 (Table 1) suggested possible collapses of the salt pond dike and non-existing of the dike at far south of AD-1. This is, therefore, allowing the heperhaline waters at the western section of the wetland to naturally flow by force of gravity due to the sloppy terrain in the eastward direction despite the blockage at AD-2. The partition exacerbates concentration of ions through evaporation and the body of waters shrinks due to the surface-to-volume ratio increase as a result of an accelerated rate of evaporation. This may cause already shallow wetlands to suffer dryness and susceptible to wind erosion.

The slight alkaline (pH 8.26) nature of waters at AD-1 could also be associated with seawater. While about neutral pH 7.03 and 7.79 (Table 1) also suggested freshwater inflows from the lower Volta River Basin and mixing of seawater by surface runoffs from the northern section of the wetland. However, the slight acidity (pH between 6.93 and 6.65) nature of the waters at the mid-section (AD-6, AD-7 and AD-8) (Table 1) may be results of breakdown of organic matter from litter falls of white mangroves. Anaerobic breakdown of organic matter in the presence of sulphate ions, humic acid and hydrogen sulphide are produced (Xu and Mills, 2018). Humic acid are considered as the most contributors of CO_2 in the wetland ecosystem that combine with water molecules to produce acidic conditions (Xu and Mills, 2018). Nevertheless, oxidation-reduction potential (ORP) levels assumed more positive values than negative values suggesting that oxidation reactions are more favoured in the wetland. This is reflected in relative high levels of dissolved oxygen (Table 1) across the study area. This could be due to the mixing effects by wind and reversal in the outflow of waters of the wetland at the east due to ebbing tides at the estuary near Ada-Foah.

The erratic nature of the turbidity levels, especially the high levels at the eastern section (AD-11, AD-10, AD-9 and AD-8 (Table 1) could be as a results of physical interaction of fast-moving waters out of the wetland due to ebbing tides at the Volta estuary near Ada-Foah. While the high turbidity at AD-3 and AD-4 are possible wave-induced turbulence. The locations AD-3 and AD-4 have limited vegetation covers and wind fetch could cause wave to interact with the bottom floor thereby introducing suspended matter into the water column.

Nitrate and ammonia displayed relatively high levels at AD-1 and they decreased to uniform levels across the study area suggested an increased nutrients load of waters of the western section of the wetland (Figure 2A and B). The high levels of nitrate and ammonia at AD-1 and their association with high levels of sulphate, salinity, TDS and conductivity are indications of possible physical and biogeochemical interactions of the water quality parameters with fauna and flora (Xu and Mills, 2018). For instance, high levels of TDS indicates excess ions in solution. The excess ions in solution cause the cells of living organisms to lose water through ion gradients to their immediate surroundings and thereby causing their cells to shrinks and collapse (Carter, 1991). The high nitrate and ammonia levels at AD-1 could be a result of oxidation and reduction of decaying organic matter of fauna and microphyte through mortality caused by hyperhaline conditions at the west of the wetland. This explained the low abundance and diversity of fish species reported by Dankwa et al. (2004) in the Songor Lagoon as compared to the Keta Lagoon.

The exceptionally, relatively high levels of reactive phosphate and silicate at AD-11 and decreases towards the western section of the wetland (Figure 2C and E) suggested anthropogenic impacts of freshwaters intrusion from the Volta River through the Big-Ada community. The high levels of phosphate compared to the finding of Obirikorang et al. (2013) suggested that the nutrient load is of immediate anthropogenic influence. Due to lack of proper drainage systems in the rural communities of the developing countries which could be the case of the Bid-Ada, where most domestic wastes contaminated with detergents are discharged into the opened drains. This contaminated swages could by arriving in the wetland with the rising tides. The variability in the total suspended solids (TSS) levels across the study areas is an indication of a localized effect (e.g., wind-induced turbulence) on the water quality. The relatively high levels of TSS at locations AD-3 and AD-4 could be attributed to disturbance of bottom sediment due to wind-induced wave interactions with the bottom bed.

Pearson coefficient correlation

The Pearson Coefficient Correlation analysis (PCCA) is a

multi-task form of relating variables and a positive association indicates a relation of increment and negative is opposite combinations. Thus, positive relation will cause an increment in a variable if the other variable is increased. Whereas, negative relation shows a decrease in a variable if the other variable is increased. As such the positive moderate correlations between temperature and TDS, conductivity, salinity and sulphate (Table 2) could be an indication of an increase in thermal vibration and excitation of the internal composition of ions and molecules of the elements in the water as well as dissolution with increasing temperature. While the negative moderate correlation between temperature and TSS (Table 2) is evidence of poor transmission of heat energy by suspended solid particles in solution suggests that the more the suspended solid particles the less the temperature and vice versa of the waters of the Songor Wetland.

We can also infer from the relationship established between conductivity and salinity, TDS and sulphate (strong significant [$p < 0.01$] positive correlation (Table 2)) that the assessed hydrographic parameters demonstrate the hydrological pathways of the Songor Wetland. The hypersaline waters of the wetland at the western section is flowing by the force gravity to the eastern section is been mixed with freshwaters from the lower Volta River and surface runoffs from the northern section. As a result, there is a corresponding increase in conductivity, TDS, salinity and sulphate levels from the east to west (Table 1).

The infiltration of the heperhaline waters from the western section of the Songor Wetland is also established by the PCCA between alkalinity and temperature, pH, conductivity, TDS and sulphate levels (Tables 1 and 2 respectively). The quality of the natural aquatic ecosystems is reflected by the levels of hardness, alkalinity, pH, free CO_2 and other physicochemical parameters (Xu and Mills, 2018). Therefore, the increment in the alkalinity values (Table 1) with corresponding TDS, salinity, conductivity, sulphate and temperature is the mixing of heperhaline waters of the wetland emanating from the western section to the eastern section of the Songor Wetland.

Principal component analysis

Principal Component Analysis (PCA) is a useful tool for background assessment and for tracing sources and the origins of variables within an ecosystem. The performed PCA indicated that salinity is the main discriminant variable (-0.935) (Table 3) affecting water quality parameter and highlighted the spatial distribution of waters within the Songor Wetland. This implies conductivity, TDS, sulphate and alkalinity inclusively indicating the hydrological pathways of the wetland. The PCA also implicated turbidity and dissolved oxygen (DO) levels as significant contributors to water quality variabilities within the wetland.

The placing of location AD-1 as an outlier with salinity as the discriminating factor (i.e. salinity, conductivity, TDS, sulphate, and partly pH [i.e. pH and alkalinity] and temperature), followed by AD-3 and AD-4; AD-2, AD-5, AD-6 and AD-8; and AD-11 (Figure 3, Tables 3 and 4), therefore, traces the hydrological pathways of the Songor Wetland. The PCA indicating turbidity as the second variable of significant PC 2 [26.9%] (Table 3) impact but of localized influence on the water quality of the wetland could be termed as natural influence as a result of limited vegetation cover and tidal impacts. The dominance of water depth as the third variable loaded on PC3 with 9% contribution to the total variables associated with locations AD-7 and AD-9 (Table 4), could be related to natural and anthropogenic impacts. The human activities like dipping and widening of the water channels couple with flow of gravity could be the causes influencing the depth of waters at locations AD-7 and AD-9 respectively. As such the natural flows both heperhaline and freshwaters of the wetland are expected collect at location AD-7 and its adjoining areas of the wetland. The loading of DO and it's high scores for locations AD-10, AD-11 and AD-4 (Tables 3 and 4) are also an indication of tidal influences and wind-induced effects. Location AD-4 which is located near Toku and Wassakuse communities had limited vegetation and hence fewer windbreakers. This is might, therefore, causing the sea-breeze from the Atlantic Ocean to have full fetch and maximum mixing of the waters.

The established second-order polynomial equation shows a linear relation between salinity and sulphate; salinity and conductivity respectively. This has confirmed the linearity of conductivity (TDS) and salinity and salinity. It should be noted that conductivity is one of the basic water quality parameters and the basis for calculating TDS and salinity (Carter, 1991). As such this study has also proved that conductivity could be used to estimate sulphate levels through salinity (Figure 4B).

Spatial distribution of flora

The distribution patterns of the crude descriptive assessment of the vegetation cover suggested freshwater dominating plants been replaced by saline tolerant plant. They observed stunted growth of the palnts are an indication of the effect of heperhaline waters at the west. The occurrences of *A. nitida* (White mangrove) and *Sesuvium portulacastrum* at locations AD-6, AD-5 and AD-4 indicated brackish or saline environment. This suggested the distribution of the aquatic plants (macrophytes) follows the salinity gradient of the wetland. Similar observations were also noted by Finlayson et al. (2000) in the past in sections of the Songor Wetland and the Keta Lagoon. Most of the saline tolerating aquatic plants adopted mechanisms for coping with the high saline waters. For instance, *A. nitida* are well known for

their adaptability strategies in coping with harsh saline water environment by excreting excess salt through their stomata which formed salt crystal underneath their leaves. In the case of *S. portulacastrum*, a well reduced to thick spongy leaves with cuticle lining is adaptive features for withstand dehydration and desiccation. The effect of the hypersaline waters in the wetland and its resources might inform the dredging and widening of some of the channels that supply the wetland with freshwater. This suggested that the wetland might have been experiencing desiccations which are reflecting in the vegetation distributions from the west to the east with salinity as the main factor, and evaporations and limited flow of freshwater as the driving forces.

Conclusion

The study identified two main sources of water supply systems to the wetland. The saline water from the west and the freshwater from the lower section of River Volta as well as surface and groundwater recharges from the northern section of the wetland. The hydrological networks of marine and freshwater origins are being affected by anthropogenic, and natural landscape in the form of elevated sand dunes and the slope of the wetland terrain. This is predominantly affecting the freshwater supply and being override by seawater inflow and evaporation and therefore subjecting the Songor Wetland to desiccation at the western section. This is causing salinity, sulphate, conductivity, TDS levels to rise at the western section and flowing toward the lower sections of the wetland by force of gravity. The high levels of nitrate and ammonia in the western were indicative of toxicity of excess ions to the aquatic organism. This is also affecting vegetation cover of the wetland which is at various stages of depletion and extinction. Furthermore, the excess silicate and phosphate levels at the east of the wetland could result in eutrophication. There is a need for further investigation on the hydrological and water quality impacts on the distribution of aquatic flora and fauna (e.g, ostracods) in Songor Wetland.

CONFLICT OF INTERESTS

The authors have not declared any conflict of interests.

ACKNOWLEDGEMENTS

The authors are grateful to Mr.Le and Molar of Dan's and Ma Company limited for facilitating the field campaign. Thanks to Mr K. F. Anyan of Department of Marine and Fisheries Sciences and Mr A. Adu-Gymfi of Plant and Environmental Biology Department, the University of Ghana Legon for their technical assistance in the field and in the lab. Many thanks go to Mr Emmanuel Brempong for his assistant in plotting the coordinate in ArcGIS.

REFERENCES

Addo MA, Okley GM, Affum HA, Acquah S, Gbadago J K (2011). Water quality and level of some heavy metals in water and sediments of Kpeshie Lagoon, La-Accra, Ghana. Research Journal of Environmental Earth Sciences 3(5):487-497.

Allersma E, Tilmans WMK (1993). Coastal conditions in West Africa-A review. Ocean and Coastal Management 19:199-240.

Amekudzie A, Faanu A, Darko EO, Awudu AR, Adukpo O, Quaye LA N, Quaye R, Kpordzro B, Agyemang, Ibrahim A (2011). Natural radioactivity concentrations and dose assessment inshore sediments along the coast of Greater Accra, Ghana. World Applied Sciences Journal 13(11):2338-2343.

American Public Health Association (APHA) (1989). Standard methods for examination of water and wastewater, 17th [eds]. Washington DC 1193 p.

Biney CA (1990). A review of some characteristics of freshwater and coastal ecosystems in Ghana. Hydrobiologia 208:45-53.

Berner EK, Berner RA (1987). The global water cycle. Englewood Cliffs, NJ: Prentice-Hall 397 p.

Bojang F, Ndeso-Atanga A (2009). The relevance of mangrove forests to African fisheries, wildlife and water resources. Nature and Faune 24(1):135.

Bollen M, Trouw K, Lerouge F, Gruwez V, Bolle A, Hoffman B, Leyssen G, De Kesel Y, Mercelis P (2011). Design of a coastal protection scheme for Ada at the Volta River mouth (Ghana). Coastal Engineering Proceedings 1(32):36.

Carter V (1991). Technical Aspects of Wetlands Wetland Hydrology, Water Quality, and Associated Functions. United States Geological Survey Water-Supply pp. 1-26.

Cang LT, Czerniak P, Thanh NC, Schwarzer K, Ricklefs K (2007). Suspended sediment dynamics in mangrove areas, Dong Tranh estuary, Can Gio mangrove forest, Ho Chi Minh City, South Vietnam. Annual Report of FY 2007 pp. 439-450.

Dankwa HR, Shenker JM, Lin J, Ofori-Danson PK, Ntiamoa-Baidu Y (2004). Fisheries of two tropical lagoons in Ghana, West Africa. Fisheries Management and Ecology 11(6):379-386.

Helfield JM, Diamond ML (1997). Use of constructed wetlands for urban stream restoration: A critical analysis. Environmental Management 21(3):329-341.

Finlayson C, Gordon C, Ntiamoa-Baidu Y, TumbultoJ, Storrs M (2000). The hydrobiology of Keta and Songor lagoons : implications for coastal wetland management in Ghana. Supervising Scientist, Supervising Scientist Report Dwarin 152 p.

Gampson EK, Nartey VK, Golow AA, Akiti TT, Sarfo MA, Salifu M, Aidoo F, Fuseini AR (2017). Physical and isotopic characteristics in peri-urban landscape: a case study at the lower Volta River Basin, Ghana. Applied Water Science 7:729-744.

HACH (1992). Water Analysis Handbook. Hach Company, Loveland, Colorado, USA., pp. 401-402, 427-428, 537-538.

Hammer DA (1992). Creating freswater wetlands.Chelsea Mich., Lewis Publishers 298 p.

Kadlec RH, Wallace SD (2009). Treatment wetlands seconded. CRC Press, Boca Raton, FL.

Karikari A, Asante K, Biney C (2009). Water quality characteristics at the estuary of Korle Lagoon in Ghana. West Africa Journal of Applied Ecology 10:1.

Kendall M (1975). Multivariate analysis. Hafuer Press (MacMillan), New York.

McCartney M, Rebelo LM, Senaratna SS, de Silva S (2010). Wetlands, agriculture and poverty reduction. In: IWMI Research Report 137. International Water Management Institute, Colombo, Sri Lanka 39 p.

Morton RA (2003). an Overview of Coastal Land Loss: With Emphasis on the Southeastern United States.

Nyarko E, Klubi E, Laissaoui A, Benmansour B (2016). Estimating recent sedimentation rates using lead-210 in tropical estuarine systems: Case study of Volta and Pra Estuaries in Ghana, West

Africa. Journal of Oceanography and Marine Research 4:1.
Obirikorang KA, Amisah S, Adjei-Boateng D (2013). Habitat description of the threatened freshwater clam, Galatea paradoxa (Born 1778) at the Volta Estuary, Ghana. Current World Environment 8(3):331-339.
Oteng-Ababio M, Owusu K, Addo KA (2011). The vulnerable state of the Ghana coast : The case of Faana-Bortianor. Journal of Disaster Risk Studies 3(2):429-442.
Tano RA, Aman A, Toualy E, Kouadio YK, François-Xavier BBD, Addo KA (2018). Development of an Integrated Coastal Vulnerability Index for the Ivorian Coast in West Africa pp. 1171-1184.
Thanh-Nho N, Strady E, Nhu-Trang T, David F, Marchand C (2018). Trace metals partitioning between particulate and dissolved phases along a tropical mangrove estuary. Chemosphere 196:311-322.
World Health Organisation (WHO) (1987). Global environmental monitoring system/ Water operation guide. WHO, Geneva 489pp.
Venice System (1959). Final resolution. The Venice System for the classification of marine waters according to salinity. In: Symposium on the classification of brackish waters. In: D Ancon [eds.], Archivio di Oceanografia e Limnologia pp. 243-248.
Xu X, Mills GL (2018). Do constructed wetlands remove metals or increase metal bioavailability? Journal of Environmental Management 218:245-255.

Vol. 13(12), pp. 524-534, December 2019
DOI: 10.5897/AJEST2019.2770
Article Number: E8F232962421
ISSN: 1996-0786

http://www.academicjournals.org/AJEST

ACADEMIC JOURNALS
expand your knowledge

African Journal of Environmental Science and Technology

Full Length Research Paper

Active and passive air quality bio-monitoring in the tropics: Intra-urban and seasonal variation in atmospheric particles estimated by leaf saturated isothermal remanent magnetisation of *Ficus benjamina* L (Moraceae)

N'guessan Achille Koffi[2]*, Kobenan Pierre N'Gouran[1], Yao Sadaiou Sabas Barima[1] and Djédoux Maxime Angaman[2]

[1]Université Jean Lorougnon Guédé, Unité de Formation et de Recherche en Environnement, BP 150 Daloa, Côte d'Ivoire.
[2]Université Jean Lorougnon Guédé, Unité de Formation Agroforesterie, BP 150 Daloa, Côte d'Ivoire.

Received 7 October, 2019; Accepted 18 November, 2019

Atmospheric pollutant emissions are likely to increase continously in developing cities like Abidjan (Ivory Coast) where air quality strategies are ineffective or not yet implemented. This could result in a big risk to human health. Local meteorological parameters can have both positive or negative effect on habitat quality depending on the biomonitoring approach used. This study investigates the sources and factors affecting the spatio-temporal variation in particulate pollution in a tropical area in Abidjan (Ivory Coast) using a passive and active biomonitoring approach. Leaf saturated isothermal remanent magnetisation (SIRM) of *Ficus benjamina* L. was monitored for 2-6 months over 2 consecutive years in four distinct urban land use classes (main roads, industrial zones, residential zones and parks) based on several meteorological parameters (wind speed, temperature, relative humidity and precipitation) and season. Results showed leaf SIRM varied among land use classes and season with main roads and industrial zones presenting higher leaf SIRM during the dry season. This suggests that vehicular exhaust emissions and industrial smokestacks were the main sources of particulate matter (PM) pollution in Abidjan. These results show also the contribution of natural particles from harmattan dust during the dry season. Leaf SIRM was negatively correlated with precipitation intensity, suggesting a wash-off effect of particles on leaves. Results, however, differed between the dry and wet season. During the dry season, leaf SIRM of young leaves was higher than that of old leaves. This trend was reversed during the raining season. This suggests combined effects of meteorology and plant growth/physiology.

Key words: Air pollution, saturated isothermal remnant magnetism, particulate matter, ficus benjamina, tropical humid area.

INTRODUCTION

Urbanization continues at a record pace all over the world, especially in emerging and developing economies. In these areas, cities are seen as destinations, especially for young people in search of employment, education,

social contacts and cultural advantages (UN-Habitat, 2008). Indeed, large cities in developing countries contain the majority of the industries of this country, most of which are highly polluting manufacturing and mining industries, and the high proportion of motor vehicles. These factors lead to environmental damage, including air pollution like atmospheric particulate matter (PM) (WHO, 2006).

In general, sources of atmospheric PM are both natural (for example volcanic ash, wind-blown sand, etc.) and anthropogenic (for example industrial facilities, transportation, etc.). Both sources result in direct emission of PM (primary PM) and emission of gaseous aerosol precursors, leading to secondary PM. It is reported that at least 3400 million tons of PM is emitted on a global scale per year (Houghton et al., 2001; Gerasopoulos et al., 2006). Anthropogenic sources in urban areas include vehicular traffic by fossil fuel combustion, vehicle braking and industrial smokestacks (Petroff et al., 2008; Bukowiecki et al., 2010).

Epidemiological studies point to a causal association between population exposure to fine PM (diameter less than 2.5 µm) in air and cardiovascular and lung cancer mortality (Cachon et al., 2014; Goudie, 2014), and poor semen quality (Zhou et al., 2014). Several studies in West African countries like Ghana (Dionisio et al., 2010), Guinea (Weinstein et al., 2010), Senegal (Dieme et al., 2012), Benin (Cachon et al., 2014) and Cape Verde (Gonçalves et al., 2014) have shown that atmospheric PM concentration in these countries, and in the West African region in general, by far exceeded the WHO limits (25 $\mu g.m^{-3}$ daily for fine PM and 50 $\mu g.m^{-3}$ daily for PM diameter more than 10 µm) (WHO, 2006).

Most techniques used to study atmospheric PM pollution make use of electronic devices and physico-chemical processes. However, the majority of these methods are not able to estimate the integrated, biological exposition effects of the different and continuously changing concentrations of air pollutants, but instead provide only a physico-chemical indication about the exposition to a sole pollutant, or at most, to a combination of some pollutants (Falla et al., 2000). Moreover, most of the physico-chemical methods are expensive, limiting their use in developing countries, and making them impractical for assessing the pollution distribution with a high spatial resolution.

Biological monitoring or biomonitoring, that may be defined as the measurement of the response of living organisms to the state or to changes in their environment (Jakubowski and Trzcinka-Ochocka, 2005), could be an alternative or a complement to these physico-chemical methods. In general, plants are more sensitive (in terms of physiological reaction) to the most prevalent air pollutants than humans and animals. Biomonitoring with plants can be achieved through active and passive approaches. Passive biomonitoring may be performed through observation and analyses on native and cultivated vegetation already present in a given study area. Active biomonitoring can be carried out with selected test plants of standard genetic origin and developmental state, which are exposed to ambient air at the study site under standardized conditions (Nali and Lorenzini, 2007).

In Abidjan (Ivory Coast), the magnetic leaf properties of *Amaranthus spinosus*, *Eleusine indica*, *Panicum maximum* and *Ficus benjamina* were used as passive bioindicators of habitat pollution by atmospheric PM (Barima et al., 2014). This study showed that atmospheric PM concentration in different land-use classes of this tropical urban environment can be best determined from leaf SIRM of *F. benjamina* and *A. spinosus*. Barima et al. (2014) recommended using the tree species (*F. benjamina*) for biomonitoring compared to grass because trees are generally more effective in capturing atmospheric particles than herbaceous plants (Fowler et al., 1989; Barima et al., 2014). Barima et al. (2014) conducted a study using passive biomonitoring and did not extend over a long period of the year. Therefore, this study did not determine the influence of meteorological parameters on leaf SIRM plants. Nevertheless, it is known that meteorological parameters can have a positive or negative effect on habitat quality (Kassomenos et al., 2014; Rodríguez-Germade et al., 2014).

Such information is necessary to determine the total PM deposition during a season or year, particularly in regions with high rainfall.

The main objective of this study is to determine the impact of season (dry vs rainy) and meteorological variables (rainfall, temperature, humidity and wind speed) on leaf SIRM of *F. benjamina*, obtained using passive and active biomonitoring. To achieve this goal, first, the influence of seasonal variation on leaf SIRM was examined, and the most important meteorological variables affecting leaf SIRM were identified. Next, the effect of exposure time to atmospheric PM on leaf SIRM was determined.

Rainfall and temperature heavily characterise seasons in tropical areas (Amara and Bouazza, 2016). Therefore, it is hypothesized that leaf SIRM of *F. benjamina* is influenced by these two meteorological variables.

MATERIALS AND METHODS

Test species

F. benjamina was chosen as a test species because it is

*Corresponding author. E-mail: achille.koffi@yahoo.fr, byssabas@gmail.com.

widespread in the study area and across the different land use classes as a decorative plant. It is a tropical evergreen tree belonging to the *Moraceae*. This species reaches a height of 30 m in natural conditions; it has glossy, oval leaves of 6-13 cm long, waxy with an acuminate tip. Its roots are adventitious. *F. benjamina* is a popular tree worldwide cultivated for reforestation and ornamental purposes; in the latter case its height usually hardly exceeds 4 m.

Sampling area

The study was conducted in Abidjan, the largest city in Ivory Coast (5°00'- 5°30 N, 3°50'- 4°10'W) by its population size (> 4 million inhabitants) and economic importance in West Africa. The city was subdivided into 4 land use classes as comprehensively described in a former study (Barima et al., 2014): main roads (MR, 4 sites); industrial zones (IZ, 2 sites); residential zones (RZ, 2 sites) and parks (2 sites).

Its climate is tropical, hot and humid with a long dry season (November to April), a long rainy season (May-June-July), a short dry season (August) and a short rainy season (September-October). Passive biomonitoring was performed in February, March, April, May, June and July 2014. The first three months are in the dry season while the last is in the rainy season. Active biomonitoring was carried out in 2015 during the same months. The local climatic characteristics of this period are shown in Figure 1.

Biomonitoring methodology

Passive biomonitoring was carried out continuously from February to July 2014. For this passive approach *F. benjamina* trees planted by the Environment Service of the municipality were selected according to accessibility and geographical distribution criteria. Sites prohibited by civil protection as areas of gas storage of highly toxic waste and power stations have been avoided. Sampling locations were determined based on the availability of *F. benjamina*. Active biomonitoring was carried out from February to July 2015. Air layering techniques were performed for vegetative propagation of *F. benjamina* seedlings used in the passive biomonitoring. Three weeks later, the layerings are placed in pots (13 litres) filled with compost and soil, in which they were kept for three months. During this entire stage plants were kept in a municipal garden relatively far from any source of motor vehicle and industrial pollution. After three months of growth, two pots of *F. benjamina* which reached a height of about 1 m, were placed side-by-side in the selected sites in all considered land use classes. In each land use class, these plants have remained exposed to ambient air for three consecutive months during the dry season. The same process is carried out during the rainy season; new plants were placed at the beginning of the rainy season.

Leaf sampling

At each site, six mature and undamaged leaves were collected on the same plant and carefully placed in paper envelopes. The area of these six leaves was quantified with ImageJ (Version 1.43u) software after scanning the leaves in the laboratory soon after sampling. Leaves were dried at ambient temperature. After drying, all six dried leaves of each sampling location were tightly packed together by cling film, avoiding the movement of any leaf parts.

Biomagnetic leaf properties

Magnetic properties were carried out using a protocol described by Mitchell et al. (2010) and Kardel et al. (2011). All six dried leaves of each sampling location, packed by cling film were pressed into a 10 cm^3 plastic tube. Each tube was magnetised in a direct current (DC) field of 1 mT with a Molspin pulse magnetiser (Molspin Ltd, UK). Saturation Isothermal Remanent Magnetisation (SIRM) of the samples ($A.m^2$) was measured using a Molspin Minispin magnetometer (Molspin Ltd, UK) with high sensitivity. Each sample was measured twice to avoid measurement errors. After every ten measurements, the magnetometer was calibrated using a magnetically-stable rock specimen. Measured SIRM values (mA/m) were normalized for plastique tube volume (10 cm^{-3}) and leaf area (m^2) which leads to a final SIRM expressed as A. Magnetic measurements were carried out at the Laboratory of Environmental and Urban Ecology of the University of Antwerp (Belgium).

Data analysis

Statistical analysis was performed using Statistica 7.1 (Stat Soft France). A significance level of 0.05 was used for all the tests. A regression was performed, by Pearson's method, between SIRM and monthly averages of air temperature, air humidity, and wind speed, and total monthly rainfall to determine the main seasonal parameters influencing leaf SIRM. These meteorological data were obtained from the archives of tutiempo Network (Data provided by the weather station: 655780 (DIAP)), SL (https://fr.tutiempo.net/climat/ws-655780.html).

To find the effect of exposure time on leaf SIRM, *F. benjamina* leaves from active biomonitoring were sampled after one and three months of exposure. The effect of exposure time was tested using a t-test intra season and between seasons. Differences in leaf SIRM between the four land use classes were tested for significance by using a one-way analysis of variance (ANOVA) procedure and a Tukey-HSD test.

RESULTS

Intra-urban variation in leaf SIRM

SIRM of *F. benjamina* leaves showed great variability within the different land use classes for both active and passive biomonitoring (Figure 2). Leaf SIRM obtained via passive biomonitoring can be grouped into two classes according to the land use classes. The first group consists of MR and IZ and displays a statistically higher SIRM ($p < 0.05$) than the second group (RZ and Park). For the first group, Leaf SIRM ranged between 70.31µA (IZ-2015) and 110.03 µA (MR-2015). The lower leaf SIRM was the second group whose values are below 22 µA (Figure 2), at least three times lower than in the first group. There were no significant differences between SIRM within each land-use class in 2014 and 2015 ($p > 0.05$).

Seasonal variation in leaf SIRM

Leaf SIRM varied significantly between and within seasons (Figure 3). This in-season variation differs among the considered land-use classes. Except for July (last rainy month), leaf SIRM values obtained during the dry season are higher than those obtained during the

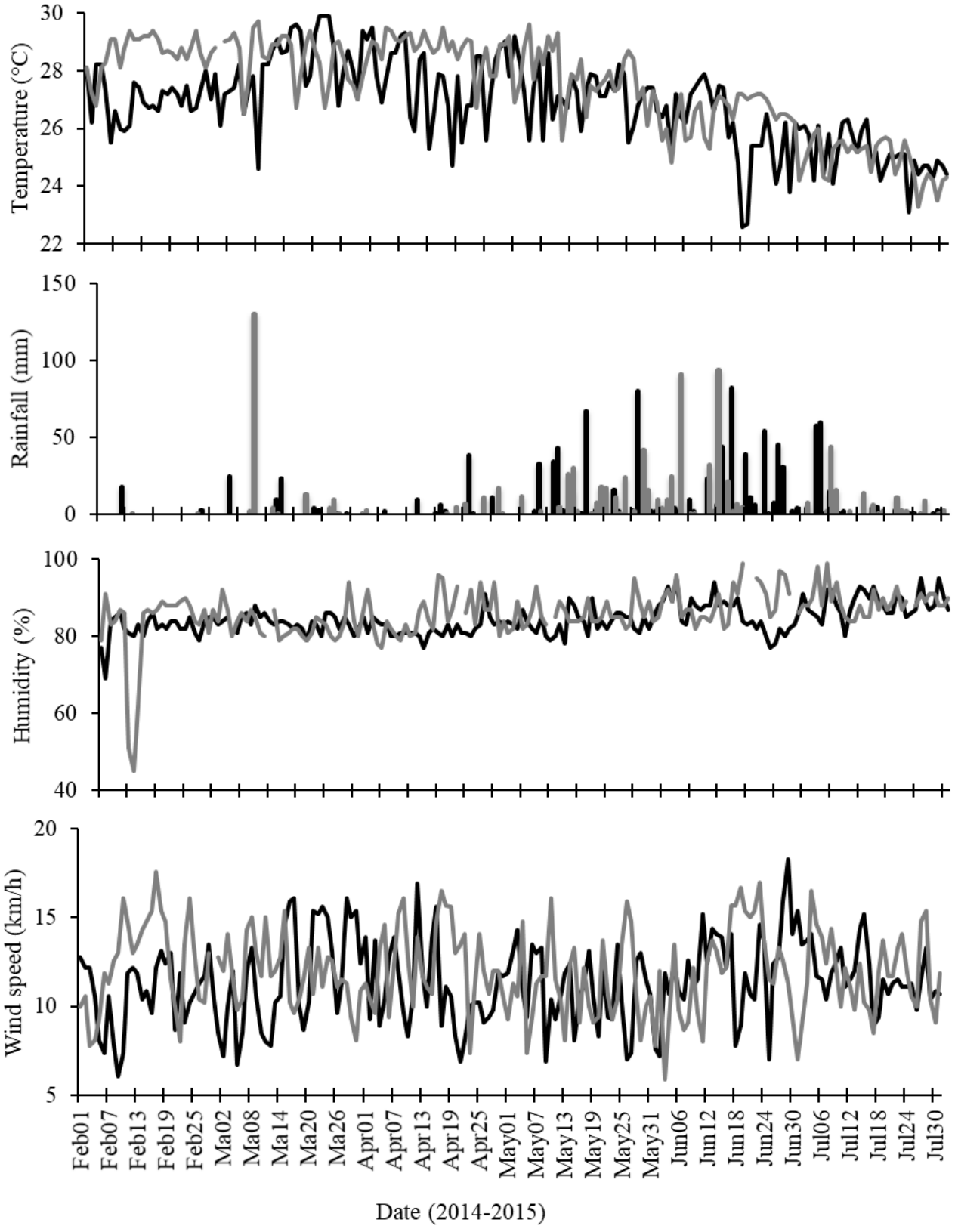

Figure 1. The daily mean of temperature, rainfall, humidity and wind speed during the experimental period from February to July 2014 (black line) and February to July 2015 (grey line). Values were taken each week for the following months: Feb: February, Ma: March, Apr: April, May: May, Jun: Jun, Jul: July. Data source: www.tutiempo.net or https://fr.tutiempo.net/madrid.html.

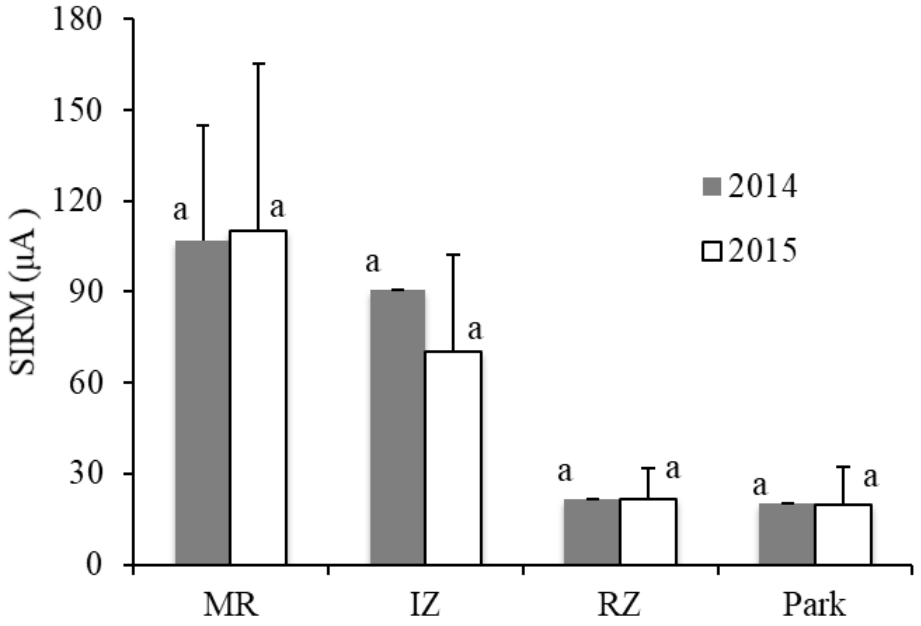

Figure 2. Leaf SIRM for *Ficus benjamina* as observed in main roads (MR), industrial zones (IZ), residential zones (RZ) and parks). Different letters indicate significant differences between land use classes for each considered period.

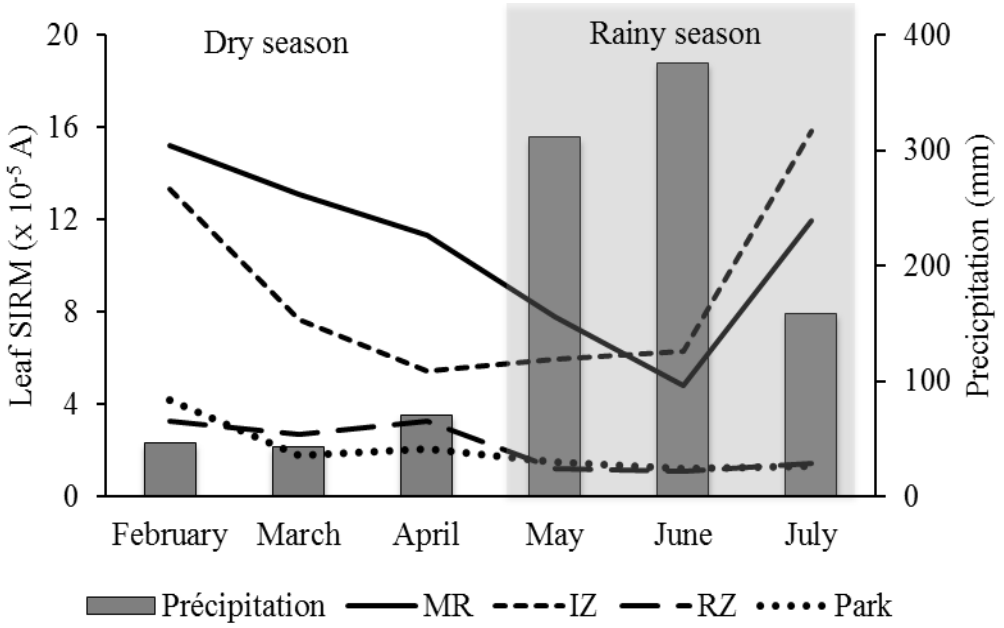

Figure 3. Leaf SIRM of *Ficus benjamina* and monthly rainfall from February to July 2014 for the passive biomonitoring.

rainy season. For MR and IZ, respectively, leaf SIRM decreased from 152.10 µA to 47.90 µA and from 133.0 µA to 62.70 x 10^{-5} A from February to June ($p < 0.05$). However, at the end of the rainy season (July), leaf SIRM rose to tend towards the value obtained during the end of the dry season. The same trends were observed for the active biomonitoring approach (Figure 4). In sum, whatever the month and season, leaf SIRM was higher

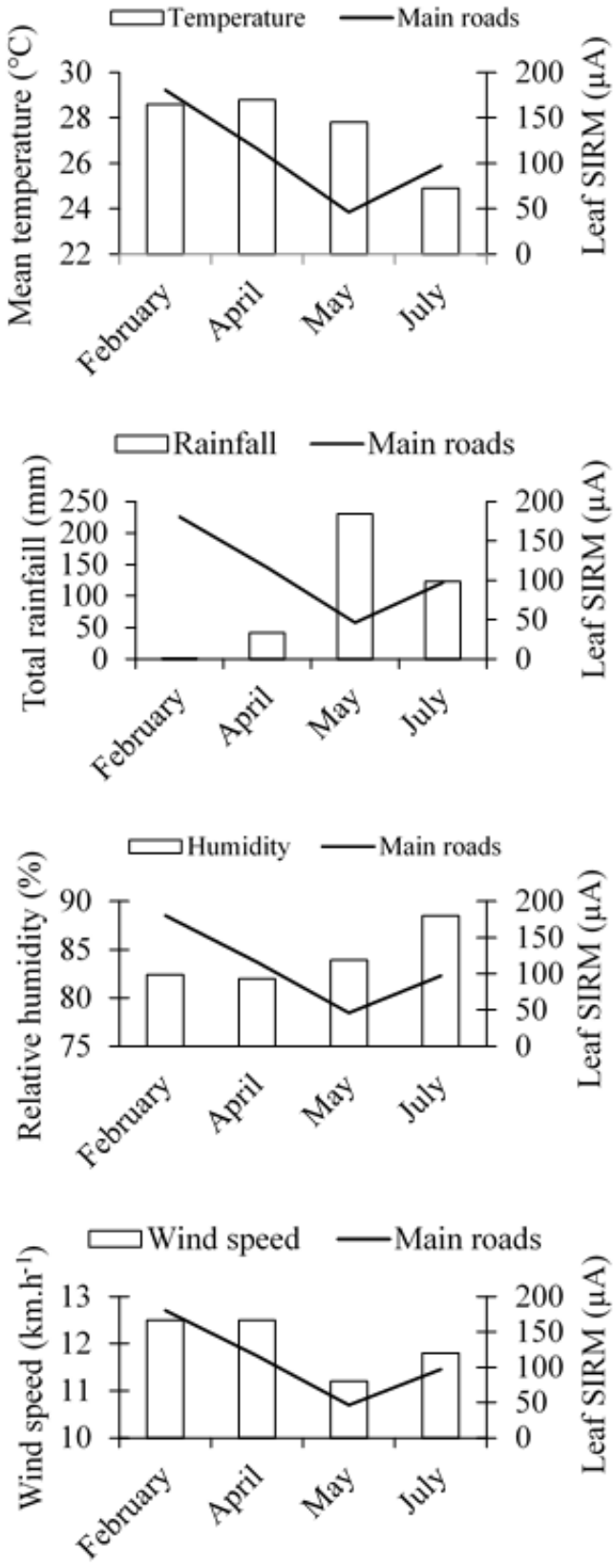

Figure 4. Leaf SIRM of *Ficus benjamina* near the main roads derived from active biomonitoring during the dry season (February to April) and the rainy season (May to July).

during the dry season than the rainy season ($p < 0.05$).

Effects of meteorological variables on leaf SIRM in a passive biomonitoring approach

Among the meteorological studies, precipitation seems to be best correlated to changes in leaf SIRM ($p < 0.05$). This negative correlation is observed in all land use classes (Table 1, Figure 3). The highest correlations were obtained from monthly rainfall in MR (r = -0.94; $p = 0.004$) and RZ (r = -89; $p = 0.010$).

Effect of plant exposure duration to air on leaf SIRM – Seasonal effect

The comparison of leaf SIRM derived from active biomonitoring in the dry (April to May) and rainy season showed a statistical difference near the MR ($t = 3.038$; $p = 0.003$) and in IZ ($t = 2.546$; $p = 0.043$). Mean leaf SIRM is higher in dry season (148.3 µA for MR and 80.07 µA for IZ) than in rainy season (71.75 µA for MR and 98.40 µA for IZ). During the dry season (February to April), SIRM of leaves subjected to one-month exposure ("young leaves"; 180.50 µA) is important than those subjected to three months exposure ("old leaves"; 116.10 µA) ($t = 2.98$; $p = 0.013$). A reversed trend was observed, during the raining season (May to July), SIRM of "old leaves" (97.10 µA) was higher than that of the "younger" leaves (46.40 µA) (t = -3.29; $p = 0.007$) (Table 2). No clear statistical difference was found in the intra seasonal variations of the other land use classes (Table 2).

Monthly rainfall events could have had an influence on the observed variation in leaf SIRM in MR, with an increase in rain event resulting in a decrease in leaf SIRM (Figure 3). During the dry season in February leaf SIRM amounted > 180.0 µA, while when rainfall during the whole month exceeded 130 mm in July, leaf SIRM fell down to 100.0 µA. The other parameters, that is, air humidity, air temperature and wind speed did not appear to affect leaf SIRM in MR.

DISCUSSION

Intra-urban variation in leaf SIRM between land use classes

No significant differences in *F. benjamina* leaf SIRM were observed between the land use classes with both passive and active biomonitoring. The highest values were observed in MR and IZ (Figures 2 and 3). These results confirm that these sites were potentially more polluted than RZ and Park as it has been already demonstrated in a previous study in Abidjan (Barima et al., 2014). In other countries, similar classifications in these two groups have been found, e.g. Belgium (Kardel et al., 2012), India (Deshmukh et al., 2013), United Kingdom (Mitchell et al., 2010), Portugal (Sant'Ovaia et al., 2012), Greece (Kassomenos et al, 2014), China (Li et al., 2014), Korea (Yoo et al., 2014). Parks are particularly known to have better air quality than other urban land use classes (Serbula et al., 2010; Dias et al., 2012). Indeed, air quality was better within parks (urban background) due to the absence of motorised traffic, and worsened when approaching roads (Barima et al., 2014). These results confirm that the major urban pollution source determined with leaf SIRM is caused by fuel driven traffic (Bukowiecki et al., 2010; Kardel et al., 2012). However, Kardel et al. (2012) and Hofman et al. (2014a) showed that in addition to fuel-driven traffic, the railway is a major source of pollution in the urban area. But transportation from trains is not developed and tram being inexistent in Ivory Coast, we have not targeted these classes. In IZ sources of particles can be dual, partly from the ferromagnetic industry, partly from the local traffic.

Seasonal variation in leaf SIRM from passive and active biomonitoring

Leaf SIRM of *F. benjamina* varied, both in the wet and dry season and within the same season on MR and IZ (Figures 3 and 4). This variation was not similar to the different land use classes. In general, leaf SIRM during the dry season was higher than during the rainy season. In temperate climatic regions and for deciduous species, several authors like Mitchell et al. (2010), Kardel et al. (2011) and Hofman et al. (2014b) also found a seasonal effect of leaf SIRM, but they observed an increase of leaf SIRM with increasing exposure time. Using PM sensors, other authors found similar trends. Instead, authors like Kassomenos et al. (2014) obtained in Greece and Spain, higher PM concentrations during the warm period. These variations of leaf SIRM or PM content in the atmosphere showed that the concentration of these pollutants is influenced by weather or meteorological conditions (Kassomenos et al., 2014).

In this study area, and in the West African tropical zone in general, PM prevalence in the atmosphere during the dry season could be explained by the harmattan dust. Indeed, in the dry season, from December to March, the West African region is subject to a dry dust-laden wind, the harmattan, blowing from the Sahara Desert. The harmattan wind carries the Sahara mineral dust to long distances (Gonçalves et al., 2014). Transport of particles by these winds has already been demonstrated in Mediterranean countries including Greece (Kassomenos et al., 2014), Portugal (Wagner et al., 2009) and Spain (Sagnotti and Winkler, 2012; Rodríguez-Germade et al., 2014).

In drier atmospheric conditions, PM concentrations are higher. Moreover, due to the lack of rain, there is little wash-off, which is observed during the rainy season and which is in contrast with the findings of Kardel et al.

Table 1. Results of simple regressions performed with *Ficus benjamina* leaf SIRM in a land-use class and meteorological variables (temperature, humidity, monthly rainfall and wind speed. *r*: Pearson coefficient of correlation. The number of samples per month = 109. Significant correlations ($p < 0.05$) are given in bold.

Parameter		Temperature (°C)	Humidity (%)	Monthly rainfall (mm)	Wind speed (km.h^{-1})
Main roads	r	0.29	-0.69	-0.94	0.38
	p	0.570	0.128	0.004	0.450
Industrial zones	r	-0.57	0.07	-0.34	0.13
	p	0.234	0.896	0.040	0.804
Residential zones	r	0.60	-0.79	-0.89	0.57
	p	0.202	0.062	0.010	0.232
Parks	r	0.27	-0.71	-0.59	-0.68
	p	0.604	0.116	0.221	0.134

Table 2. Student T-test results of the seasonal evolution of mean leaf SIRM (µA ± standard deviation) derived from active biomonitoring in the dry (April-May) and rainy season (May-July). Significant effects are shown in bold ($p < 0.05$). Values assigned by the same letter are not statistically different (ANOVA, Turkey test).

Paramater		Main roads	Industrial zones	Residential zones	Parks
February		180.50^{a}	69.76^{ab}	35.80	38.60^{a}
April		116.10^{a}	11.31^{a}	17.90	14.10
	t	2.98	-4.87	1.29	7.52
	p	**0.013**	0.128	0.418	0.084
May		46.40	36.80^{a}	11.50	11.20
July		97.10	61.60^{a}	21.50	15.20
	t	-3.29	-1.87	-1.83	-0.84
	p	**0.007**	0.312	0.318	0.554
Seasonal mean	t	3.038	2.546	1.214	1.123
	p	**0.003**	**0.043**	0.270	0.123

(2011) and Hofman et al. (2014b).

Rainfall effect on leaf SIRM

It is well known that atmospheric PM and dust concentrations vary due to variation in meteorological conditions, even with constant emissions to the environment, as meteorological conditions play a vital role in governing the fate of air pollutants (Deshmukh et al., 2013). Among the considered meteorological variables, rainfall is statistically and negatively correlated with leaf SIRM (Table 1, Figures 3 and 4). It seems that the heavy rain events wash off the intercepted dust from the leaves. This wash-off effect was also found by other authors (Matzka and Maher, 1999; Sant'Ovaia et al., 2012; Li et al., 2014), while others did not observe such an effect (Kardel et al., 2011; Hofman et al., 2014c).

Studies showed that leaf surface characteristics have a strong influence on the retention of particles by the leaf surfaces, and therefore on the intensity of wash off effect. Thus, leaves with complex shapes, waxy cuticles, ridged surface fine hairs or emitting sticky substances may accumulate particles efficiently (Freer-Smith et al., 1997; Kardel et al., 2011; Freer-Smith et al., 2004; Wang et al., 2013). However, within these characteristics, atmospheric PM amount, a species with ridged leaf surfaces, was significantly higher than species with waxy leaf surfaces (Wang et al., 2013). Furthermore, plants accumulated atmospheric PM both on foliage surfaces and waxes. In terms of quantity, atmospheric PM on leaf surface generally exceeded wax PM, with variable rates depending on the species and land use clases (Przybysz et al., 2014). In nature, atmospheric PM on leaf surface can easily be washed off from foliage by rain, as also pointed out by other authors (Beckett et al., 2000; Van Heerden et al., 2007). Moreover, increased direct exposure to rain event conditions might cause a more intensive mechanical and chemical abrasion of the wax layer (Wang et al., 2013) like *F. benjamina* (simple and

waxy leaves) in our study case.

Effect of exposure duration on leaf SIRM

During the dry season, the mean values of leaf SIRM decreased significantly ($p < 0.05$) from February to April in MR (Table 2). However, during the rainy season (May to July), this trend changed ($p < 0.05$); SIRM increased after a longer exposure time. This decrease in SIRM with time during the dry season is in contrast with the results of Kardel et al. (2011) and Rodriguez-Germade et al. (2014), while it is in agreement with their conclusions during the rainy season. The first authors showed that SIRM of *Tilia platyphyllos* and *Carpinus betulus* leaves increased during the season with a limited effect of rain-induced wash off. A similar trend was also reported for *Platanus hispanica* (Rodríguez-Germade et al., 2014). Some authors have proposed that part of the particulate material responsible for the magnetic signal is not found on the leaves' surface but rather is incorporated into their structure through the stomata cavities or their cuticle waxy protective layer (Sagnotti and Winkler, 2012; Burkhardt and Pariyar, 2014; Przybysz et al., 2014).

F. benjamina, an evergreen tree, showed an increase in leaf SIRM with time during the rainy season. This result suggests that the encapsulation of magnetic particles into the leaf tissue mainly occurs during the rainy season (growth phase) compared to the dry season probably due to a higher wax regeneration or formation activity during this growth season (Mitchell et al., 2010; Kardel et al., 2011). Mitchell et al. (2010) showed the evergreen trees may incorporate a larger proportion of particles within the leaf structure.

However, lower leaf SIRM after three months of exposure to air during the dry season could be explained, in a tropical humid area, during this season, by the severity of drought and harmattan is more rigorous (Weinstein et al., 2010). Plant adaptation to drought stress (high temperature and low rainfall) and harmattan leads to stomata closure (Koffi et al., 2014) and a reduction of epicuticular wax production; it reduces the encapsulation of particles by leaf and thus a subsequent SIRM decline (Hofman et al., 2014b). In any event, rain-induced wash off of magnetic particles from tree leaves is likely to vary according to species and leaf characteristics, in addition to rain intensity, canopy position and degree of shelter (Mitchell et al., 2010; Hofman et al., 2014b).

Active biomonitoring versus passive biomonitoring

The choice of a biomonitoring method will depend on season (dry and rainy). Given the harsh environmental conditions of the dry season *F. benjamina* used with active biomonitoring could reduce their encapsulation of atmospheric particles because of their response to environmental stress (Hofman et al., 2014b) as explained in the previous section. Thus, a passive biomonitoring approach may be advisable in a dry season because the plant in an urban environment has already adapted to drought conditions compared to those from active biomonitoring that are spending there in the dry season for the first time.

During the rainy season, active biomonitoring would be useful since plants are in their growth phase. Moreover, sampling of leaves in late growth phase may optimise magnetic differentiation between sites with differing urban habitat quality differences in leaf SIRM; thus the atmospheric PM between sites became more pronounced later during the growing season (Kardel et al., 2011), especially for high spatial resolution biomonitoring studies (Kardel et al., 2010). However, a disadvantage of measurements in the rainy season is the wash-off effect caused by intense rain events. Using passive biomonitoring approach, differences in soil parameters, plant age and treatment, and even study plants availability in urban area are practical constraints.

In total, passive biomonitoring methods seem more appropriate than active biomonitoring approach to study PM deposition via leaf SIRM of *F. benjamina* in an African tropical urban environment like Ivory Coast.

Conclusion

There are no significant differences between the leaf SIRM of *F. benjamina* near main roads and industrial zones. Industrial smokestacks and vehicle exhausts seem the main sources of pollution in the city. Leaf SIRM varied between and within seasons. Leaf SIRM was higher during the dry season compared to the rainy season, suggesting a rain-induced wash-off effect of leaf deposited PM. The effect of exposure time on leaf SIRM showed contrasting results based on seasons. Leaf SIRM was the highest at the beginning of the dry season and lowest at the end of this season. In contrast, leaf SIRM was higher at the end of the rainy season than in the beginning but these values are lower than those obtained during the dry season. PM deposition process on the leaf surface and its encapsulation during the plant growth period could explain these results.

CONFLICT OF INTERESTS

The authors have not declared any conflict of interests.

ACKNOWLEDGMENTS

This work was supported by grants received from David and Alice Van Foundation, Belgian Federal Science Policy Office (BELSPO) co-funded by the Marie Curie

Actions from the European Commission and International Foundation for Science (IFS) and “Programme d’Appui Stratégique à la Recherche Scientifique” (PASRES). We acknowledge Buuren and the Commission for Cooperation in Development (formerly CIUF-CUD) for funding the fieldwork and VLIR UOS for allowing the analysis of the samples in Belgium.

REFERENCES

Amara M, Bouazza M (2016). The synergistic action of aridity and human impacts on plant biodiversity in the algerian extreme northwest (Tellian plain of maghnia). Plant Archives 16(2):907-917.

Barima YSS, Angaman DM, N'Gouran KP, Koffi NA, Kardel F, De Cannière C, Samson R (2014). Assessing atmospheric particulate matter distribution based on Saturation Isothermal Remanent Magnetization of herbaceous and tree leaves in a tropical urban environment. Science of the Total Environment 470-471:975-982.

Beckett KP, Freer-Smith P, Taylor G (2000). Effective tree species for local air quality manage- ment. J Arboric. Journal of Arboriculture 26(1):12-19.

Bukowiecki N, Lienemann P, Hill M, Furger M, Richard A, Amato F, Prévôt ASH, Baltensperger U, Buchmann B, Gehrig R (2010). PM10 emission factors for non- exhaust particles generated by road traffic in an urban street canyon and along a freeway in Switzerland. Atmospheric Environment 44:2330-2340.

Burkhardt J, Pariyar S (2014). Particulate pollutants are capable to ‘degrade’ epicuticular waxes and to decrease the drought tolerance of Scots pine (*Pinus sylvestris* L.). Environmental Pollution 184:659-667.

Cachon BF, Firmin SP, Verdin A, Ayi-Fanou L, Billet S, Cazier F, Martin PJ, Aissi F, Courcot D, Sanni A, Shirali P (2014). Proinflammatory effects and oxidative stress within human bronchial epithelial cells exposed to atmospheric particulate matter (PM2.5 and PM>2.5) collected from Cotonou, Benin. Environmental Pollution 185:340-351.

Deshmukh DK, Deb MK, Mkoma SL (2013). Size distribution and seasonal variation of size-segregated particulate matter in the ambient air of Raipur city, India. Air Quality, Atmosphere, and Health 6:259-276.

Dias D, Tchepel O, Carvalho A, Miranda AI, Borrego C (2012). Particulate Matter and Health Risk under a Changing Climate: Assessment for Portugal. The Scientific World Journal pp. 1-10.

Dieme D, Cabral-Ndior M, Garçon G, Verdin A, Billet S, Cazier F, Courcot D, Diouf A, Shirali, P (2012). Relationship between physicochemical characterization and toxicity of fine particulate matter (PM2.5) collected in Dakar city (Senegal). Environmental research 113:1-13.

Dionisio KL, Arku RE, Hughes AF, Vallarino J, Carmichael H, Spengler JD, Agyei-Mensah S, Ezzati M (2010). Air pollution in Accra neighborhoods: spatial, socioeconomic, and temporal patterns. Environmental Science & Technology 44(7):270-2276.

Falla J, Laval-Gilly P, Henryon M, Morlot D, Ferard JF (2000). Biological air quality monitoring: A review. Environmental Monitoring and Assessment 64(3):627-644.

Fowler D, Cape JN, Unsworth MH (1989. Deposition of atmospheric pollutants on forests. Philosophical Transactions of the Royal Society of London 324B:247-265.

Freer-Smith PH, El-Khatib AA, Taylor G (2004). Capture of particulate pollution by trees: a comparison of species typical of semi-arid areas (Ficus nitida and Eucalyptus globulus) with European and North American species. Water, Air, and Soil Pollution 155(1-4):173-187.

Freer-Smith PH, Holloway S, Goodman A (1997). The uptake of particulates by an urban woodland: site description and particulate composition. Environmental Pollution 95:27-35.

Gerasopoulos E, Kouvarakis G, Babasakalis P, Vrekoussis M, Putaud JP, Mihalopoulos N (2006). Origin and variability of particulate matter (PM10) mass concentrations over the Eastern Mediterranean. Atmospheric Environment 40:4679-4690.

Gonçalves C, Alves C, Nunes T, Rocha S, Cardoso J, Cerqueira M, Pio C, Almeida SM, Hillamo R, Teinilä K (2014). Organic characterisation of PM10 in Cape Verde under Saharan dust influxes. Atmospheric Environment 89:425-432.

Goudie AS (2014). Desert dust and human health disorders. Environment International 63:101-113.

Hofman J, Lefebvre W, Janssen S, Nackaerts R, Nuyts S, Mattheyses L, Samson R (2014a). Increasing the spatial resolution of air quality assessments in urban areas: A comparison of biomagnetic monitoring and urban scale modelling. Atmospheric Environment 92:130-140.

Hofman J, Wuyts K, Van Wittenberghe S, Samson R (2014b). On the temporal variation of leaf magnetic parameters: seasonal accumulation of leaf-deposited and leaf-encapsulated particles of a roadside tree crown. Science of the Total Environment 493:766-772.

Hofman J, Wuyts K, Van Wittenberghe S, Brackx M, Samson R (2014c). On the link between biomagnetic monitoring and leaf-deposited dust load of urban trees: Relationships and spatial variability of different particle size fractions. Environmental Pollution 189:63-72.

Houghton JT, Ding Y, Griggs DJ, Noguer M, Van Der Linden PJ, Dai X, Johnson CA (2001). Intergovernmental Panel on Climate Change (IPCC). Climate Change 2001: The Scientific Basis. Contribution of Working Group I to the Third Assessment Report of the Intergovernmental Panel on Climate Change pp. 881-881.

Jakubowski M, Trzcinka-Ochocka M (2005). Biological monitoring of exposure: Trends and key developments. Journal of Occupational Health 47(1):22-48.

Kardel F, Wuyts K, Babanezhad M, Vitharana UWA, Wuytack T, Potters G, Samson R (2010). Assessing urban habitat quality based on specific leaf area and stomatal characteristics of *Plantago lanceolata* L. Environmental Pollution 158:788-794.

Kardel F, Wuyts K, Maher BA, Hansard R, Samson R (2011). Leaf saturation isothermal remanent magnetization (SIRM) as a proxy for particulate matter monitoring: Inter-species differences and in-season variation. Atmospheric Environment 45:5164-5171.

Kardel F, Wuyts K, Maher BA, Samson R (2012). Intra-urban spatial variation of magnetic particles: Monitoring via leaf saturation isothermal remanent magnetisation (SIRM). Atmospheric Environment 55:111-120.

Kassomenos PA, Vardoulakis S, Chaloulakou A, Paschalidou AK, Grivas G, Borge R, Lumbreras J (2014). Study of PM10 and PM2.5 levels in three European cities: Analysis of intra and inter urban variations. Atmospheric Environment 87:153-163.

Koffi NA, Barima YSS, Angaman DM, Dongui BK (2014). Stomatal leaf characteristics of Ficus benjamina L. as potential bioindicators of air quality in the Abidjan city (Côte d'Ivoire). Journal of Applied Biosciences 78:6675-6684.

Li W, Wang C, Wang H, Chen J, Yuan C, Li T, Wang W, Shen H, Huang Y, Wang R, Wang B, Zhang Y, Chen H, Chen Y, Tang J, Wang X, Liu J, Coveney JrRM, Tao S (2014). Distribution of atmospheric particulate matter (PM) in rural field, rural village and urban areas of northern China. Environmental Pollution 185:134-140.

Matzka J, Maher BA (1999). Magnetic biomonitoring of roadside tree leaves: identification of spatial and temporal variations in vehicle-derived particulates. Atmospheric Environment 33(28):4565-4569.

Mitchell R, Maher BA, Kinnersley R (2010). Rates of particulate pollution deposition onto leaf surfaces: Temporal and inter-species magnetic analyses. Environmental Pollution 158(5):1472-1478.

Nali C, Lorenzini G (2007). Air quality survey carried out by schoolchildren : An innovative tool for urban planning. Environmental Monitoring and Assessment 131(1-3):201-210.

Petroff A, Mailliat A, Amielh M, Anselmet F (2008). Aerosol dry deposition on vegetative canopies. Part I: review of present knowledge. Atmospheric Environment 42(16):3625-3653.

Przybysz A, Sæbø A, Hanslin HM, Gawroński SW (2014). Accumulation of particulate matter and trace elements on vegetation as affected by pollution level, rainfall and the passage of time. Science of the Total Environment 481:360-369.

Rodríguez-Germade I, Mohamed KJ, Rey D, Rubio B, García AL (2014). The influence of weather and climate on the reliability of magnetic properties of tree leaves as proxies for air pollution monitoring. Science of the Total Environment 468-469:892-902.

Sagnotti L, Winkler A (2012). On the magnetic characterization and quantification of the superparamagnetic fraction of traffic-related urban airborne PM in Rome, Italy. Atmospheric Environment 59:131-140.

Sant'Ovaia H, Lacerda MJ, Gomes C (2012). Particle pollution - An environmental magnetism study using biocollectors located in northern Portugal. Atmospheric Environment 61:340-349.

Serbula SM, Antonijevic MM, Milosevic NM, Milic SM, Ilic AA (2010). Concentrations of particulate matter and arsenic in Bor (Serbia). Journal of Hazardous Materials 181:43-51.

UN-Habitat (2008). United Nations Human Settlements Programme & United Nations. Economic Commission for Africa. (2008). The state of African city 2008. A framework for addressing urban challenges in Africa.

Van Heerden P, Krüger GHJ, Kilbourn Louw M (2007). Dynamic responses of photosystem II in the Namib Desert shrub, Zygophyllum prismatocarpum, during and after foliar deposition of limestone dust. Environmental Pollution 146:34-45.

Wagner F, Bortoli D, Pereira S, Costa MJ, Silva AM, Weinzierl B, Esselborn M, Petzold A, Rasp K, Heinold B, Tegen I (2009). Properties of dust aerosol particles transported to Portugal from the Sahara desert. Tellus B: Chemical and Physical Meteorology 61(1):297-306.

Wang H, Shi H, Li Y, Yu Y, Zhang J (2013). Seasonal variations in leaf capturing of particulate matter, surface wettability and micromorphology in urban tree species. Frontiers of Environmental Science & Engineering 7(4):579-588.

Weinstein JP, Hedges SR, Kimbrough S (2010). Characterization and aerosol mass balance of PM2.5 and PM10 collected in Conakry, Guinea during the 2004 Harmattan period. Chemosphere 78:980-988.

World Health Organization (WHO) (2006). Air quality guidelines for particulate matter, ozone, nitrogen dioxide and sulfur dioxide: global update 2005: summary of risk assessment (No. WHO/SDE/PHE/OEH/06.02). Geneva: World Health Organization.

Yoo JM, Lee YR, Kim D, Jeong MJ, Stockwell WR, Kundu PK, Oh SM, Shin DB, Lee SJ (2014). New indices for wet scavenging of air pollutants (O3, CO, NO_2, SO_2, and PM10) by summertime rain. Atmospheric Environment 82:226-237.

Zhou N, Cui Z, Yang S, Han X, Chen G, Zhou Z, Zhai C, Ma M, Li L, Cai M, Li Y, Ao L, Shu W, Liua J, Cao J (2014). Air pollution and decreased semen quality: A comparative study of Chongqing urban and rural areas. Environmental Pollution 187:145-152.

Related Journals: